Faculty of Aerospace Engineering

Incremental Nonlinear Dynamic Inversion Flight Control

Stability and Robustness Analysis and Improvements

R. C. van 't Veld

September 29, 2016

Delft University of Technology

Challenge the future

Incremental Nonlinear Dynamic Inversion Flight Control

Stability and Robustness Analysis and Improvements

Master of Science Thesis

For obtaining the degree of Master of Science in Aerospace Engineering
at Delft University of Technology

R. C. van 't Veld

September 29, 2016

Faculty of Aerospace Engineering · Delft University of Technology

Delft University of Technology

Delft University Of Technology
Department Of
Control and Simulation

The undersigned hereby certify that they have read and recommend to the Faculty of Aerospace Engineering for acceptance a thesis entitled **"Incremental Nonlinear Dynamic Inversion Flight Control"** by **R. C. van 't Veld** in partial fulfillment of the requirements for the degree of **Master of Science**.

Dated: September 29, 2016

Readers:

dr. Q. P. Chu

dr.ir. E. van Kampen

dr. B. F. Santos

Abstract

Incremental Nonlinear Dynamic Inversion (INDI) is a variation on Nonlinear Dynamic Inversion (NDI) retaining the high-performance advantages of NDI, while increasing controller robustness to model uncertainties and decreasing the dependency on the vehicle model. After a successful flight test with a multirotor Micro Aerial Vehicle (MAV), the question arises whether this technique can be used to successfully design a Flight Control System (FCS) for aircraft in general. This requires additional research on aircraft characteristics that could cause issues related to the stability and performance of the INDI controller. Typical characteristics are additional time delays due to data buses and measurement systems, slower actuator and sensor dynamics, and a lower control frequency. The main contributions of this article are 1) an analytical stability analysis showing that implementing discrete-time INDI with a sampling time smaller than 0.02s results in large stability margins regarding system characteristics and controller gains; 2) a simulation study showing significant performance degradation requiring controller adaptation due to actuator measurement bias, angular rate measurement noise, angular rate measurement delay and actuator measurement delay; 3) the use of a real-time time delay identification algorithm based on latency to successfully synchronize the angular rate and actuator measurement delay together with pseudo control hedging (PCH) to prevent oscillatory behavior; and 4) recommendations regarding control modes, assessment criteria and PH-LAB Cessna Citation specific issues to be used by future contributors to a flight test with INDI on the PH-LAB aircraft.

Contents

Acronyms

AHRS	Attitude and Heading Reference System
ASDF	Average Square Difference Function
CAP	Control Anticipation Parameter
CHR	Cooper-Harper Rating
CINDI	Continuous Incremental Nonlinear Dynamic Inversion
CV	Control Variable
DADC	Digital Air Data Computer
DINDI	Discrete Incremental Nonlinear Dynamic Inversion
DLR	German Aerospace Center
ESO	Extended State Observer
FBW	Fly-by-Wire
FCS	Flight Control System
FL	Feedback Linearization
FTIS	Flight Test and Instrumentation System
INDI	Incremental Nonlinear Dynamic Inversion
LOES	Lower Order Equivalent System
MAV	Micro Aerial Vehicle
MIMO	Multiple Input Multiple Output
MRAC	Model Reference Adaptive Control
MUAD	Maximum Unnoticeable Added Dynamics
NDI	Nonlinear Dynamic Inversion
NN	Neural Network
PCH	Pseudo Control Hedging
PID	Proportional-Integral-Derivative
PIO	Pilot Induced Oscillation
RMS	Root Mean Square
SISO	Single Input Single Output

List of Symbols

Roman Symbols

A	Generic matrix function
a	Generic scalar function
b	Generic scalar function
C_l	Dimensionless rolling moment coefficient
C_m	Dimensionless pitching moment coefficient
C_n	Dimensionless yawing moment coefficient
e	Tracking error
F	(Linearized) System matrix
$\underline{f}$	Generic vector function
G	(Linearized) Control effectiveness matrix
$\underline{g}$	Generic vector function
H	Generic transfer function
h	Generic scalar function
$\underline{h}$	Generic vector function
K	Gain
k	Gain
L	Rolling moment, [Nm]
M	Pitching moment, [Nm]
N	Yawing moment, [Nm]
n	Normalized specific forces, [g]

n	Order of system, [-]
p	Roll rate, [deg/s or rad/s]
q	Pitch rate, [deg/s or rad/s]
r	Yaw rate, [deg/s or rad/s]
r	Relative degree of system, [-]
s	Laplace variable
T	Sampling time, [s]
t	Time, [s]
u	Velocity along x-body axis, [m/s]
u	Physical control input
$\underline{u}$	Physical control input vector
V	Velocity, [m/s]
v	Velocity along y-body axis, [m/s]
w	Velocity along z-body axis, [m/s]
X	Force along x-body axis, [N]
x	Position along x-axis, [m]
x	State variable
$\underline{x}$	State vector
Y	Force along y-body axis, [N]
y	System output scalar
y	Position along y-axis, [m]
$\underline{y}$	System output vector
Z	Force along z-body axis, [N]
z	Position along z-axis, [m]
z	Discrete variable

Greek Symbols

α	Angle-of-attack, [deg or rad]
β	Sideslip angle, [deg or rad]
Γ	Discrete input matrix
γ	Control effectiveness uncertainty ratio, [-]
γ	Flight path angle, [deg or rad]
Δ	Increment

δ	Control effector state, [- or deg or rad]
θ	Pitch angle, [deg or rad]
λ	Eigenvalue
μ	Aerodynamic roll angle, [deg or rad]
ν	Virtual control input
$\underline{\nu}$	Virtual control input vector
Φ	Discrete system matrix
ϕ	Roll angle, [deg or rad]
χ	Heading angle, [deg or rad]
ψ	Yaw angle, [deg or rad]

Subscripts

0	Current point in time
a	Velocity axis
a	Aileron
$b/body$	Body axis
d	Desired
e	Elevator
EAS	Equivalent Air Speed
eci	Earth-centered inertial axis
$filt$	Filter
$flap$	Flap
k	Discrete indice
n	Nominal
NED	Vehicle-carried normal earth axis
r	Rudder
T	Throttle
t	trim
u	Actuator
x	Control
x	x-axis
y	y-axis
z	z-axis

Chapter 1

Introduction

This chapter introduces the Master of Science thesis report: "Incremental Nonlinear Dynamic Inversion Flight Control: Stability and Robustness Analysis and Improvements". The thesis was written at the Control & Simulation department of the faculty of Aerospace Engineering of Delft University of Technology. The introduction presents a motivation for the project given in Section 1-1. Moreover, the research objectives and question are presented in Section 1-2. Finally, Section 1-3 presents the outline of the report.

1-1 Project Motivation

Before the 1990s almost all Flight Control Systems (FCSs) of fixed-wing aircraft were developed based on classical, linear control techniques (Balas, 2003). These techniques have yielded satisfactory results in nominal conditions for many years. However, the design of these FCSs are costly due to the scheduling and iteration difficulties (Adams & Banda, 1993; Enns, Bugajski, Hendrick, & Stein, 1994). Additionally, these techniques suffer from performance degradation due to nonlinearities, uncertainties and failures encountered in reality (Slotine & Li, 1991).

Besides being a disadvantage in itself, this performance degradation can also be related to safety issues. A worldwide survey considering the period from 1993 to 2007 has shown that loss of control in-flight is the second most important occurrence causing fatal accidents, as well as involving the second most fatalities (Anon., 2008). Also, the survey concluded that the loss of control accident rate has been approximately constant since 1995. Another worldwide survey for the period from 2006 to 2011 has confirmed this trend and again lists loss of control in-flight as the second most important occurrence causing fatal accidents (Anon., 2013). Moreover, this survey even lists loss of control in-flight as the most important cause of fatalities over this period of time.

The last few decades, academia developed new control techniques to design FCSs to alleviate problems related to development cost and time, performance and safety. Examples are methods such as eigenstructure assignment, H_∞ loop-shaping, linear quadratic regulator/Gaussian, μ-synthesis, Model Reference Adaptive Control (MRAC), Nonlinear Dynamic Inversion (NDI) and Neural Networks (NNs) (Honeywell & Lockheed Martin, 1996; Balas, 2003). Unfortunately, the FCS architecture, synthesis approach and software are considered confidential by some companies within the aerospace industry. Still, a significant trend towards the use of advanced multivariable techniques in industry is visible considering all publicly available information (Balas, 2003; Balas & Hodgkinson, 2009). Moreover, according to Balas and Hodgkinson (2009), NDI is currently the most applied multivariable control technique, especially in military applications.

The introduction of new multivariable control techniques led to FCSs with increased complexity. This increased complexity has a severe disadvantage regarding the clearance of flight control laws for certification (Fielding, Varga, Bennani, & Selier, 2002). The objective of the clearance process is to prove to authorities that the FCS functions adequately over the whole flight envelope considering all uncertain parameters and potential failure conditions. The increased complexity of flight control laws makes the clearance of these laws an increasingly lengthy and expensive process. Especially adaptive controllers using some form of system identification or online learning to optimize FCS are difficult to certify (Jacklin, 2008). The main reason of this difficulty is the absence of means with which the adaptive controllers can be certified. This issue is mainly caused by increased difficulty to define software performance requirements together with all derived requirements as well as to provide software verification plans, test cases and procedures and software life cycle data.

As mentioned above, NDI is currently the most applied multivariable control technique. The main advantages of NDI are that it avoids gain-scheduling and that NDI directly incorporates nonlinearities into the control laws (Enns et al., 1994). Moreover, the handling quality dependent part of an NDI FCS is isolated from the airframe/engine dependent part, such that the desired handling qualities can directly be enforced within the controller design process (Walker & Allen, 2002). As result, the use of NDI leads to reduced development cost and time, easier reuse across various airframes, greater ability to cope with changing models and improved performance at high angle-of-attack compared to classical control techniques. However, a drawback of NDI is that model mismatches and measurement errors reduce performance and can even result in unstable situations (Sieberling, Chu, & Mulder, 2010).

In light of all issues mentioned above, the development of Incremental Nonlinear Dynamic Inversion (INDI) was triggered. INDI is a variation onNDI retaining the advantages of NDI, while increasing controller robustness to model uncertainties and decreasing the controller dependency on the vehicle model. This reduced dependency on an exact mathematical model of the to-be-controlled system is beneficial for controller certification (Heise, Falconí, & Holzapfel, 2014). INDI shows promising results compared with NDI, however theory on INDI is still being developed. Additional research on INDI regarding time delays, (slow) actuator dynamics, sensor dynamics, controller frequency and discretization are required (Sieberling et al., 2010; Simplício, Pavel, van Kampen, & Chu, 2013; Smeur, Chu, & de Croon, 2016). Moreover, only two flight test with an INDI controller have been documented in literature (Smith & Berry, 2000; Smeur et al., 2016). The first test was merely a proof of concept flight test, at a time when most issues regarding INDI were not identified yet (Smith & Berry, 2000). The second test used a multirotor Micro Aerial Vehicle (MAV) to successfully show the advantages of INDI (Smeur et al., 2016).

Still, it is unknown whether the results obtained on a multirotor MAV successfully translate to design a FCS for aircraft in general. This requires additional research on typical aircraft characteristics such as additional time delays due to the use of data buses and measurement systems, slower actuator and sensor dynamics and a lower controller frequency. To investigate these characteristics, this thesis applies INDI to a model of the PH-LAB Cessna Citation, a CS-25 certified fixed-wing aircraft, co-owned by Delft University of Technology. Moreover, a flight test with INDI on the PH-LAB, which has a Fly-by-Wire (FBW) system with which experimental controllers can be tested, was initially part of the project plan. However, due to factors like funding and planning together with other MSc students, the flight test with the PH-LAB could not be executed within the time frame of this project. The research objective is to further develop the theory on INDI, particularly with regard to the implementation of INDI in a CS-25 certified fixed-wing aircraft. This project ultimately contributes to safer, cheaper FCSs with shorter development periods, straightforward certification and increased performance.

1-2 Research Objectives and Questions

The research objective presented in Section 1-1 is to further develop the theory on INDI, particularly with regard to the implementation of INDI in a CS-25 certified fixed-wing aircraft. This objective is realized by comparing the performance of an INDI controller in a perfect and realistic world on the PH-LAB Cessna Citation platform in a simulated environment. This utilizes the high fidelity simulation model of the PH-LAB available at Delft University of Technology. Furthermore, the performance of a Proportional-Integral-Derivative (PID) controller in a perfect and realistic world on the PH-LAB platform in a simulated environment is also compared. The PID controller is used to put the results obtained with the INDI controller into perspective.

As mentioned, a flight test with the PH-LAB was originally included within the project plan. Therefore, part of the project objective also included an investigation into the FBW system of the PH-LAB aircraft. To prevent any confounds, it is important to understand whether some PH-LAB specific issues and characteristics can lead to performance degradation of an INDI controller. Otherwise, this performance degradation might be wrongly connected to INDI controlled aircraft in general. Although the flight test was not executed during this project, it is still expected and recommended that the flight test is executed in the future. Therefore, the results presented within this report can be useful for all contributors to the flight test.

The research objective is used to phrase a main research question. This main question is subdivided into multiple sub-questions. The combination of the answers to all sub-questions will form the answer to the main questions. The main questions and sub-questions are formulated as follows:
Which measures are required to prevent performance degradation of an INDI controller when implemented in a CS-25 certified fixed-wing aircraft?

1. Which criteria and control modes are relevant for assessing the performance of an INDI controller?

2. Which phenomena should be included within a simulated environment to emulate reality?
3. Which of the selected phenomena cause performance degradation of an INDI controller within a simulated environment emulating reality?
4. Which measures are required to prevent any observed performance degradation?
5. Which measures are required to implement an INDI controller together with the FBW system of the PH-LAB Cessna Citation?

1-3 Report Outline

This report is split into three parts. Part I is a research paper, which concisely presents all results of the project. As such, Part I can be read as a standalone document.

Part II of the report contains all literature studies performed. Chapter 2 presents the basic theory and principles of INDI. This chapter includes the mathematical description of both NDI and INDI control. Moreover, the concepts of internal dynamics and time-scale separation are introduced. Chapter 3 reviews the state-of-the-art on FCSs, NDI and INDI, providing insight into the gap between science and industry at which the thesis is aimed. Chapter 4 discusses relevant criteria to assess controller performance in a simulation environment and reality. Chapter 5 shows all real-world phenomena that could potentially degrade the INDI controller performance. Finally, Chapter 6 presents measures suggested in literature to prevent any performance degradation observed in other research on INDI.

Part III of the report contains additional derivations and results. This part can be seen as an appendix to the research paper of Part I. Chapter 7 presents detailed derivations of Discrete Incremental Nonlinear Dynamic Inversion (DINDI) in support of Section II of the research paper. Chapter 8 presents the detailed analytical stability analysis in support of Section III of the research paper. Chapter 9 presents additional simulation results in support of Sections V and VI of the research paper. Chapter 10 investigates the PH-LAB aircraft characteristics based on a previous flight test in support of Section V of the research paper. Finally, Chapter 11 discusses PH-LAB specific issues related to flight testing an INDI controller. This chapter was not included in the paper as its main focus is to provide information for future contributors to a flight test with INDI on the PH-LAB aircraft. Finally, the report is completed by Chapter 12 presenting the conclusions and recommendations.

Part I

Research Paper

Stability and Robustness Analysis and Improvements for Incremental Nonlinear Dynamic Inversion Control

R. C. van 't Veld, E. van Kampen and Q. P. Chu

Delft University of Technology, Delft, Zuid-Holland, 2629 HS, the Netherlands

Incremental nonlinear dynamic inversion (INDI) is a variation on nonlinear dynamic inversion (NDI), retaining the high-performance characteristics, while reducing model dependency and increasing robustness. After a successful flight test with a multirotor micro aerial vehicle, the question arises whether this technique can be used to successfully design a flight control system for aircraft in general. This requires additional research on aircraft characteristics that could cause issues related to the stability and performance of the INDI controller. Typical characteristics are additional time delays due to data buses and measurement systems, slower actuator and sensor dynamics, and a lower control frequency. The main contributions of this article are 1) an analytical stability analysis showing that implementing discrete-time INDI with a sampling time smaller than 0.02s results in large stability margins regarding system characteristics and controller gains; 2) a simulation study showing significant performance degradation requiring controller adaptation due to actuator measurement bias, angular rate measurement noise, angular rate measurement delay and actuator measurement delay; and 3) the use of a real-time time delay identification algorithm based on latency to successfully synchronize the angular rate and actuator measurement delay together with pseudo control hedging (PCH) to prevent oscillatory behavior.

Nomenclature

A_x, A_y, A_z	Specific forces along body X/Y/Z axis, m/s^2
b, $\bar{c}$	Wing Span and Mean aerodynamic chord, m
C_l, C_m, C_n	Dimensionless Rolling, Pitching and Yawing moment coefficients
F, G	Linearized System and Control effectiveness matrix
g	Gravity constant, m/s^2
I	Inertia matrix, kg·m^2
K	Gain
k, N	Variable number
$\underline{M}$	Aerodynamic moment vector, Nm
m	Mass, kg
n_y	Normalized specific force along body Y axis, g
p, q, r	Roll, Pitch and Yaw rates around the body X/Y/Z axis, rad/s
$\hat{R}$	Average square difference function estimator
S	Wing area, m^2
s	Laplace variable
T, t	Sampling time and Time, s
u	Physical control input
u, v, w	Velocity components along body X/Y/Z axis, m/s
V	Velocity, m/s
x	State
z	Complex variable for z-transform
β, ϕ, θ	Sideslip, Roll and Pitch angle, rad
γ	Control effectiveness uncertainty ratio
δ	Control surface deflection, rad

ζ	Filter damping ratio
μ	Bias mean
ν	Virtual control input
ρ	Air density, kg/m^3
σ	Noise variance
τ	Variable number
Φ, Γ	Discrete System and Control effectiveness matrix
$\underline{\omega}$	Angular rate vector, rad
ω_n	Filter natural frequency, rad/s
Subscript	
a, e, r	Aileron, Elevator and Rudder
c, d, u, x	Commanded, Desired, Actuator, Control
h, rm	Hedge, Reference model
k	Discrete index
0	Current point in time

I. Introduction

Before the 1990s, the design of almost all flight control laws for aircraft was based on classical control techniques.[1,2] However, in recent years the use of advanced, multivariable control techniques has become the standard. Moreover, nonlinear dynamic inversion (NDI) has been the most popular technique of these advanced, multivariable techniques. The advantage of NDI over classical techniques is that NDI avoids gain-scheduling, directly incorporates nonlinearities into the control laws and isolates the handling quality dependent part of the control laws from the airframe/engine dependent part.[3,4]

These advantages ultimately result in improved performance and reduced development cost and time. Furthermore, NDI can be used to improve safety by avoiding aircraft accidents due to loss of control in flight.[5] This is important as two surveys from 1993 to 2007 and from 2006 to 2011 show that loss of control has consistently been an important cause of fatal accidents as well as fatalities.[6,7] Within the 2006 to 2011 period, loss of control in flight even was the most import cause of fatalities.

A drawback of NDI is that model mismatches and measurement errors reduce performance and can even result in unstable situations.[8] In light of these issues, the development of incremental nonlinear dynamic inversion (INDI) was triggered. INDI is a variation on NDI retaining the advantages of NDI, while decreasing the controller dependency on the vehicle model. As result, the controller robustness regarding model uncertainties and measurement errors is increased.[8] Moreover, these benefits are obtained by relatively simple means compared to, for example, the extension of NDI with neural networks.[9] Therefore, using INDI to design the flight control system (FCS) of an aircraft can also be beneficial regarding controller certification.[10]

INDI shows promising results compared with NDI in simulation studies applied to various aeronautical and space vehicles.[8,11,12] However, in practice INDI has only been flight tested twice. The first test was performed within the VAAC Harrier aircraft, but the test was merely a proof of concept at a time when INDI had not been thoroughly investigated yet.[13] Recently, INDI was successfully applied to a multirotor micro aerial vehicle (MAV) confirming the results obtained in simulations.[14]

Due to the successful application of INDI in a multirotor MAV, the question arises whether using INDI to design FCSs could contribute to safer, cheaper aircraft with shorter development periods, straightforward certification and increased performance. However, before a flight test is performed, additional research on aircraft characteristics that could cause issues related to the stability and performance of the INDI controller is required. Typical characteristics are additional time delays due to data buses and measurement systems, slower actuator and sensor dynamics, and a lower controller frequency.[8,12,14] To investigate these characteristics, this paper applies INDI to a model of the PH-LAB Cessna Citation, a CS-25 certified fixed-wing aircraft, co-owned by Delft University of Technology.

This paper presents three main contributions. First, the closed-loop system stability of a general linear system controlled by INDI is investigated as a sampled-data system, i.e. a system with a continuous-time plant and a discrete-time controller. As such, the effect of time delay, control gain, control effectiveness uncertainty and controller frequency on INDI stability is investigated. Second, the effect of real-world phenomena, e.g. sensor bias, noise and time delays, on an INDI controlled aircraft are investigated. Third, the paper provides solutions to prevent performance degradation of the INDI controlled system due to any of the investigated real-world phenomena significantly affecting controller performance.

The outline of the paper is as follows. Sec. II shows the derivation of discrete-time INDI compared to continuous-time INDI. Sec. III discusses the investigation of the stability of discrete-time INDI. Sec. IV describes the development of two attitude controllers, based on INDI and PID control. The effect of real-world phenomena on these controllers is investigated in Sec. V. Moreover, Sec. V also provides solutions to prevent performance degradation due to these phenomena based on literature. Additionally, Sec. VI presents a real-time time delay identification method essential to compensate for unsynchronized time delay. Finally, Sec. VII gives the conclusions and recommendations.

II. Incremental Nonlinear Dynamic Inversion

Originally, INDI was developed for continuous-time systems. However, INDI has to be developed as discrete-time controller to be able to investigate the closed-loop system as sampled-data system. The derivation of continuous-time INDI is reviewed to support the derivation of discrete-time INDI.

A. Continuous-time INDI

The continuous-time INDI derivation starts from a general nonlinear system, see Eq. (1).[8,12]

$$\dot{\underline{x}} = \underline{f}(\underline{x}, \underline{u}) \tag{1}$$

The system of Eq. (1) can be linearized about the current point in time indicated by the subscript '0', see Eq. (2). As such, the variables $\underline{x}_0$, $\dot{\underline{x}}_0$ and $\underline{u}_0$ are given by the latest available measurements, while the variables $\underline{x}$, $\dot{\underline{x}}$ and $\underline{u}$ are in the future. Note that the linearization is based on the assumptions of a small sampling time and instantaneous control effectors.

$$\begin{aligned} \dot{\underline{x}} &\approx \underline{f}(\underline{x}_0, \underline{u}_0) + \left.\frac{\partial \underline{f}(\underline{x}, \underline{u})}{\partial \underline{x}}\right|_{\underline{x}=\underline{x}_0, \underline{u}=\underline{u}_0} (\underline{x} - \underline{x}_0) + \left.\frac{\partial \underline{f}(\underline{x}, \underline{u})}{\partial \underline{u}}\right|_{\underline{x}=\underline{x}_0, \underline{u}=\underline{u}_0} (\underline{u} - \underline{u}_0) \\ \dot{\underline{x}} &\approx \dot{\underline{x}}_0 + F(\underline{x}_0, \underline{u}_0)(\underline{x} - \underline{x}_0) + G(\underline{x}_0, \underline{u}_0)(\underline{u} - \underline{u}_0) \end{aligned} \tag{2}$$

The time-scale separation principle is assumed to hold for Eq. (2). The change in control input, $\underline{u}$, is considered significantly faster than the change in system state, $\underline{x}$, based on the assumptions of small sampling time and instantaneous control effectors.[12] Thus, assuming $\underline{x} \approx \underline{x}_0$ while $\underline{u} \neq \underline{u}_0$. As a result $\underline{x} - \underline{x}_0 = 0$ is assumed, which can be used to simplify Eq. (2) to Eq. (3). Eq. (3) can be used to develop a control law by defining the virtual control input as $\underline{\nu} = \dot{\underline{x}}$. Concluding, the physical control input u can be computed using Eq. (4), the latest available measurements ($\dot{\underline{x}}_0$,$\underline{x}_0$,$\underline{u}_0$) and the virtual control input, $\underline{\nu}$. This virtual control input is to be designed. Moreover, the control effectiveness matrix, $G(\underline{x}_0, \underline{u}_0)$ of the system has to be known and invertible.

$$\dot{\underline{x}} = \dot{\underline{x}}_0 + G(\underline{x}_0, \underline{u}_0)(\underline{u} - \underline{u}_0) \tag{3}$$

$$\underline{u} = \underline{u}_0 + G^{-1}(\underline{x}_0, \underline{u}_0)(\underline{\nu} - \dot{\underline{x}}_0) \tag{4}$$

B. Discrete-time INDI

The start of the derivation of discrete-time INDI is equal to the continuous-time INDI derivation, including all assumptions, up to Eq. (3). Eq. (3) can be seen as the combination of two linear state-space systems, Eqs. (5) and (6), both with $F(\underline{x}_0, \underline{u}_0) = 0$.

$$\dot{\underline{x}} = F(\underline{x}_0, \underline{u}_0)\underline{x} + G(\underline{x}_0, \underline{u}_0)\underline{u} \tag{5}$$

$$\dot{\underline{x}}_0 = F(\underline{x}_0, \underline{u}_0)\underline{x}_0 + G(\underline{x}_0, \underline{u}_0)\underline{u}_0 \tag{6}$$

The discrete counterpart of such a linear state-space systems is known, Eq. (7).[15] Considering that $F(\underline{x}_0, \underline{u}_0) = 0$, Eq. (7) can be simplified to Eq. (8).

$$\begin{gathered} \underline{x}_{k+1} = \Phi(\underline{x}_0, \underline{u}_0)\underline{x}_k + \Gamma(\underline{x}_0, \underline{u}_0)\underline{u}_k \\ \Phi = I + \Delta t F + \frac{\Delta t^2}{2!}F^2 + \frac{\Delta t^3}{3!}F^3 + \cdots \qquad \Gamma = \Delta t G + \frac{\Delta t^2}{2!}FG + \frac{\Delta t^3}{3!}F^2 G + \cdots \end{gathered} \tag{7}$$

$$\frac{\underline{x}_{k+1} - \underline{x}_k}{\Delta t} = G(\underline{x}_0, \underline{u}_0)\underline{u}_k \tag{8}$$

Using Eq. (8) to discretize both Eqs. (5) and (6) and combining these as in Eq. (3) results in Eq. (9). Eq. (9) is rewritten by defining $\underline{x}_{0_k} = \underline{x}_{k-1}$ and $\underline{u}_{0_k} = \underline{u}_{k-1}$ to obtain Eq. (10), based on the definition of the '0' subscript in continuous-time. These definitions imply that the variables with the 'k-1' subscript are given by the latest available measurements.

$$\frac{\underline{x}_{k+1} - \underline{x}_k}{\Delta t} = \frac{\underline{x}_{0_{k+1}} - \underline{x}_{0_k}}{\Delta t} + G(\underline{x}_{0_k}, \underline{u}_{0_k})(\underline{u}_k - \underline{u}_{0_k}) \tag{9}$$

$$\frac{\underline{x}_{k+1} - \underline{x}_k}{\Delta t} = \frac{\underline{x}_k - \underline{x}_{k-1}}{\Delta t} + G(\underline{x}_{k-1}, \underline{u}_{k-1})(\underline{u}_k - \underline{u}_{k-1}) \tag{10}$$

Eq. (10) can be inverted to obtain the discrete-time INDI control law, Eq. (11). However, the direct inversion of Eq. (10) would require the future state $\underline{x}_k$ to be known. To obtain a usable control law, the term $\frac{\underline{x}_k - \underline{x}_{k-1}}{\Delta t}$ is considered to represent the forward difference approximation of $\underline{\dot{x}}_{k-1}$ and can be replaced by the backward difference approximation $\frac{\underline{x}_{k-1} - \underline{x}_{k-2}}{\Delta t}$.

$$\underline{u}_k = \underline{u}_{k-1} + G^{-1}(\underline{x}_{k-1}, \underline{u}_{k-1}) \left(\underline{\nu}_k - \frac{\underline{x}_{k-1} - \underline{x}_{k-2}}{\Delta t} \right) \tag{11}$$

$$\underline{\nu}_k = \frac{\underline{x}_{k+1} - \underline{x}_k}{\Delta t} \tag{12}$$

Concluding the physical control input u_k can be computed using Eq. (11), the latest available measurements ($\underline{x}_{k-1}$,$\underline{u}_{k-1}$), the previous measurements, $\underline{x}_{k-2}$, and the virtual control input, $\underline{\nu}_k$. This discrete-time virtual control input is again to be designed, similar to continuous-time INDI. Moreover, the control effectiveness matrix, $G(\underline{x}_{k-1}, \underline{u}_{k-1})$ of the system has to be known and invertible.

III. Analytical Stability

The stability of the theoretically developed INDI control law of Eq. (11) is analyzed for a general mathematical system with actuator dynamics, see Fig. 1. To keep the analysis clear, only a single-input single-output first-order linear system is used, Eq. (13), together with a first-order actuator, Eq. (14). Moreover, the virtual control input is designed based on a simple P-controller with gain K_x, Eq. (15). First, the effect of the mathematical system characteristics in combination with the controller sampling time are analyzed for the baseline system. Afterwards, the effect of variations based on time delay and control effectiveness uncertainty on the closed-loop stability are presented.

$$\dot{x} = Fx + Gu \tag{13}$$

$$\dot{u} = K_u(u_c - u) \tag{14}$$

$$\nu_k = K_x(x_{d_k} - x_{k-1}) \tag{15}$$

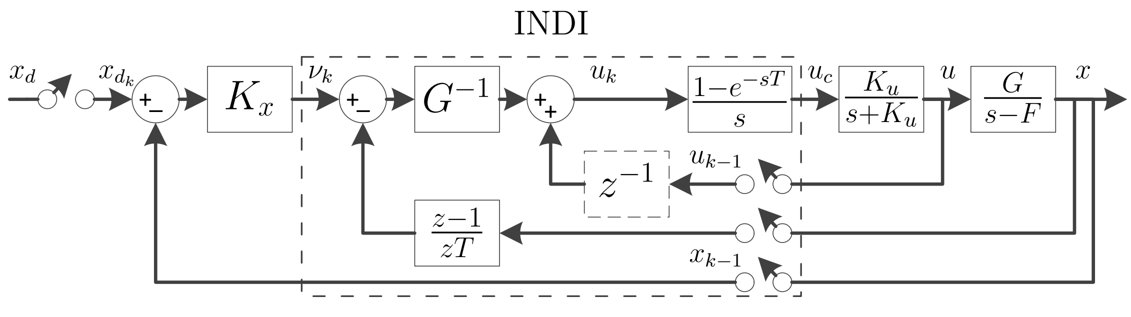

Figure 1: Sampled-data system with discrete-time INDI controller and continuous-time linear system

A. Analysis Method

The closed-loop system of Fig. 1 contains both continuous- and discrete-time components as well as samplers and a zero-order hold block, $\frac{1-e^{-sT}}{s}$, converting continuous signals into discrete signals and vice verse. The discrete equivalent of the sampled-data system has to be found to analyze the system. This discrete equivalent is found by adding phantom samplers and rearranging the block diagram, such that there are samplers in front and behind all continuous (series of) transfer function(s). The combination of the two samplers with the continuous (series of) transfer function(s) can then be converted to a discrete transfer function via tables combining z- and s-transforms.[16]

The discrete-time system can be reduced to a single transfer function. The characteristic polynomial of this transfer function can then be used for the stability analysis. Note that the system is asymptotically stable if and only if all roots of the characteristic polynomial have a magnitude smaller than one. To avoid having to solve all the roots of the characteristic polynomial, Jury's stability criterion is used to check the system's stability based on a tabular method.[17]

B. Baseline System

First, the stability of a baseline system without time delays or control effectiveness uncertainties is investigated. The baseline closed-loop system used is the system depicted in Fig. 1 with the dashed unit delay block not included. The stable regions of the baseline INDI controller are given in Fig. 2. The constant values, $F = 2$, $K_u = 13$ and $K_x = 7$, used throughout the figures were selected to obtain stability regions typical for the PH-LAB Cessna Citation model. Note that the closed-loop stability is independent of the control effectiveness matrix when uncertainties are not considered.

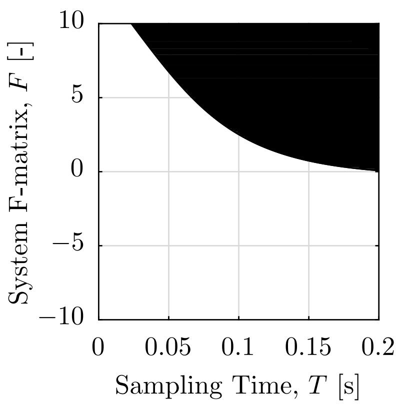

(a) $K_u = 13$, $K_x = 7$

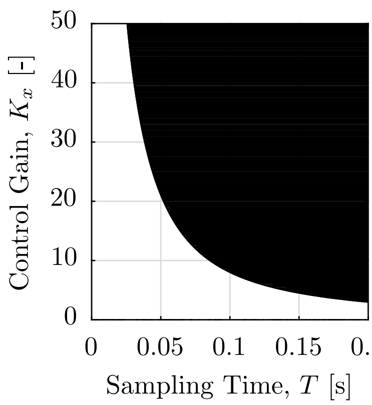

(b) $F = 2$, $K_u = 13$

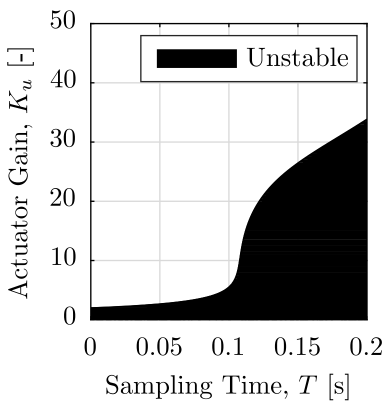

(c) $F = 2$, $K_x = 7$

Figure 2: Stability for baseline INDI controller

In general, logical trends can be observed regarding the stability of the baseline INDI controller. Fig. 2a shows that systems implemented with smaller sampling time can control systems with less natural stability, i.e. a higher F-matrix value. Similarly, Figs. 2b and 2c show that the same conclusion can be drawn for more aggressive control laws, i.e. a higher control gain, and slower actuators, i.e. a lower actuator gain.

Another observation based on Fig. 2 is that the system is stable for sampling times smaller than 0.02s in all three figures. The only exception is a system with small actuator gains, however this instability is not a result of any discrete effects as the same unstable region appears when analyzing a continuous-time controller. Unfortunately, nonlinear effects like control saturation and system nonlinearities are not included within the analysis. Moreover, the effect of multiple inputs, multiple outputs, multirate feedback signals and multiloop controllers can be added to the analysis to increase the accuracy of the results. Therefore, it is difficult to set a maximum sampling time, which would ensure system stability when using a discrete-time INDI controller. Still, a sampling time smaller than 0.02s seems to provide a large stable region regarding variation in F, K_u and K_x when considering the typical values of the PH-LAB Cessna Citation.

C. Measurement Time Delay

The stability of INDI controllers subjected to measurement time delay is an issue for INDI controllers.[8,14] Especially, when the actuator measurements, u_{k-1} and the state derivative measurement, the $\frac{z-1}{zT}$ block, are not equally delayed. Moreover, there is a disagreement whether or not the unit delay of the actuator measurement, u_{k-1}, indicated by the dashed unit delay block in Fig. 1, has to be included[12,14] or not.[11,18] Therefore, four different systems are investigated: 1) a baseline system, Fig. 2c; 2) a system with a unit delay on the state derivative measurement Fig. 3a; 3) a system with a unit delay on the actuator measurement, Fig. 3b; and 4) a system with a unit delay on both actuator and state derivative measurements, Fig. 3c.

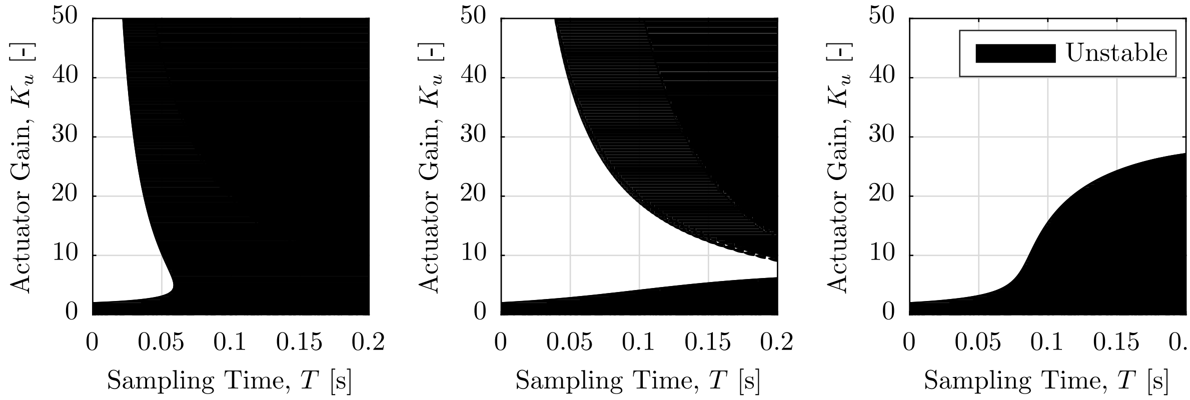

(a) State derivative (b) Actuator (c) Actuator and state derivative

Figure 3: Stability with unit delays on actuator measurements and/or state derivative: $F = 2$, $K_x = 7$

Clearly, the baseline system and the system with both the actuator and state derivative measurements delayed have the largest stable region compared with the systems with either the actuator or state derivative measurements delayed. This shows the importance of delaying both measurement signals equally. Moreover, it shows that when the combination of discrete-time controller and continuous-time system is used, the unit delay of the actuator measurements degrades system stability and should not be included in the controller.

Furthermore, comparing Figs. 2c and 3c shows that the INDI controller can handle some overall time delay within the system. Additionally, there is a significant difference between the tolerance to state derivative delay and actuator delay in Figs. 3a and 3b. This difference is attributed to the fact that the state derivative signal is used via negative feedback, while the actuator measurements are used via positive feedback. Delaying a negative feedback signal results in magnified control inputs, resulting in relatively fast system instability. On the other hand, delaying a positive feedback signal results in damped control inputs, resulting in relatively slow system instability. This effect is also seen in the results of Sec. VI.

D. Control Effectiveness Uncertainties

The stability of INDI controllers subjected to model uncertainties should not be an issue for INDI controllers.[8,14] The results of this section are independent of uncertainties in the system matrix, however control effectiveness uncertainties can still affect the controller. The effect of control effectiveness uncertainties is seen in Fig. 4. The uncertainties have been implemented into the system of Fig. 1 by substituting $(G + \Delta G)^{-1}$ for G^{-1}, the uncertainty ratio used is defined by Eq. (16).

$$\gamma = \frac{G}{G + \Delta G} \tag{16}$$

Fig. 4 shows that the INDI controller remains stable over a large range of control effectiveness uncertainty, given that the controller runs at a sampling time smaller than the aforementioned 0.02s. This conclusion is supported by similar observations made in literature.[12,14] Furthermore, note that the system instability for low and negative values of γ is not the result of any discrete effects and also appears when analyzing a continuous-time closed-loop system.

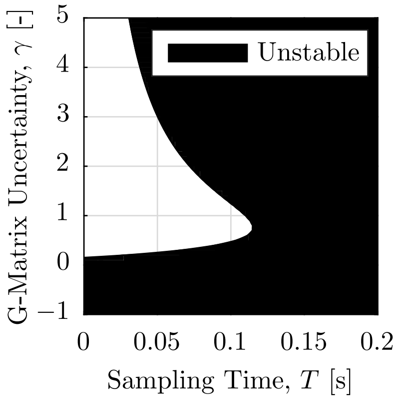

Figure 4: Stability with control effectiveness uncertainty: $F = 2$, $K_u = 13$, $K_x = 7$

IV. Attitude Controller

Two attitude controllers are developed to investigate the effect of real-world phenomena on an INDI controlled aircraft. One controller is based on discrete-time INDI and the other controller is based on PID control. The PID controller is used to put the results obtained with the INDI controller into perspective, see Sec. V. The INDI attitude controller is based on a cascaded design with an angular rate inner loop and attitude outer loop.

A. Angular Rate Inner Loop

The angular rate inner loop is based on Euler's equations of motion, Eq. (17), which is similar in form to Eq. (1). To obtain the discrete-time control law of Eq. (11), the G-matrix is obtained based on Eq. (17), see Eq. (18).[8] Therefore, the angular rate controller is given by Eqs. (19) and (20). Note that the developed inner loop neglects the actuator dynamics of the system and assumes instantaneous control effectors.

$$\dot{\underline{\omega}} = I^{-1}\underline{M} - I^{-1}(\underline{\omega} \times I\underline{\omega}) \tag{17}$$

$$G(\underline{x}_{k-1}, \underline{u}_{k-1}) = I^{-1}\frac{1}{2}\rho V^2 S \begin{bmatrix} bC_{l_{\delta_a}} & 0 & bC_{l_{\delta_r}} \\ 0 & \bar{c}C_{m_{\delta_e}} & 0 \\ bC_{n_{\delta_a}} & 0 & bC_{n_{\delta_r}} \end{bmatrix} \tag{18}$$

$$\underline{u}_k = \underline{u}_{k-1} + \frac{2I}{\rho V^2 S} \begin{bmatrix} bC_{l_{\delta_a}} & 0 & bC_{l_{\delta_r}} \\ 0 & \bar{c}C_{m_{\delta_e}} & 0 \\ bC_{n_{\delta_a}} & 0 & bC_{n_{\delta_r}} \end{bmatrix}^{-1} \left(\underline{\nu}_k - \frac{\underline{\omega}_{k-1} - \underline{\omega}_{k-2}}{\Delta t} \right) \tag{19}$$

$$\underline{\nu} = \begin{bmatrix} \nu_p \\ \nu_q \\ \nu_r \end{bmatrix}; \quad \underline{\omega} = \begin{bmatrix} p \\ q \\ r \end{bmatrix}; \quad \underline{u} = \begin{bmatrix} \delta_a \\ \delta_e \\ \delta_r \end{bmatrix} \tag{20}$$

Similar to Eq. (15) in Sec. III, the virtual control input is designed based on the tracking error. However, the angular rate inner loop uses PI-control instead of just P-control, because the integral controller can compensate for potential bias in the actuator measurements, as further explained in Sec. V. The overall control structure and tuning is presented in Sec. IV.D.

B. Attitude Outer Loop

The attitude outer loop consist of the control of the roll, pitch and sideslip angles. The sideslip angle is preferred above the yaw angle, as a controller aimed at keeping the sideslip angle at zero results in coordinated flight. The principle of time-scale separation is used to develop the roll and pitch angle outer loop around the angular rate inner loop. The slow outer loop is defined such that the output is used as input of the faster inner-loop. As such, the dynamics of the inner-loop are neglected and the angular rates are assumed to be equal to the commanded values. The relation between attitude angles and angular rates is based on a kinematic equation independent of aircraft characteristics, see Eq. (21). Therefore, this loop is based on the standard NDI technique instead of INDI.

$$\begin{bmatrix} \dot{\phi} \\ \dot{\theta} \end{bmatrix} = \begin{bmatrix} 1 & \sin\phi\tan\theta & \cos\phi \\ 0 & \cos\phi & -\sin\phi\tan\theta \end{bmatrix} \begin{bmatrix} p \\ q \\ r \end{bmatrix} \tag{21}$$

To obtain the NDI outer loop Eq. (21) is inverted. Moreover, the attitude rates, $\dot{\phi}$ and $\dot{\theta}$, are replaced by the virtual control inputs ν_ϕ and ν_θ respectively. Similar to INDI these virtual control inputs are designed based on tracking error, but for this loop only P-control is used. The r_c is based on the separate sideslip outer loop designed next and as discussed before, the p_c and q_c are used as inputs for the inner loop. The roll and pitch outer loop is given by Eq. (22).

$$\begin{bmatrix} p_c \\ q_c \end{bmatrix} = \begin{bmatrix} 1 & \sin\phi\tan\theta \\ 0 & \cos\phi \end{bmatrix}^{-1} \left\{ \begin{bmatrix} \nu_\phi \\ \nu_\theta \end{bmatrix} - \begin{bmatrix} \cos\phi\tan\theta \\ -\sin\phi \end{bmatrix} r_c \right\} \tag{22}$$

The control law used for the sideslip outer-loop is given by Eq. (23), which is equivalent to the control law used by Miller.[19] Mathematically, the sideslip outer loop can be developed similar to the roll and pitch outer loop.[20] However, the PH-LAB Cessna Citation does not have accurate, fast sensors measuring the required body velocities (u, v, w) and sideslip angle itself. Therefore, the sideslip controller cannot be based on Eq. (24) and several assumptions are made such that Eq. (23) is obtained. The coordinated flight is the main purpose of the sideslip outer-loop, therefore the sideslip angle, β, and its derivative, $\dot{\beta}$, are assumed zero and consequently $v = 0$. Moreover, it is assumed that the effect of the wp term is negligible. The overall control structure and tuning is presented in Sec. IV.D.

$$r_d = \frac{g}{V}(n_y + \sin\phi\cos\theta) \tag{23}$$

$$\dot{\beta} = \frac{1}{\sqrt{u^2+w^2}} \left(\frac{-uv}{V^2}(A_x - g\sin\theta) + \left(1 - \frac{v}{V^2}\right)(A_y + g\sin\phi\cos\theta) - \frac{vw}{V^2}(A_z + g\cos\phi\cos\theta) + wp - ur \right) \tag{24}$$

C. Pseudo Control Hedging

An important concern for NDI and INDI based controllers is the violation of the assumptions made regarding instantaneous actuator and inner loop dynamics.[12,21] These dynamics are not actually instantaneous and actuators also have position and rate limits introducing control saturation into the closed-loop system. Unfortunately, no solutions were found in literature that completely eliminate the performance degradation that can arise from breaking these assumptions.

Pseudo control hedging (PCH) is used by several authors to at least alleviate the performance degradation issues due to control saturation.[12,21] PCH reduces the magnitude of the commanded signals to a level achievable by the saturated controller.[22] PCH has two potential benefits for the controller developed in this paper. First, PCH can act as an anti-windup technique for the PI-controller used to compute the virtual control input of the inner loop.[21] Second, as explained next PCH adds an additional tunable variable to the system, which can be used to tune the influence of various feedback signals on controller performance, see Sec. VI. Therefore, PCH is selected to complement the developed angular rate inner loop.

PCH consist of a first-order reference model (RM), which imposes the desired dynamics on the output, Eqs. (25) and (26). Moreover, the RM can provide the derivative of the command signal, $\underline{\nu}_{rm}$ which is used as feedforward control term. The RM is adjusted to an achievable level by the command hedge $\underline{\nu}_h$, Eq. (27). However, since $\underline{u}_k$ is not known the command hedge is computed for the previous time step, see Eq. (28). Note that the command hedge can also be computed internally using the desired control input in combination with an actuator model, instead of measuring $\underline{u}_{k-1}$.[21]

$$\underline{\nu}_{rm} = K_{rm}(\underline{\omega}_c - \underline{\omega}_{rm}) \tag{25}$$

$$\underline{\omega}_{rm} = \frac{1}{s}(\underline{\nu}_{rm} - \underline{\nu}_h) \tag{26}$$

$$\begin{aligned}
\underline{\nu}_h &= \underline{\nu}_c - \underline{\nu} \\
\underline{\nu}_h &= \left[\frac{\underline{x}_{k-1} - \underline{x}_{k-2}}{\Delta t} + G(\underline{x}_{k-1}, \underline{u}_{k-1})(\underline{u}_{c_k} - \underline{u}_{k-1})\right] - \left[\frac{\underline{x}_{k-1} - \underline{x}_{k-2}}{\Delta t} + G(\underline{x}_{k-1}, \underline{u}_{k-1})(\underline{u}_k - \underline{u}_{k-1})\right] \\
\underline{\nu}_h &= G(\underline{x}_{k-1}, \underline{u}_{k-1})(\underline{u}_{c_k} - \underline{u}_k)
\end{aligned} \tag{27}$$

$$\underline{\nu}_h = I^{-1}\frac{1}{2}\rho V^2 S \begin{bmatrix} bC_{l_{\delta_a}} & 0 & bC_{l_{\delta_r}} \\ 0 & \bar{c}C_{m_{\delta_e}} & 0 \\ bC_{n_{\delta_a}} & 0 & bC_{n_{\delta_r}} \end{bmatrix} (\underline{u}_{c_{k-1}} - \underline{u}_{k-1}) \tag{28}$$

Due to the use of the RM, each INDI loop has an additional tunable variable. The K_{rm} imposes the general desired dynamics on the system, while the linear controller used within the original INDI loop can be used to further adapt some fine dynamics and characteristics of the system. The overall controller structure combining the angular rate inner loop with PCH and the attitude outer loop is presented in Fig. 5. As discussed, the linear controllers (LCs) used to design the virtual control inputs are based on PID-control.

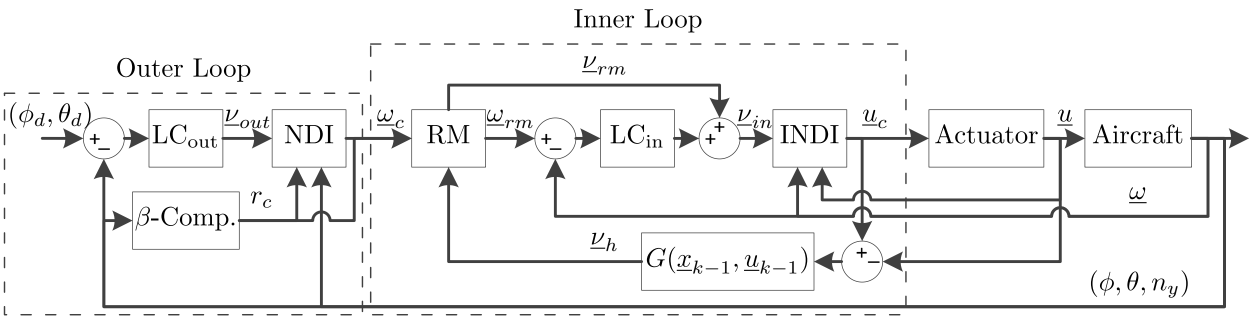

Figure 5: Attitude controller structure based on NDI, INDI and PCH

D. Controller Tuning and PID Controller

The control gains used to tune the developed controller depicted in Fig. 5 are lised in Table 1. Note that initially, the inner loop LC was based on PI-control, while the inner loop RM used P-control. However, as discussed in Sec. V this solution did not perform as expected and a solution using an inner loop based on P-control for the LC and PI-control for the RM was adopted. Furthermore, the controller without PCH used in Sec. VI uses the RM gains as LC gains as this controller does not have a RM.

Table 1: PID and INDI control gains

Channel	PID				INDI			
	Inner		Outer		Inner			Outer
	K_P	K_I	K_P	K_D	$K_{P_{in}}$	$K_{P_{rm}}$	$K_{I_{rm}}$	$K_{P_{out}}$
Roll, p-ϕ	-0.4	-0.75	1.5	0	20	7	1.4	1.5
Pitch, q-θ	-0.4	-1.0	1.5	0	20	6	1.2	1.5
Yaw, r-n_y	-0.4	-0.75	-1.0	-0.3	20	7	1.4	n.a.

A controller based on PID control is developed, besides the INDI controller, to support the investigation on the effect of real-world phenomena on the INDI controller, see Sec. V. The inner loop of the PID controller controls the angular rates (p, q, r), just like the INDI controller. The outer loop of the PID controller controls the attitude angles (ϕ, θ) together with the lateral acceleration (n_y). The lateral acceleration is used to minimize the sideslip angle. Similar to INDI, the sideslip angle itself cannot be used as the PH-LAB Cessna Citation does not have accurate, fast sensors measuring the sideslip angle or body velocities. The PID controller combines an PI-control inner loop with a PD-control outer loop, see Table 1.

V. Effect of Real-World Phenomena on INDI Controlled Aircraft

Before a flight test with an INDI controlled aircraft is performed in future research as follow up on the flight test with INDI in a multirotor MAV, the effect of real-world phenomena on an INDI controlled aircraft are investigated. For this investigation, the controller developed in the previous section is implemented together with the PH-LAB Cessna Citation model.

A. Real-World Phenomena to be Investigated

The two previous flight tests with INDI provide an indication which real-world phenomena are most important to investigate. However, as only two flight tests have been performed, also flight tests with NDI controllers are used within this section.

First, bias, defined as all constant disturbances, is considered. Bias can be introduced into the system as input to the airframe, e.g. wind, and as addition to measured feedback signals. Both NDI and INDI have shown to reject bias as input to the airframe during flight tests.[14,20] However, other flight test have shown that NDI performance can degrade due to severe winds and erroneous measurements.[23,24] Therefore, bias is included as phenomenon that should be investigated.

Second, the topic of discretization is considered. The effect of controller frequency is included in the investigation to confirm the theoretical findings of Sec. III. Other discretization effects can be found in feedback signals through sampling and quantization. The effect of feedback signal sampling times is investigated to complement the investigation on controller frequency. Feedback signal quantization is mentioned as an issue in two flight tests with NDI, however both studies had relatively limited computation resources compared to today's standards.[24,25] Therefore, quantization is not expected to become in issue in any future flight test and quantization will not be investigated.

Third, the effect of model mismatches is considered. The outstanding robustness of INDI with respect to model mismatches was already shown on an MAV.[14] Additionally, almost every simulation study available on the topic of INDI has shown the robustness of INDI. As such, the inclusion of model mismatches is deemed superfluous. Especially, since Sec. III also showed that INDI remains stable over a large range of control effectiveness uncertainty.

Fourth, noise, defined as all random disturbances, will be included in the simulation. Analogous to bias, noise appears as input to the airframe as well as in feedback signals. Flight test have shown that NDI performance can degrade due to severe turbulence and erroneous measurements.[23,24] Moreover, noise within feedback systems is reported for both NDI and INDI to potentially degrade controller performance.[13,20]

Fifth, it is also important to include time delays, as already indicated in Sec. III. This is also confirmed in literature as time delay, for example, caused system instability through a pilot induced oscillation.[4]

The magnitude of all real-world phenomena used in this section is based on previous flight test data with the PH-LAB Cessna Citation, see Table 2. The bias acting on the feedback signals is based on the mean of the disturbances, while the noise acting on the signals is based on the variances of the disturbances. Moreover, a constant wind is implemented as bias with a total velocity of 25 m/s split across all three axes. Additionally, atmospheric turbulence is implemented as noise using the Dryden model with $\sigma = 1\text{m}^2/\text{s}^2$ and $L_g = 150\text{m}$.[15]

Table 2: PH-LAB Cessna Citation real-world phenomena characteristics

	Bias [μ]	Noise [σ^2]	Delay [s]	Sampling Time [s]
p, q, r [rad/s]	$3 \cdot 10^{-5}$	$4 \cdot 10^{-7}$	0.128	0.0192
V [m/s]	2.5	$8.5 \cdot 10^{-4}$	0.1	0.0625
δ_a, δ_e, δ_r [rad]	$4.5 \cdot 10^{-3}$	$5.5 \cdot 10^{-7}$	0.0397	0.01
ϕ, θ [rad]	$4 \cdot 10^{-3}$	$1 \cdot 10^{-9}$	0.128	0.0192
n_y [g]	$2.5 \cdot 10^{-3}$	$1.5 \cdot 10^{-5}$	0.128	0.0192

B. Results

The effect of the real-world phenomena on the controller performance is investigated using 40 second simulation runs. Each run includes four consecutive 3211 maneuvers on the roll and pitch angles starting at an altitude of 6000 m and a velocity of 100 m/s. Both PID and INDI controllers run at 100 Hz, while the PH-LAB model is simulated using variable sampling time to emulate continuous-time. Previous flight test with the PH-LAB aircraft also ran experimental controllers at 100 Hz and according to the results of Sec. III this should result in a stable closed-loop system.

The controller performance is assessed using the sum of the root mean square (RMS) tracking errors of the outer loop control variables (ϕ, θ, β). Tables 3 and 4 show the RMS tracking error for the PID and INDI controllers respectively. The tables show the effect of the real-world phenomena on each signal separately and combined. Note that the PID controller does not use the velocity and control surface deflections measurements as feedback signals. The tables also show a baseline run without real-world phenomena running at 50 and 100 Hz. Furthermore, the total effect of all real-world phenomena combined is presented. As the constant wind has a significant effect on this number hiding the stability issues of INDI, also the total effect without wind is given.

Table 3: RMS tracking error PID

	Bias	Noise	Delay	Sampling	Baseline (100Hz)
Combined	0.2294	0.1915	0.1749	0.1891	0.1902
p, q, r	0.1902	***0.1902***	***0.1758***	0.189	Baseline (50Hz)
V	n.a.	n.a.	n.a.	n.a.	0.1895
δ_a, δ_e, δ_r	n.a.	n.a.	n.a.	n.a.	Total
ϕ, θ	0.1901	0.1902	0.1921	0.1903	0.4265
n_y	0.2032	0.1902	0.1906	0.1902	Total (-wind)
Wind/Turb.	***0.2428***	0.1913	n.a.	n.a.	***0.1928***

Table 4: RMS tracking error INDI

	Bias	Noise	Delay	Sampling	Baseline (100Hz)
Combined	0.2665	0.1895	0.2083	0.1892	0.1891
p, q, r	0.1891	***0.1891***	***0.2068***	0.1891	Baseline (50Hz)
V	0.1894	0.1891	0.1891	0.1891	0.1888
δ_a, δ_e, δ_r	***0.2129***	0.1891	***0.1914***	0.1891	Total
ϕ, θ	0.1903	0.1891	0.1909	0.1892	0.2604
n_y	0.1897	0.1891	0.1891	0.1891	Total (-wind)
Wind/Turb.	***0.2554***	0.1895	n.a.	n.a.	***0.2396***

Table 5: RMS tracking error INDI+

	Bias	Noise	Delay	Sampling	Baseline (100Hz)
Combined	0.2585	0.1914	0.1825	0.1895	0.191
p, q, r	0.191	***0.191***	***0.1811***	0.1894	Baseline (50Hz)
V	0.1916	0.191	0.191	0.191	0.1909
δ_a, δ_e, δ_r	***0.1929***	0.191	***0.1933***	0.191	Total
ϕ, θ	0.1924	0.191	0.193	0.1911	0.2479
n_y	0.1917	0.191	0.1911	0.191	Total (-wind)
Wind/Turb.	***0.2573***	0.1914	n.a.	n.a.	***0.1846***

Comparing Table 3, Table 4 and output response observations, five simulation runs show significant performance degradation caused by actuator measurement bias, wind bias, angular rate measurement noise, angular rate measurement delay and actuator measurement delay. Sec. V.C discusses solutions to prevent performance degradation due to these phenomena. As seen in Table 5 and Fig. 6f, the performance of INDI significantly improves when these solutions are implemented, referred to as INDI+. Fig. 6 shows the difference in pitch angle response between the INDI and INDI+ controllers for all phenomena causing performance degradation.

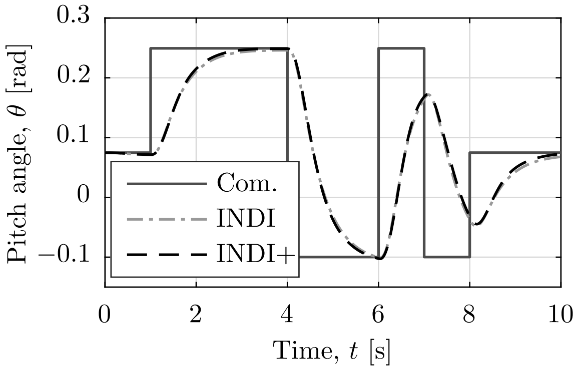

(a) Actuator bias

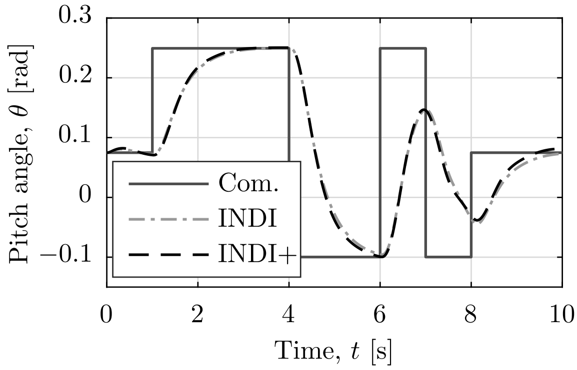

(b) Wind bias

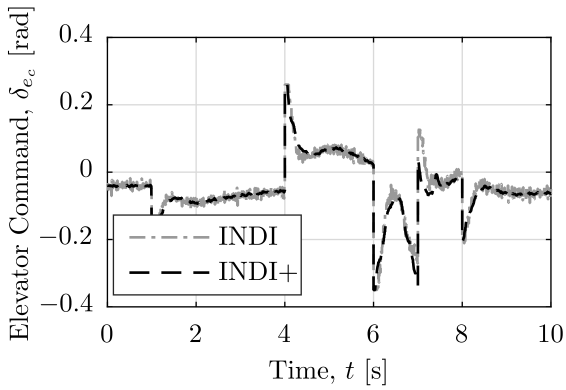

(c) Angular rate noise

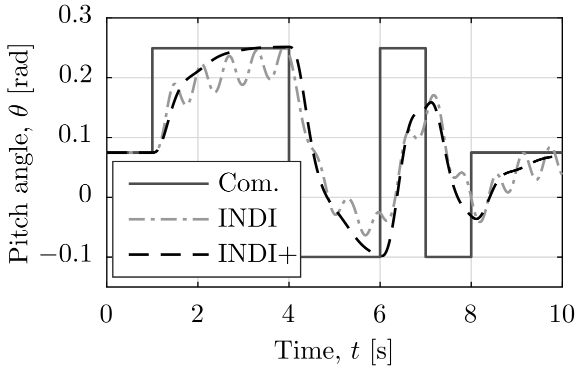

(d) Angular rate delay

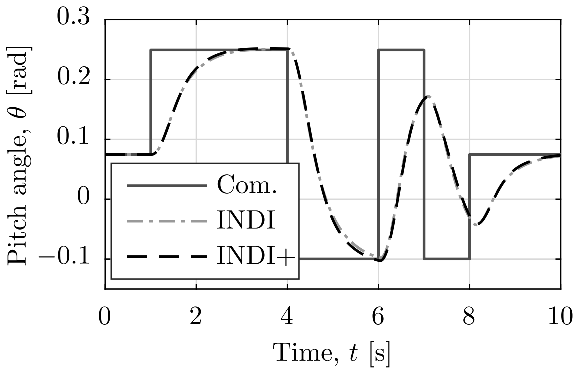

(e) Actuator delay

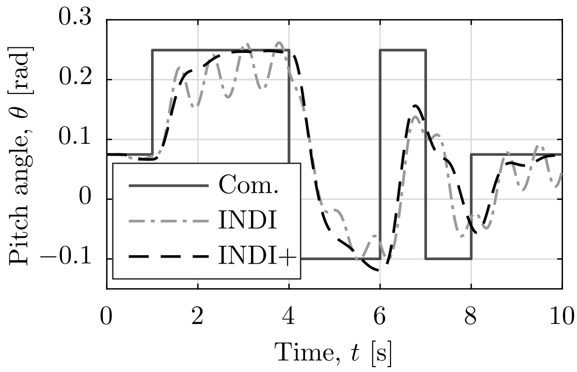

(f) Total excluding constant wind

Figure 6: Pitch response subjected to selected phenomena for INDI with and without solutions

C. Solutions for Performance Degradation

The baseline INDI attitude controller developed in Sec. IV has to be adapted to solve the issues related to real-world phenomena and improve performance. A requirement imposed on the adaptations proposed in this paper is that no additional model dependencies should be added to the controller to avoid losing one of the main benefits of INDI control. First, Fig. 6a shows that a bias on the actuator position measurements causes a steady-state error within the closed-loop response. Initially, a combination of PI-control to design the virtual control input with PCH as anti-windup technique was used to solve the steady-state error. However, when PCH is used based on the latest available actuator measurement, the PCH RM also adapts to the bias in these measurements such that the steady-state error remains.

Two options can be implemented that do eliminate the steady-state error: PCH could be implemented based on an actuator model instead of actuator measurements or the PCH RM could be based on PI-control. The first option has the benefit of having an anti-windup for the integrator element at the expense of additional model dependency within the controller. The second option does not require the actuator model, but also loses the anti-windup benefit. As discussed, the lack of model dependencies, one of the main benefits of INDI control, is considered more important and therefore the second option is selected. Still, Sec. VI shows that PCH is a valuable addition even when the anti-windup benefit is lost.

Second, Fig. 6b shows that the INDI controller has to adapt to the constant wind conditions increasing the RMS tracking error. Fortunately, as expected from literature, the constant wind does not cause a steady-state error as the bias is eventually rejected by the INDI controller.[14] Therefore, no solution is required for this phenomenon.

Third, Fig. 6c shows that differentiation amplifies the noise on the control input signals and signals used for identification in Sec. VI. Implementing a second-order filter, see Eq. (29), on the angular rate measurements can be used to reduce the noise on these signals.[14,26] Using Tustin's transformation, the continuous-time filter of Eq. (29) is converted into the discrete-time equivalent. Adequate filter performance was obtained using $\omega_n = 40$ rad/s and $\zeta = 0.6$.

$$H(s) = \frac{\omega_n^2}{s^2 + 2\zeta\omega_n s + \omega_n^2} \tag{29}$$

Finally, Fig. 6d shows that unsynchronized delays between the actuator and angular rate measurements cause oscillatory behavior. Note that Fig. 6e does not show this behavior as the actuator measurement delay of the PH-LAB is significantly smaller than the angular rate measurement delay, see Table 2. To improve system performance the two signals should be synchronized. This synchronization can partially be performed by filtering the actuator measurements with the exact same filter dynamics as the angular rates, since filters also introduce lag into a system.[14] Moreover, either the actuator or the angular rate measurements can be delayed with a multiple of the controller frequency, such that the delay originating from using different type of sensors and data buses can be eliminated. This does require successful identification of the difference in delay between the two feedback signals, an issue which is discussed in detail in Sec. VI.

VI. Unsynchronized Time Delay

The previous section identified that unsynchronized delays between the actuator and angular rate measurements cause oscillatory behavior. Therefore, successful identification of the difference in delay between the two feedback signals is vital for adequate INDI controller performance. The identified difference can then be added to the appropriate signal to synchronize the time delay.

A. Performance Degradation

First, the performance degradation characteristics due to unsynchronized time delay are investigated. Fig. 7 shows the RMS tracking error as function of both actuator and angular rate delay for an INDI controller with PCH and affected by real-world phenomena. As expected based on the results of Sec. III and Sec. V the best performance is obtained when both delays are about equal. Still, Fig. 7 also shows that a small mismatch between both delays is acceptable. Additionally, with the current controller gains a delay of about 220 ms in both signals results in overall controller degradation. This is 100 ms above the delay of 130 ms identified from PH-LAB flight test data. Furthermore, it can be seen that the controller performance is less sensitive to actuator delay than angular rate delay, as discussed in Sec. III.

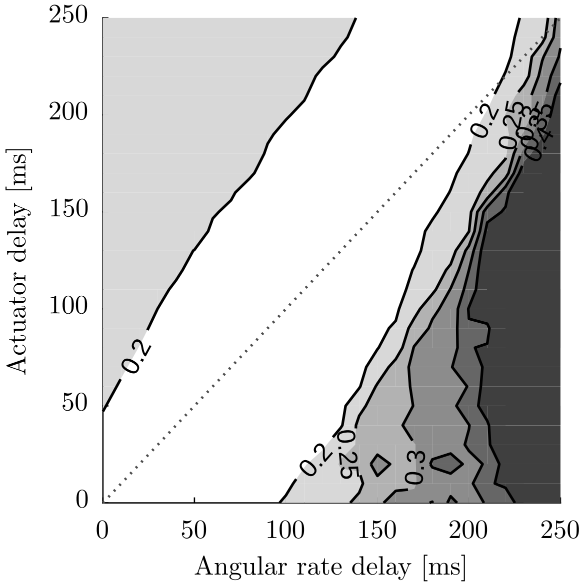

Figure 7: RMS performance for INDI with PCH affected by real-world phenomena

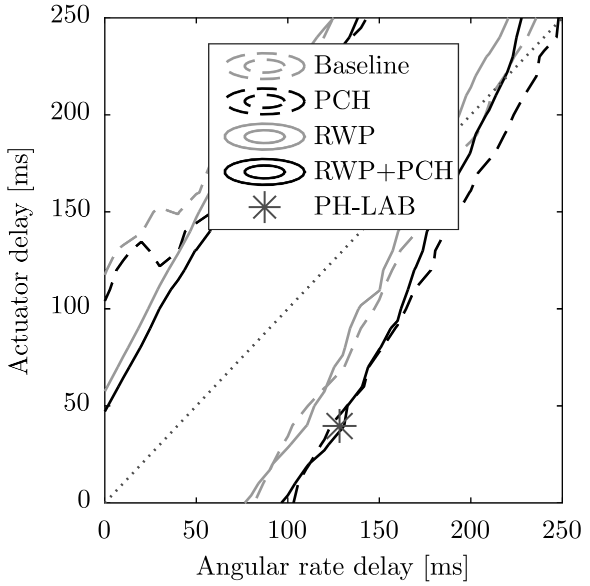

Figure 8: INDI performance boundaries, RMS=0.2, with/without PCH and real-world phenomena

Fig. 8 shows the performance boundaries for the INDI controller with/without real-world phenomena (RWP) and with/without PCH. The performance boundary is set at an RMS of 0.2, which is the value at which oscillatory behavior starts to appear. Fig. 8 shows that the performance of the INDI controlled PH-LAB is degraded independent of which combination of RWP and PCH is taken. The figure also shows that the addition of RWP does slightly reduce the region of adequate performance.

Interestingly, Fig. 8 also shows that the region of adequate performance shifts towards larger angular rate delays when PCH is used. As explained in Sec. IV, the inner loop K_P gain is larger for the controller with PCH compared with the controller without PCH. As such, the influence of the virtual control input, based on the inner loop tracking error, on the actual control input increases compared with the angular rate derivative feedback. This shift in influence reduces performance degradation due to angular rate delay, because the angular rate derivative feedback is the cause of oscillatory behavior leading to performance degradation.

B. Real-Time Time Delay Identification

The real-time time delay identification algorithm used is based on the concept of latency. Latency is the time delay between when a control command is given and the corresponding measurement is collected. The difference in latency between the actuator and angular rate measurements is a measure of the unsynchronized delay between these signals. The latency of the actuator measurement signal is based on control commands of (δ_a, δ_e, δ_r) and the measurements of these signals. The latency of the angular rates is based on the virtual control inputs (ν_p, ν_q, ν_r) and the filtered angular acceleration estimates ($\dot{p}$, $\dot{q}$, $\dot{r}$). Sharp peaks within the signals are most useful for identification, as these are easiest to match between the command and the actual response. Therefore, the derivatives of the mentioned signals are used, as it magnifies those parts of the signals with large derivatives.

To obtain an estimate of the latency of these signals, the average square difference function (ASDF) is used.[27] This function does not introduce additional model dependencies into the controller as only already available signals are used. Moreover, the ASDF is computationally efficient and is not affected by the mean of the signal like, for example, the correlation function. Literature indicates that the ASDF has adequate performance for signals with a signal-to-noise ratio (SNR) larger than 15 dB.[28] Fortunately, the SNR of the flight test signals was estimated around 20 dB, based on the PH-LAB with 3211 maneuvers on pitch and roll angles with a 10 degree magnitude. Other, more complex, algorithms exist in literature that could deal with low SNR signals, when the threshold of 15 dB cannot be met.

The ASDF can be computed by obtaining the argument minimizing Eq. (30).[27] Eq. (30) can be converted into a recursive formula, Eq. (31) to reduce memory and computational resources. Furthermore, the latency of both the roll and pitch channel can be identified separately, after which an average can be used within the controller improving identification accuracy.

$$\hat{R}(\tau) = \frac{1}{N}\sum_{k=1}^{N}[x_1(kT) - x_2(kT+\tau)]^2 \tag{30}$$

$$\hat{R}_k(\tau) = \frac{1}{N_k}[N_{k-1}\hat{R}_{k-1} + (x_{1_{k-\tau}} - x_{2_k})^2] \tag{31}$$

C. Results

The success of the real-time time delay algorithm can be seen in Fig. 9. This figure shows the final delay identification error after the 40 second simulations. The error ranges between -10ms, a surplus in angular delay added to the controller, and 30 ms, a surplus in actuator delay added to the controller. This range shows that it is difficult for the algorithm to perfectly estimate the time delay, however the range is within the region of best performance, based on Fig. 8, up to about 200 ms of total delay. Less aggressive control gains can be used to increase the total delay tolerated. The identification error is mainly caused by the bias, noise and sampling time phenomena. For example, the PH-LAB obtains angular rate measurements with a sampling time of 19.2 ms, while the algorithm tries to identify with a resolution of 10 ms, equivalent to the controller sampling time.

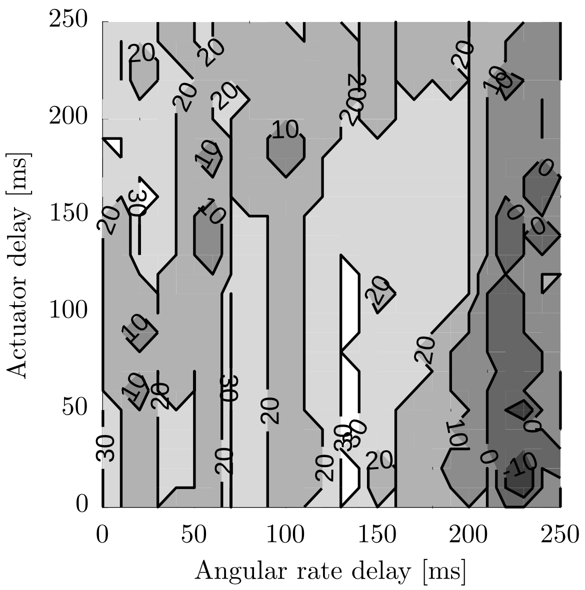

Figure 9: Delay identification error after 40 seconds with real-world phenomena and PCH

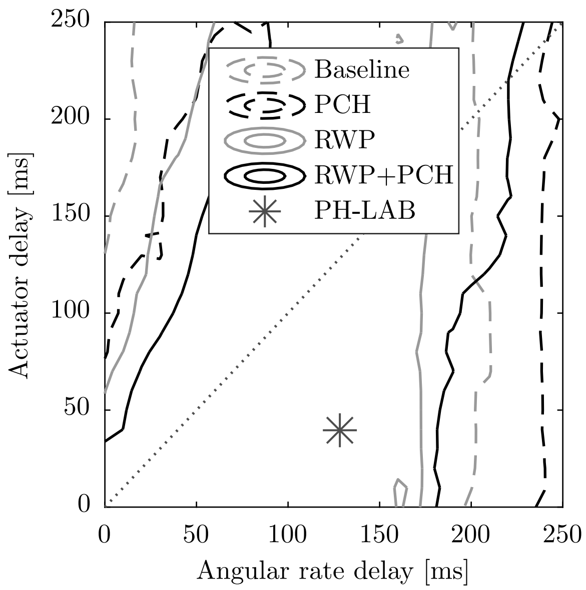

Figure 10: INDI performance boundaries, RMS=0.2, with delay identification

The performance boundaries of INDI with the real-time time delay algorithm activated are given in Fig. 10. Clearly, the performance of INDI has improved compared to Fig. 8, as expected based on the results of Fig. 9. Especially, when it is considered that the left performance boundary is not too important regarding stability, as INDI is not as sensitive to a surplus of actuator delay. Moreover, the performance of the system including PCH and phenomena inevitably degrades for time delays larger than 220 ms, as discussed based on Fig. 7. However, some parts of Fig. 10 still have an RMS larger than 0.2 due to a worse transient response in which the time delay is identified. Besides, Fig. 10 shows that without additional phenomena simulated, the algorithm in combination with PCH has adequate performance up to a total delay of 240 ms.

VII. Conclusion

Incremental nonlinear dynamic inversion (INDI) is a promising control technique that could contribute to safer, cheaper flight control systems (FCSs) with shorter development periods, straightforward certification and increased performance. This paper has shown that performance degradation due to typical aircraft characteristics can be prevented to retain the advantages of INDI as proven on other application platforms.

An analytical stability analysis showed that implementing discrete-time INDI with a smaller sampling time results in larger stability margins regarding system characteristics and controller gains. More specifically, the analysis concluded that sampling times smaller than 0.02s result in large stability margins. Moreover, the artificial unit delay of the actuator measurements implemented by some other authors was found to degrade system stability.

The effect of the real-world phenomena, bias, discretization, noise and time delay on an INDI controlled aircraft were investigated. Four phenomena showed significant performance degradation requiring controller adaptation: actuator measurement bias, angular rate measurement noise, angular rate measurement delay and actuator measurement delay.

Fortunately, the performance degradation can be prevented using a combination of three solutions without introducing additional model dependencies into the controller. First, using PI-control to design the virtual control input of the inner loop prevents a steady-state error due to actuator measurement bias. Second, a second-order low-pass filter can be used to reduce noise in the control input signal due to angular rate measurement noise. Third, the measurement delay of the angular rate and actuator measurements have to be synchronized to prevent oscillatory behavior, although a small mismatch between the delay in both signals is acceptable.

The importance of synchronizing the measurements was confirmed by both the analytical stability analysis and simulations with an INDI controlled aircraft. Moreover, both methods also showed that INDI is inherently more sensitive to a surplus of angular rate delay compared with a surplus of actuator delay. Part of this effect can be counteracted using pseudo control hedging (PCH), which favorably shifts the region of adequate performance towards a surplus of angular rate delay.

To synchronize the measurements a real-time time delay identification algorithm based on the concept of latency was proposed. The latency of both actuator and angular rate measurements with respect to the values commanded by the controller are identified using the average square difference function (ASDF). The difference in latency between the actuator and angular rate measurements is a measure of the unsynchronized delay between these signals. The unsynchronized delay is successfully identified by the algorithm with only a small error range. As such, the controller can fly with each combination of actuator and angular rate delay for values well above typical delays for aircraft. An additional benefit of the algorithm is that it does not introduce additional model dependencies into the controller as only already available signals are used.

References

[1]Balas, G. J., "Flight Control Law Design: An Industry Perspective," *European Journal of Control*, Vol. 9, No. 2-3, 2003, pp. 207–226.

[2]Balas, G. J. and Hodgkinson, J., "Control Design Methods for Good Flying Qualities," *AIAA Atmospheric Flight Mechanics Conference*, AIAA, Chicago, IL, USA, 2009.

[3]Enns, D., Bugajski, D., Hendrick, R., and Stein, G., "Dynamic Inversion: An Evolving Methodology for Flight Control Design," *International Journal of Control*, Vol. 59, No. 1, 1994, pp. 71–91.

[4]Walker, G. P. and Allen, D. A., "X-35B STOVL Flight Control Law Design and Flying Qualities," *2002 Biennial International Powered Lift Conference and Exhibit*, AIAA, Williamsburg, VA, USA, 2002.

[5]Lombaerts, T. J. J., Huisman, H. O., Chu, Q. P., Mulder, J. A., and Joosten, D. A., "Nonlinear Reconfiguring Flight Control based on Online Physical Model Identification," *Journal of Guidance, Control, and Dynamics*, Vol. 32, No. 3, 2009, pp. 727–748.

[6]Anon., "Civil Aviation Safety Data: 1993-2007," Tech. rep., Civil Aviation Authority of the Netherlands (CAANL), The Hague, the Netherlands, 2008.

[7]Anon., "State of Global Aviation Safety," Tech. rep., International Civil Aviation Organization (ICAO), Montreal, Canada, 2013.

[8]Sieberling, S., Chu, Q. P., and Mulder, J. A., "Robust Flight Control using Incremental Nonlinear Dynamic Inversion and Angular Acceleration Prediction," *Journal of Guidance, Control, and Dynamics*, Vol. 33, No. 6, 2010, pp. 1732–1742.

[9]Johnson, E. N. and Kannan, S. K., "Adaptive Trajectory Control for Autonomous Helicopters," *Journal of Guidance, Control, and Dynamics*, Vol. 28, No. 3, 2005, pp. 524 – 538.

[10]Heise, C. D., Falconí, G. P., and Holzapfel, F., "Hexacopter Outdoor Flight Test Results of an Extended State Observer

based Controller," *2014 IEEE International Conference on Aerospace Electronics and Remote Sensing Technology*, IEEE, Yogyakarta, Indonesia, 2014, pp. 26–33.

[11]Acquatella B., P., Falkena, W., van Kampen, E.-J., and Chu, Q. P., "Robust Nonlinear Spacecraft Attitude Control using Incremental Nonlinear Dynamic Inversion," *AIAA Guidance, Navigation, and Control Conference*, AIAA, Minneapolis, MN, USA, 2012.

[12]Simplício, P., Pavel, M. D., van Kampen, E., and Chu, Q. P., "An Acceleration Measurements-based Approach for Helicopter Nonlinear Flight Control using Incremental Nonlinear Dynamic Inversion," *Control Engineering Practice*, Vol. 21, No. 8, 2013, pp. 1065–1077.

[13]Smith, P. and Berry, A., "Flight Test Experience of a Non-Linear Dynamic Inversion Control Law on the VAAC Harrier," *Atmospheric Flight Mechanics Conference*, AIAA, Denver, CO, USA, 2000, pp. 132–142.

[14]Smeur, E. J. J., Chu, Q. P., and de Croon, G. C. H. E., "Adaptive Incremental Nonlinear Dynamic Inversion for Attitude Control of Micro Air Vehicles," *Journal of Guidance, Control, and Dynamics*, Vol. 39, No. 3, 2016, pp. 450–461.

[15]Mulder, J. A., van der Vaart, J. C., and Mulder, M., *AE4304: Atmospheric Flight Dynamics*, Faculty of Aerospace Engineering, Delft University of Technology, Delft, the Netherlands, 2007.

[16]Nise, N. S., *Control Systems Engineering*, John Wiley & Sons, Inc., Asia, 6th ed., 2011.

[17]Jury, E. I., "A Modified Stability Table for Linear Discrete Systems," *Proceedings of the IEEE*, Vol. 53, No. 2, 1965, pp. 184–185.

[18]Lu, P. and van Kampen, E.-J., "Active Fault-Tolerant Control for Quadrotors Subjected to a Complete Rotor Failure," *2015 IEEE/RSJ International Conference on Intelligent Robots and Systems*, IEEE/RSJ, Hamburg, Germany, 2015, pp. 4698–4703.

[19]Miller, C. J., "Nonlinear Dynamic Inversion Baseline Control Law: Architecture and Performance Predictions," *AIAA Guidance, Navigation, and Control Conference*, AIAA, Portland, OR, USA, 2011.

[20]Lombaerts, T. J. J. and Looye, G. H. N., "Design and Flight Testing of Nonlinear Autoflight Control Laws," *AIAA Guidance, Navigation, and Control Conference*, AIAA, Minneapolis, MN, USA, 2012.

[21]Lombaerts, T. J. J. and Looye, G. H. N., "Design and Flight Testing of Manual Nonlinear Flight Control Laws," *AIAA Guidance, Navigation, and Control Conference*, AIAA, Portland, OR, USA, 2011.

[22]Johnson, E. N. and Calise, A. J., "Pseudo-Control Hedging: A New Method for Adaptive Control," *Advances in Navigation Guidance and Control Technology Workshop*, Redstone Arsenal, AL, USA, 2000.

[23]Schierman, J. D., Ward, D. G., Hull, J. R., Gandhi, N., Oppenheimer, M. W., and Doman, D. B., "Integrated Adaptive Guidance and Control for Re-Entry Vehicles with Flight-Test Results," *Journal of Guidance, Control, and Dynamics*, Vol. 27, No. 6, 2004, pp. 975–988.

[24]Johnson, E. N. and Turbe, M. A., "Modeling, Control, and Flight Testing of a Small Ducted-Fan Aircraft," *Journal of Guidance, Control, and Dynamics*, Vol. 29, No. 4, 2006, pp. 769 – 779.

[25]Bauschat, J.-M., Mönnich, W., Willemsen, D., and Looye, G., "Flight Testing Robust Autoland Control Laws," *AIAA Guidance, Navigation, and Control Conference and Exhibit*, AIAA, Montreal, Canada, 2001.

[26]Bacon, B. J., Ostroff, A. J., and Joshi, S. M., "Reconfigurable NDI Controller using Inertial Sensor Failure Detection & Isolation," *IEEE Transactions on Aerospace and Electronic Systems*, Vol. 37, No. 4, 2001, pp. 1373–1383.

[27]Jacovitti, G. and Scarano, G., "Discrete Time Techniques for Time Delay Estimation," *IEEE Transactions on Signal Processing*, Vol. 41, No. 2, 1993, pp. 525–533.

[28]Nandi, A. K., "On the Subsample Time Delay Estimation of Narrowband Ultrasonic Echoes," *IEEE Transactions on Ultrasonics Ferroelectrics and Frequency Control*, Vol. 42, No. 6, 1995, pp. 993–1002.

Part II

Literature Studies

Chapter 2

Basic Theory & Principles

This chapter presents an introduction of the basic theory and principles of Incremental Nonlinear Dynamic Inversion (INDI). The report introduction of Chapter 1 already noted that INDI is a variation on Nonlinear Dynamic Inversion (NDI). Moreover, the INDI controller developed uses an INDI inner loop combined with an NDI outer loop. Hence, also an understanding of the basic theory and principles of NDI are considered important for this report. Note that a more detailed version of this chapter can be found in the preliminary thesis (van 't Veld, 2016).

First, Section 2-1 presents the fundamentals regarding NDI by providing a mathematical description of NDI and the relation between NDI and Feedback Linearization (FL). Second, Section 2-2 presents the fundamentals regarding INDI. Third, Section 2-3 discusses the issue of internal dynamics, which can cause system instability, that is inherently connected to NDI and INDI. Fourth, Section 2-4 describes the concept of time-scale separation, widely used in literature, which can simplify an NDI or INDI controller. Finally, the effect of model uncertainties on the response of systems controlled by NDI and INDI is discussed in Section 2-5.

2-1 Nonlinear Dynamic Inversion (NDI)

NDI is a nonlinear control system technique based on the algebraic transformation of nonlinear system dynamics into a, fully or partial, linear system. This algebraic transformation is performed by exact state transformations and feedback, contrary to conventional linear methods, which use Jacobian linearization to obtain linear approximations of the dynamics. NDI is also referred to as FL in literature due to the nature of the control technique. FL is applied through the companion form, Subsection 2-1-1, input-state linearization or input-output linearization, Subsections 2-1-2 and 2-1-3. Note that NDI is of the input-output linearization form. The technique can only be applied to nonlinear systems, which are feedback linearizable. If applied successfully, the relation between virtual control input and system output reduces to simple integrators. A linear control law can then be adopted to set the desired output dynamics. (Slotine & Li, 1991)

2-1-1 NDI for Systems in Companion Form

The principle of NDI is most easily demonstrated on a Single Input Single Output (SISO) system in companion form. A system is in companion form, if the system dynamics are described by Eq. (2-1), in which x is a scalar output, $\underline{x} = \begin{bmatrix} x & \dot{x} & \cdots & x^{(n-1)} \end{bmatrix}^T$ is the state vector and u is a scalar physical control input. Moreover, the functions $a(\underline{x})$ and $b(\underline{x})$ are nonlinear functions depending solely on the state vector $\underline{x}$. Additionally, this example uses a control-affine nonlinear system, i.e. the states linearly depend on the control input and nonlinearly depend on the states themselves. Eq. (2-1) can also be presented in a state-space representation as seen in Eq. (2-2). (Slotine & Li, 1991)

$$x^{(n)} = b(\underline{x}) + a(\underline{x})u \tag{2-1}$$

$$\frac{d}{dt}\begin{bmatrix} x_1 \\ \vdots \\ x_{n-1} \\ x_n \end{bmatrix} = \begin{bmatrix} x_2 \\ \vdots \\ x_n \\ b(\underline{x}) + a(\underline{x})u \end{bmatrix} \tag{2-2}$$

The physical control input, u, can then be solved for by introducing a virtual control input, ν, as presented in Eq. (2-3), given that the inverse $a^{-1}(\underline{x})$ exists. The introduction of the virtual control input results in a linear input-state relation, as presented in Eq. (2-4).

$$u = a^{-1}(\underline{x})[\nu - b(\underline{x})] \tag{2-3}$$

$$\frac{d}{dt}\begin{bmatrix} x_1 \\ x_2 \\ \vdots \\ x_{n-1} \\ x_n \end{bmatrix} = \begin{bmatrix} 0 & 1 & 0 & \cdots & 0 \\ 0 & 0 & 1 & \cdots & 0 \\ \vdots & \vdots & \vdots & \ddots & \vdots \\ 0 & 0 & 0 & \cdots & 1 \\ 0 & 0 & 0 & \cdots & 0 \end{bmatrix} \begin{bmatrix} x_1 \\ x_2 \\ \vdots \\ x_{n-1} \\ x_n \end{bmatrix} + \begin{bmatrix} 0 \\ 0 \\ \vdots \\ 0 \\ 1 \end{bmatrix} \nu = \begin{bmatrix} x_2 \\ x_3 \\ \vdots \\ x_n \\ \nu \end{bmatrix} \tag{2-4}$$

The introduced virtual control input can now be replaced by a state feedback control law, see Eq. (2-5). This control law can be tuned using linear methods, such that the closed-loop system has exponentially stable dynamics when all poles are in the left-half complex plane. Moreover, exponentially convergent tracking can be obtained for a task with desired output $x_d(t)$ and tracking error $e(t) = x(t) - x_d(t)$ by selecting the control law as in Eq. (2-6). Note, that the $x_d^{(n)}$ term in Eq. (2-6) can be added as a feedforward term to increase controller performance regarding speed and tracking accuracy.

$$\nu = -k_0 x - k_1 \dot{x} - \cdots - k_{n-1} x^{(n-1)} \tag{2-5}$$

$$\nu = x_d^{(n)} - k_0 e - k_1 \dot{e} - \cdots - k_{n-1} e^{(n-1)} \tag{2-6}$$

Summarizing, the implementation of an NDI controller for a system in canonical form requires several features. The $a^{-1}(\underline{x})$ and $b(\underline{x})$ blocks have to be evaluated with the current state vector. Moreover, a linear controller has to be designed that computes the virtual input based on the difference between a reference state and the true or measured state. (Slotine & Li, 1991)

However, the strategy for the implementation of NDI via the companion form is not directly applicable to all systems, as not every system is in this companion form. Alternatively, an algebraic transformation can be used to put the system into a companion form. This method is referred to as input-state linearization, but this method requires complex mathematical tools. No practical examples were found in literature in which NDI control was applied via either the companion form or an input-state linearization. Therefore, only NDI control via input-output linearization, described in Subsections 2-1-2 and 2-1-3, is used throughout the remainder of this report. (van 't Veld, 2016)

2-1-2 NDI via Input-Output Linearization for SISO systems

The concept of input-output linearization is introduced by considering the system given by Eq. (2-7). The basic approach to input-output linearization is the differentiation of the output function, y, until the control input, u, appears. (Slotine & Li, 1991)

$$\begin{aligned} \dot{\underline{x}} &= \underline{f}(\underline{x}) + \underline{g}(\underline{x})u \\ y &= h(\underline{x}) \end{aligned} \tag{2-7}$$

Two mathematical notations are introduced for this process: the Lie derivative of $h(\underline{x})$ with respect to $\underline{f}(\underline{x})$, $L_{\underline{f}}h(\underline{x}) = \nabla h(\underline{x}) \cdot \underline{f}(\underline{x})$, and the gradient of $h(\underline{x})$, $\nabla h(\underline{x}) = \frac{\partial h(\underline{x})}{\partial \underline{x}}$. Note the r$^{\text{th}}$-order Lie derivative is defined as $L^r_{\underline{f}}h(\underline{x}) = L_{\underline{f}}[L^{r-1}_{\underline{f}}h(\underline{x})]$. The first differentiation of the output function is presented in Eq. (2-8). If $L_{\underline{g}}h(\underline{x}) \neq 0$ for any $\underline{x}$, then the control law can be obtained from Eq. (2-9), such that a linear relation is obtained between the output y and input u, via $\dot{y} = \nu$.

$$\dot{y} = \nabla h(\underline{x})\dot{\underline{x}} = \nabla h(\underline{x})(\underline{f}(\underline{x}) + \underline{g}(\underline{x})u) = L_{\underline{f}}h(\underline{x}) + L_{\underline{g}}h(\underline{x})u \tag{2-8}$$

$$u = \frac{1}{L_{\underline{g}}h(\underline{x})}(-L_{\underline{f}}h(\underline{x}) + \nu) \tag{2-9}$$

If $L_{\underline{g}}h(\underline{x}) = 0$ for all $\underline{x}$, then the output is differentiated again and again until the control input u appears. This can be notated formally by Eq. (2-10) with the notion that differentiation stops when $L_{\underline{g}}L^{r-1}_{\underline{f}}h(\underline{x}) \neq 0$ for some integer r, such that the linear relation $y^{(r)} = \nu$ can be obtained by defining the control law for input u as in Eq. (2-11). Furthermore, note that Eq. (2-11) is similar in structure to NDI via the companion form as seen in Eq. (2-12). Resulting in a control architecture for a control system based on NDI as seen in Figure 2-1. This figure shows the important concept that the combination of NDI controller and nonlinear system results in the transfer function $1/s^n$. This physically represents a chain of integrators equal to the number of differentiations required, such that the linear input-output relation $y^{(n)} = \nu$ is obtained.

$$y^{(i)} = L^i_{\underline{f}}h(\underline{x}) + L_{\underline{g}}L^{i-1}_{\underline{f}}h(\underline{x})u \tag{2-10}$$

$$u = \frac{1}{L_{\underline{g}}L^{r-1}_{\underline{f}}h(\underline{x})}(-L^r_{\underline{f}}h(\underline{x}) + \nu) \tag{2-11}$$

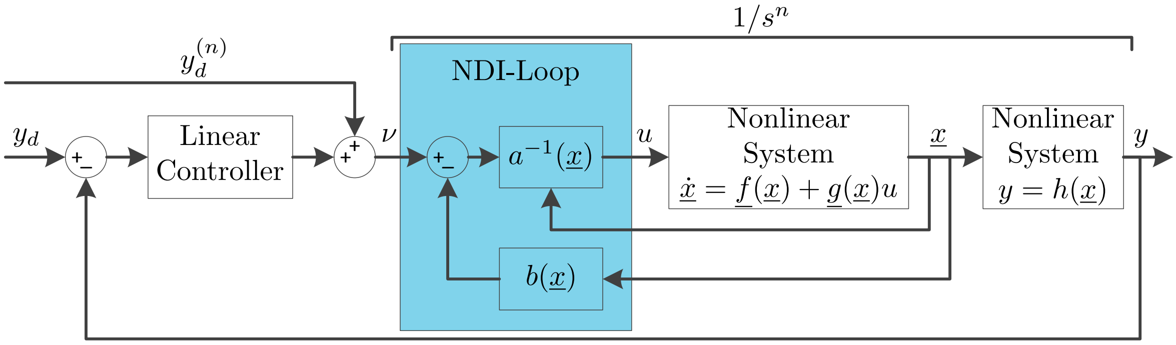

Figure 2-1: Block diagram of NDI control structure for control-affine nonlinear system via input-output linearization

$$
\begin{aligned}
&u = a^{-1}(\underline{x})[\nu - b(\underline{x})] \text{ with } \nu = y^{(n)} \\
&a^{-1}(\underline{x}) = \frac{1}{L_{\underline{g}} L_{\underline{f}}^{r-1} h(\underline{x})}; \; b(\underline{x}) = L_{\underline{f}}^{r} h(\underline{x})
\end{aligned}
\tag{2-12}
$$

The amount of differentiations r until the explicit relationship between the input and output appears is defined as the relative degree. For any partially or fully controllable system, with order n, it takes a maximum of n differentiations for the explicit input-output relation to appear, such that $r \leq n$. For systems with $r < n$ part of the system is 'unobservable' within the input-output linearization. These unobservable dynamics are referred as the internal dynamics of the system. The internal dynamics of the system do not explicitely depend on the input u and cannot be controlled (van 't Veld, 2016). The internal dynamics have to be stable for the NDI to be effective, this is further discussed in Section 2-3. For systems with $r = n$ the controlled closed-loop system has no internal dynamics. If the relation between output derivative $y^{(i)}$ and input u never appears, the system is not feedback linearizable and NDI cannot be applied to the system (Marino, 1986). (Slotine & Li, 1991)

2-1-3 NDI via Input-Output Linearization for MIMO systems

The NDI methodology for SISO systems can be extended to the more general Multiple Input Multiple Output (MIMO) case. The theory is however still applied to control-affine systems with the same number of inputs and outputs m. The mathematical tools presented in this section can easily be adapted to cope with a system with a different number of inputs than outputs. The MIMO system considered for this section is presented in Eq. (2-13). (Slotine & Li, 1991)

$$
\begin{aligned}
\underline{\dot{x}} &= \underline{f}(\underline{x}) + G(\underline{x})\underline{u} \\
\underline{y} &= \underline{h}(\underline{x})
\end{aligned}
\tag{2-13}
$$

The input $\underline{u}$ and output $\underline{y}$ are vectors with length m, $\underline{h}(\underline{x})$ is a nonlinear vector function with length m and $G(\underline{x})$ is an $m \times m$ input matrix. As for the SISO case, all output components y_j have to be differentiated until an explicit relation with one of the inputs appears. The number of differentiations required, r_j, is the relative degree of the output component. The sum of the relative degrees of all output components is defined as the total relative degree.

The relation between the virtual control input $\underline{\nu}$ and physical control input $\underline{u}$ is found in similar fashion to the SISO case, see Eq. (2-15), considering the explicit relation between input and output to be defined as presented in Eq. (2-14). The form of $A(\underline{x})$ highlights the assumptions made at the start of this section with an equal number of inputs and outputs. Without this assumption, $A(\underline{x})$ is not square and thus some sort of control allocation is required to solve for the physical control input $\underline{u}$. Besides, Eq. (2-15) also shows that each output component y_j is only affected by a single virtual input v_j.

$$y_j^{(r_j)} = L_{\underline{f}}^{r_j} h_j(\underline{x}) + \begin{bmatrix} L_{G_1} L_{\underline{f}}^{r_j-1} h_j(\underline{x}) & \cdots & L_{G_m} L_{\underline{f}}^{r_j-1} h_j(\underline{x}) \end{bmatrix} \begin{bmatrix} u_1 \\ \vdots \\ u_m \end{bmatrix} \tag{2-14}$$

$$\begin{aligned} &\underline{u} = A^{-1}(\underline{x})[\underline{\nu} - \underline{b}(\underline{x})] \text{ with } \underline{\nu} = \begin{bmatrix} \nu_1 \\ \vdots \\ \nu_m \end{bmatrix} = \begin{bmatrix} y_1^{(r_1)} \\ \vdots \\ y_m^{(r_m)} \end{bmatrix} \\ &A(\underline{x}) = \begin{bmatrix} L_{G_1} L_{\underline{f}}^{r_1-1} h_1(\underline{x}) & \cdots & L_{G_m} L_{\underline{f}}^{r_1-1} h_1(\underline{x}) \\ \vdots & \ddots & \vdots \\ L_{G_1} L_{\underline{f}}^{r_m-1} h_1(\underline{x}) & \cdots & L_{G_m} L_{\underline{f}}^{r_m-1} h_1(\underline{x}) \end{bmatrix}; \ \underline{b}(\underline{x}) = \begin{bmatrix} L_{\underline{f}}^{r_1} h_1(\underline{x}) \\ \vdots \\ L_{\underline{f}}^{r_m} h_m(\underline{x}) \end{bmatrix} \end{aligned} \tag{2-15}$$

Therefore, the dynamics of each of the outputs is completely independent and decoupled from the remaining system, provided that the system model is accurately known. Furthermore, this implies that the linear controller can be designed for each channel, as if it were a SISO case. (Slotine & Li, 1991)

2-2 Incremental Nonlinear Dynamic Inversion (INDI)

INDI is considered a variation on NDI, however the derivation of INDI starts from a more general system, see Eq. (2-16). Therefore, the use of INDI is not constrained to control-affine systems as is the case for NDI. However, the use of INDI is constrained to systems with a direct relation between the input and derivative of the desired output. (Sieberling et al., 2010; Acquatella B., Falkena, van Kampen, & Chu, 2012; Smeur et al., 2016)

$$\dot{\underline{x}} = \underline{f}(\underline{x}, \underline{u}) \tag{2-16}$$

The system of Eq. (2-16) can be linearized about the current point indicated by the subscript '0', see Eq. (2-17). Note that this expansion is based on the assumptions of a small sampling time and instantaneous control effectors. The notation of Eq. (2-17) can be simplified by defining $\left.\frac{\partial \underline{f}(\underline{x},\underline{u})}{\partial \underline{x}}\right|_{\underline{x}=\underline{x}_0,\underline{u}=\underline{u}_0} = F(\underline{x}_0, \underline{u}_0)$ and $\left.\frac{\partial \underline{f}(\underline{x},\underline{u})}{\partial \underline{u}}\right|_{\underline{x}=\underline{x}_0,\underline{u}=\underline{u}_0} = G(\underline{x}_0, \underline{u}_0)$ as well as the incremental notations $\Delta\underline{x} = (\underline{x} - \underline{x}_0)$ and $\Delta\underline{u} = (\underline{u} - \underline{u}_0)$.

$$\begin{aligned} \dot{\underline{x}} &\approx \underline{f}(\underline{x}_0, \underline{u}_0) + \left.\frac{\partial \underline{f}(\underline{x},\underline{u})}{\partial \underline{x}}\right|_{\underline{x}=\underline{x}_0,\underline{u}=\underline{u}_0} (\underline{x} - \underline{x}_0) + \left.\frac{\partial \underline{f}(\underline{x},\underline{u})}{\partial \underline{u}}\right|_{\underline{x}=\underline{x}_0,\underline{u}=\underline{u}_0} (\underline{u} - \underline{u}_0) \\ \dot{\underline{x}} &\simeq \dot{\underline{x}}_0 + F(\underline{x}_0, \underline{u}_0)\Delta\underline{x} + G(\underline{x}_0, \underline{u}_0)\Delta\underline{u} \end{aligned} \tag{2-17}$$

To further simplify Eq. (2-17), the time-scale separation principle is introduced as defined in Eq. (2-18). Section 2-4 explains the physical nature and validity of this assumption, which is also used to develop the outer loops of the NDI and INDI controllers. Using the time-scale separation assumption Eq. (2-17) is further reduced to Eq. (2-19). Eq. (2-19) can be used to develop a control law similar to NDI by defining the virtual control input as $\underline{\nu} = \dot{\underline{x}}$.

$$F(\underline{x}_0, \underline{u}_0)\Delta\underline{x} << G(\underline{x}_0, \underline{u}_0)\Delta\underline{u} \tag{2-18}$$

$$\dot{\underline{x}} \simeq \dot{\underline{x}}_0 + G(\underline{x}_0, \underline{u}_0)\Delta\underline{u} \tag{2-19}$$

$$\Delta\underline{u} \simeq G^{-1}(\underline{x}_0, \underline{u}_0)(\underline{\nu} - \dot{\underline{x}}_0) \tag{2-20}$$

As such, the physical control input u can be compute using the previous input together with the incremental input of Eq. (2-20). The combined INDI controller and nonlinear system acts as an integrator with transfer function $1/s$. This response can be further tuned by using a linear controller as in Section 2-1. The control architecture of INDI is depicted in Figure 2-2. The structure of the INDI controller is very similar to the NDI controller discussed in Section 2-1. The main difference between both methods is that INDI has replaced part of the feedback depending on the model and measured states with feedback of the estimated state derivatives. (Sieberling et al., 2010; Acquatella B. et al., 2012; Smeur et al., 2016)

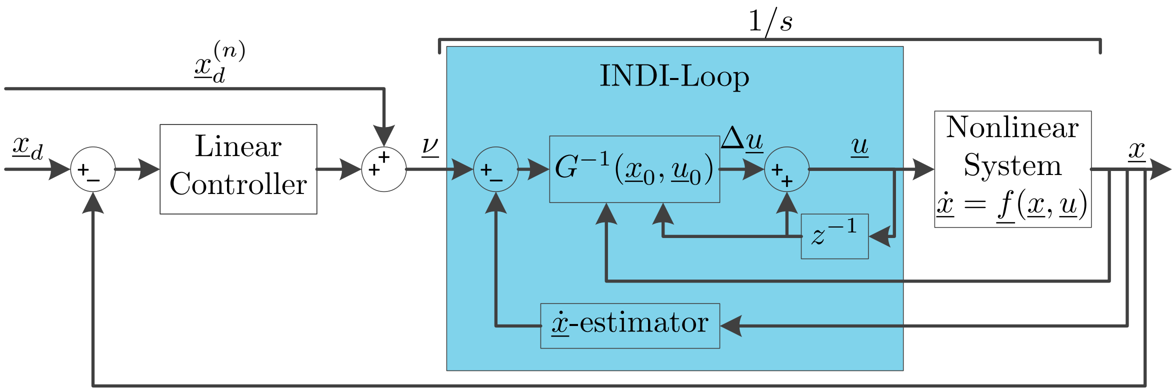

Figure 2-2: Block diagram of INDI control structure for general nonlinear system

2-3 Internal Dynamics

This section presents the concept of internal dynamics associated with NDI and INDI. The system has internal dynamics when it is not completely feedback linearized, as discussed in Section 2-1-2. Conceptually, internal dynamics are the remaining system motions, when the outputs are constrained to be constant or prescribed by the NDI or INDI controller (Enns et al., 1994). Therefore, the internal dynamics and its characteristics depend on the original system as well as the variables selected to be controlled, i.e. the Control Variables (CVs).

The internal dynamics are unstable for non-minimum phase systems only. Non-minimum phase systems are systems for which the initial output reaction to a specific input is in opposite direction of the long-term output reaction. The normal acceleration due to elevator deflection of tail-controlled airframes is an example of a system exhibiting non-minimum phase behavior (van 't Veld, 2016).

The issue related to non-minimum phase system can be explained by consider the normal acceleration as CV controlled by an elevator input in a tail-controlled configuration. When classical control theory is used, the error between the commanded and measured acceleration is converted into an elevator input. In this case, a positive error signal requires an increase in normal acceleration, which can be obtained by a negative elevator input. The designer can force this behavior into the system by properly tuning the gains. Now consider the same configuration controlled by an NDI or INDI controller. Based on the system dynamics the first derivative of the CV already yields an explicit relation with the elevator input signal. However, this explicit relation is based on the acceleration generated by the elevator itself instead of the acceleration generated by rotating the airframe. Therefore, when a positive error signal is fed to this NDI controller a positive elevator input is given to the system. The long term effect is a negative normal acceleration increasing the magnitude of the error signal, eventually causing system instability. (van 't Veld, 2016)

The previous sections have concluded that non-minimum phase systems controlled via NDI or INDI in general result in unstable closed-loop systems. However, what if one still wants to control a CV with non-minimum phase characteristics for a given to-be-controlled system. An extensive overview of five fundamental methods is available in literature (Rajput & Weiguo, 2014). However, there is no general method available that can account for unstable internal dynamics without making demands on the characteristics of the NDI or INDI controlled system (van 't Veld, 2016). Therefore, the internal dynamics are accounted for by selecting proper CVs for the to-be-controlled system. For example, an inner loop controlling the body angular rates of the airframe results in a system with minimum phase characteristics, due to the dynamics of airframes.

2-4 Time-Scale Separation

This section presents the concept of time-scale separation and its use in combination with NDI and INDI control. Moreover, this section discusses how different time-scale naturally occur within aircraft dynamics. The existence of these time-scales can be utilized to obtain a cascaded NDI or INDI controller via multiple loop closures. These loops are defined such that the outputs of the outer, slow loop are the inputs of the inner, fast loop. Although not further discussed in this report, a mathematical manner in which time scales can be investigated is by using singular perturbations theory (Naidu & Calise, 2001).

First, the physical occurrence of time-scales within aircraft dynamics is discussed. For this discussion a simple aircraft input model is used containing three types of control surfaces, namely ailerons, elevators and a rudder, together with a single engine as propulsion system. All control effectors are assumed to have first order actuator dynamics. In general, the dynamics of an aircraft are described by a combination of translation and rotational equations of motion, actuator dynamics and aerodynamic relationships (Mulder et al., 2013). By analyzing the defined dynamics an overview can be made of the effect of the available inputs on all other variables defining the system, see Figure 2-3.

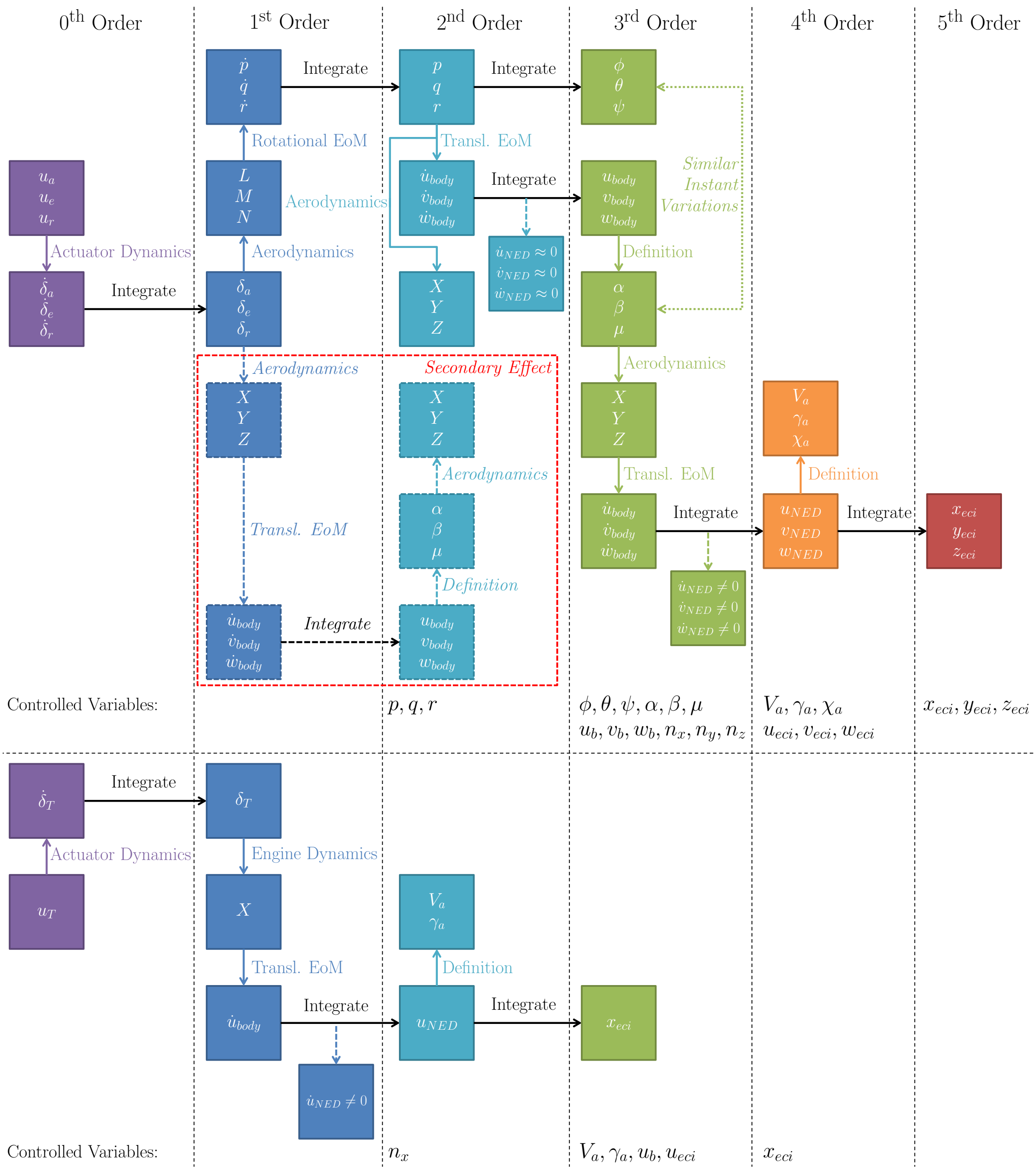

Figure 2-3: Overview of various time-scales in aircraft dynamics

Figure 2-3 shows that the dynamics of any variable with respect to the inputs is defined by a system with a certain order. This order is equal to the number of integrations used to link the variable to one of the inputs. Physically speaking, the fastness of the dynamics of a variable depends on the system order, hence the variables are in different timescales. For example, the effect of an elevator input, δ_e, on the aircrafts pitch rate, q, dynamics appears quicker than the effect of the same elevator input on the aircrafts pitch angle, θ, dynamics.

Similarly, the effect of an elevator input on the aircrafts pitch angle dynamics appears quicker than the effect of the same elevator input on the aircrafts flight path angle, γ, dynamics. The low order dynamics given in Figure 2-3 correspond to a small or fast time-scale and the high order dynamics correspond to a large or slow time-scale.

Additionally, Figure 2-3 also shows the relation between specific CVs and the aircraft inputs. This can be used to select the proper CVs for each loop of a cascaded controller, this includes Proportional-Integral-Derivative (PID), NDI and INDI controllers. The main guideline is that an outer loop must be in a slower time-scale, i.e. higher order, than the inner loop used. For example, if an outer loop controlling V_a, γ_a, χ_a is desired, then a middle loop with CVs ϕ, α, β and inner loop p, q, r can be selected (Lombaerts, Huisman, Chu, Mulder, & Joosten, 2009). According to the time-scale separation principle, the variables dictating the slow dynamics are assumed constant in the fast, inner loops. The variables dictating the fast dynamics are assumed to achieve their commanded values instantaneously in the slow, outer loops. Theoretically, this principle could result in stability issues, however it has been proven that exponential stability about the commanded values of the outer loop can be guaranteed, if inner loop gains are sufficiently large (Schumacher & Khargonekar, 1998).

Note that some variables appear multiple times in Figure 2-3, due to small secondary effects noticeable in the aircraft dynamics. These secondary effects cannot be used to properly control the aircraft, moreover these effects can even form a nuisance for the proper control of the variables affected. For example, these secondary effects are the main cause of unstable internal dynamics and non-minimum phase behavior, as explained in Section 2-3. The concept of internal dynamics can also be extended towards NDI and INDI based on time-scale separation. The sum of the order of all subsystems is equal to the total order of the system and the sum of the local relative degree of all subsystems is equal to the total relative degree of the system. No internal dynamics exist if the total relative degree of the system is equal to the total order of the system. Moreover, also each subsystem can be analyzed for internal dynamics. No local internal dynamics exist if the local relative degree is equal to the order of the subsystem. Consequently, the nuisance caused by internal dynamics is independent on the utilization of the time-scale separation principle. (Lombaerts et al., 2009; Simplício, 2011)

The main advantage of time-scale separation is that it results in a reduced mathematical complexity, while unbiased tracking can still be offered by the closed-loop system. In the example with the V_a, γ_a, χ_a outer loop, three separate inversion of a third order systems are used, instead of an inversion of a ninth order system. Moreover, the cascaded design shows increased robustness against disturbances in the fast dynamics of the system (Nise, 2011).

2-5 System Response for Model Uncertainties

One of the arguments motivating the research for INDI is that INDI has increased robustness to model uncertainties and a decreased dependency on the vehicle model, see Chapter 1. This section presents the effect of model uncertainties on the response of systems controlled by NDI and INDI. Note that uncertainties regarding sensor measurements and dynamics are not taken into account. Furthermore, as discussed in Section 2-2 instantaneous control surface deflections are assumed, i.e. the system has ideal actuators.

The system response for an NDI controlled system regarding the nominal situation indicated with a subscript n is given in Eq. (2-21), see Section 2-1. Clearly, the closed-loop response of the controlled system is linear with $\dot{\underline{x}} = \underline{\nu}$. However, real systems contain model uncertainties, therefore the real system is defined as Eq. (2-22). The real system can be combined with the control law designed for the nominal condition to obtain the system response with model uncertainties, Eq. (2-23). The resulting response presented by Eq. (2-23) is not necessarily linear. For example, for an angular rate controller with uncertainties regarding mass, inertia and aerodynamics, multiple nonlinear terms remain in the system response. (Sieberling et al., 2010)

$$\begin{aligned} \dot{\underline{x}} &= \underline{f}_n(\underline{x}) + G_n(\underline{x})\underline{u} \\ \underline{u} &= G_n^{-1}(\underline{x})[\underline{\nu} - \underline{f}_n(\underline{x})] \\ \dot{\underline{x}} &= \underline{\nu} \end{aligned} \tag{2-21}$$

$$\dot{\underline{x}} = \underline{f}_n(\underline{x}) + \Delta\underline{f}(\underline{x}) + G_n(\underline{x})\underline{u} + \Delta G(\underline{x})\underline{u} \tag{2-22}$$

$$\begin{aligned} \dot{\underline{x}} &= \underline{f}_n(\underline{x}) + \Delta\underline{f}(\underline{x}) + G_n(\underline{x})G_n^{-1}(\underline{x})[\underline{\nu} - \underline{f}_n(\underline{x})] + \Delta G(\underline{x})G_n^{-1}(\underline{x})[\underline{\nu} - \underline{f}_n(\underline{x})] \\ \dot{\underline{x}} &= [I + \Delta G(\underline{x})G_n^{-1}(\underline{x})]\underline{\nu} + \Delta\underline{f}(\underline{x}) - \Delta G(\underline{x})G_n^{-1}(\underline{x})\underline{f}_n(\underline{x}) \end{aligned} \tag{2-23}$$

Similarly, the system response for an INDI controlled system in nominal situation is given by Eq. (2-24), see Section 2-2. Again, the closed-loop response for this nominal system is linear with $\dot{\underline{x}} = \underline{\nu}$. The real system response, Eq. (2-26), is obtained by combining the control law designed for the nominal condition and the real system containing uncertainties, Eq. (2-25). (Sieberling et al., 2010)

$$\begin{aligned} \dot{\underline{x}} &= \dot{\underline{x}}_0 + G_n(\underline{x}_0, \underline{u}_0)\Delta\underline{u} \\ \Delta\underline{u} &= G_n^{-1}(\underline{x}_0, \underline{u}_0)[\underline{\nu} - \dot{\underline{x}}_0] \\ \dot{\underline{x}} &= \underline{\nu} \end{aligned} \tag{2-24}$$

$$\dot{\underline{x}} = \dot{\underline{x}}_0 + G_n(\underline{x}_0, \underline{u}_0)\Delta\underline{u} + \Delta G(\underline{x}_0, \underline{u}_0)\Delta\underline{u} \tag{2-25}$$

$$\begin{aligned} \dot{\underline{x}} &= \dot{\underline{x}}_0 + G_n(\underline{x}_0, \underline{u}_0)G_n^{-1}(\underline{x}_0, \underline{u}_0)[\underline{\nu} - \dot{\underline{x}}_0] + \Delta G(\underline{x}_0, \underline{u}_0)G_n^{-1}(\underline{x}_0, \underline{u}_0)[\underline{\nu} - \dot{\underline{x}}_0] \\ \dot{\underline{x}} &= [I + \Delta G(\underline{x}_0, \underline{u}_0)G_n^{-1}(\underline{x}_0, \underline{u}_0)]\underline{\nu} - \Delta G(\underline{x}_0, \underline{u}_0)G_n^{-1}(\underline{x}_0, \underline{u}_0)\dot{\underline{x}}_0 \end{aligned} \tag{2-26}$$

Considering the assumption of small sampling time and ideal sensor measurements the new and current state derivatives are approximated to be equal $\dot{\underline{x}} \approx \dot{\underline{x}}_0$. Given this assumption, Eq. (2-26) can be simplified such that the system responds approximately equal to the nominal system with $\dot{\underline{x}} = \underline{\nu}$, see Eq. (2-27).

$$\begin{aligned} [I + \Delta G(\underline{x}_0, \underline{u}_0)G_0^{-1}(\underline{x}_0, \underline{u}_0)]\dot{\underline{x}} &\approx [I + \Delta G(\underline{x}_0, \underline{u}_0)G_0^{-1}(\underline{x}_0, \underline{u}_0)]\underline{\nu} \\ \dot{\underline{x}} &\approx \underline{\nu} \end{aligned} \tag{2-27}$$

Concluding, when comparing the real system responses of NDI and INDI given by Eqs. (2-23) and (2-26) the INDI clearly depends less on model uncertainties than its NDI counterpart. Moreover, given the assumptions made within the derivation of INDI, the real system response even approximates the nominal system response as given by Eq. (2-27).

Chapter 3

State-of-the-Art Review

This chapter presents a state-of-the-art literature review to enhance understanding of the research area and any opposing views. This chapter should therefore provide additional insight on the research objective and questions presented in Section 1-2. To ensure that all relevant research areas are considered this section contains a review on Flight Control Systems (FCSs), Section 3-1, a review on Nonlinear Dynamic Inversion (NDI), Section 3-2, and a review on Incremental Nonlinear Dynamic Inversion (INDI), Section 3-1. Note that the state-of-the-art review focuses on literature containing flight tested controllers due to the practically oriented research objective.

3-1 Review on Flight Control Systems (FCSs)

The introduction already indicated that a few decades ago almost all FCSs were developed based on classical, linear control techniques (Balas, 2003). These linear control techniques assume the validity of a linear model within a small part of the flight envelope. However, outside of this domain the controller performance will degrade (Slotine & Li, 1991). Note, in general Proportional-Integral-Derivative (PID) controllers are used as linear controller. To obtain a satisfactory controller, the flight envelope is partitioned into several parts and separate linear controllers are designed for each part of the envelope. Afterwards, gain schedules are designed by interpolating the separate linear controllers and as such obtain a controller for the full flight envelope (Adams & Banda, 1993; Enns et al., 1994).

The classical techniques are widely used throughout industry, still the techniques are limited as these are based on local linearizations and gain scheduling. The methodology is: time consuming, expensive, depends on engineering art, difficult to re-use in other airframes, not flexible regarding design changes within the aircraft design and life cycle, difficult to use for high angle-of-attack flight and not tolerant to system failures (Adams & Banda, 1993; Enns et al., 1994; Lombaerts et al., 2009). Most of these issues are inherently connected to the nature of the classical techniques and are thus difficult to mitigate. Consequently, industry and academia have shifted towards using advanced, multivariable control techniques to develop FCSs, such as eigenstructure assignment, H_∞ loop-shaping, linear quadratic regulator/Gaussian, μ-synthesis, Model Reference Adaptive Control (MRAC), NDI and Neural Networks (NNs) (Honeywell & Lockheed Martin, 1996; Balas, 2003). To limit the extend of the research project not all of these control techniques can be considered. NDI and more specifically the INDI variation are considered for this project. The benefits of this choice and the state-of-the-art regarding NDI and INDI are explained in Section 3-2 and 3-3. This choice is also convenient since NDI is currently the most applied multivariable control technique (Balas, 2003; Balas & Hodgkinson, 2009).

3-2 Review on NDI

NDI is a control technique that fundamentally differs from the classical, linear control techniques described in the previous section. See Chapter 2 for the basic theory and principles of NDI. Note that NDI is also referred to as feedback linearization or input-output linearization in literature (Slotine & Li, 1991). As described by Enns et al. (1994) and Slotine and Li (1991), NDI globally linearizes system dynamics by using full-state feedback and an onboard model of the system dynamics. Moreover, the global linearization of the system dynamics pairs with a decoupling of control variables in a Multiple Input Multiple Output (MIMO) system. Additionally, linear control techniques can then be used for this NDI controlled system to obtain the desired output dynamics. This fundamental difference reduces the amount of time, cost and engineering art required to obtain a satisfactory FCS. Moreover, NDI can more easily be re-used in other airframes, has increased flexibility regarding changes within the aircraft design and life cycle and has improved performance for high angle-of-attack flight (Walker & Allen, 2002; Baer, 2014). Finally, the handling quality dependent part of an NDI FCS is isolated from the airframe/engine dependent part, such that flying qualities can directly be incorporated into the FCS when using NDI (Walker & Allen, 2002). This advantage was used during the development of the X-35, the predecessor of the F-35.

On the other hand, the use of NDI also has some fundamental disadvantages (Slotine & Li, 1991; Enns et al., 1994; Lombaerts et al., 2009). First, the name already indicates that the control laws contain a mathematical inversion, this can lead to singularities within the control laws resulting in infeasible inputs given to the system, see also Chapter 2. Second, NDI cannot be applied directly to so-called non-minimum phase systems as this results in unstable closed-loop dynamics, see also Chapter 2. This drawback has an impact on aerospace applications, as the vertical acceleration due to elevator deflection of tail-controlled airframes is an example of such a non-minimum phase system. Third, an accurate model of the system has to be available as model mismatches will result in an incorrect inversion, which will subsequently lead to performance degradation. Therefore, NDI itself is not tolerant to system failures or control saturation, as these significantly change the system dynamics. However, Lombaerts and Looye (2012) show that the Pseudo Control Hedging (PCH) technique, developed by Johnson and Calise (2000), can be used together with NDI to mitigate issues related to model mismatch due to control saturation. Fourth, full-state feedback has to be available and accurate to obtain adequate controller performance. Wrong measurements, due to noise, bias or time delay, have a similar effect as an inaccurate model as these result an incorrect inversion. Moreover, it should be kept in mind that some variables in aerospace applications are difficult to measure, such as angle-of-attack and sideslip angle.

The theoretical disadvantages of NDI as described above have been confirmed by flight tests. The first two disadvantages mentioned, i.e. the risk of singularities and unstable closed-loop dynamics, can be dealt with rather straightforward by selecting appropriate variables to be controlled. Any issues related to these disadvantages were not experienced during various flight tests (Bauschat, Mönnich, Willemsen, & Looye, 2001; Wacker, Munday, & Merkle, 2001; Walker & Allen, 2002; Lombaerts & Looye, 2012). The third disadvantage mentioned, i.e. the availability of an accurate model, was noticed during flight tests. Wacker et al. (2001) experienced issues as the flight test vehicle was dropped from a B-52, which created a downwash significantly affecting the aerodynamic behavior of the testing vehicle. Moreover, Walker and Allen (2002) comment on a Pilot Induced Oscillation (PIO) experienced due to a time delay in combination with higher order dynamics not taken into account by the model. Finally, also the fourth disadvantage mentioned, i.e. the accurate full-state feedback required was observed during flight tests. Bauschat et al. (2001) note that high levels of turbulence and quantization of measurements led to performance degradation. Lombaerts and Looye (2012) discuss that their first test flight failed due to measurement noise.

The disadvantages mentioned above are inherently connected to NDI and are difficult to mitigate. Therefore, the main advances regarding NDI are made by combining NDI with other control techniques. All of the flight tested variations on NDI are discussed below. A commonly found addition to NDI is the use of a NN (Johnson & Kannan, 2005; Bosworth, 2008). NNs can be used to correct model mismatches and as such prevent performance degradation of the NDI controller, although errors due to control saturation cannot be prevented by using a NN. Moreover, the addition of a NN makes the controller adaptive such that it is tolerant to system failures. However, NNs have to be trained before used and the compensating power of NNs has its limits. Another addition to NDI is the use of MRAC (Hanson, Schaefer, Burken, Johnson, & Nguyen, 2011; Schaefer, Hanson, Johnson, & Nguyen, 2011). For a flight test performed with intentional errors and simulated failures, the use of MRAC together with NDI showed equal or improved handling qualities and equal or reduced tracking errors compared with NDI only. Nevertheless, the MRAC controller showed some issues regarding PIOs, unpredictable behavior and increased pilot workload. A third addition to NDI is the use of an Extended State Observer (ESO) (Heise et al., 2014). The ESO increases system robustness to errors and uncertainties by estimating the disturbances on the system. Furthermore, this method does improve performance compared with a regular NDI controller. On the other hand, the theory lacks evaluation on various application platforms as well as performance comparisons with other control techniques. Another variation on NDI is INDI, which uses additional feedback signals to decrease model dependency and increase controller robustness. Despite the decreased model dependency, a flight test showed good performance as well as good disturbance rejection properties for the INDI controller (Smeur et al., 2016). However, also this theory lacks evaluation on various application platforms and the theory still contains some assumptions, such as fast actuator dynamics and ideal sensor dynamics, which might not hold on all application platforms (Sieberling et al., 2010).

Based on the review given in this section, NDI offers advantages over classical control theory when used to design FCSs. However, within flight tested designs the performance degradation due to model mismatches and measurement errors, i.e. noise, bias and delay, are apparent disadvantages of NDI. Consequently, researchers are developing solutions for these fundamental flaws. The use of INDI or NNs, MRAC or ESOs in combination with NDI reduces the effect of model mismatches and measurement errors. As discussed above, all solutions are improvements compared with NDI itself, however flaws in each solution still remain. Finally, it is noted by Heise et al. (2014) that the simplicity of the ESO and INDI offers a significant benefit compared with the complexity and nonlinearity of NNs and MRAC regarding certification, verification and validation of the controller.

To limit the extend of the research project not all variations on NDI are considered, similar to the discussion of Section 3-1. The INDI variation on NDI is the main focus of this research. Nevertheless, the literature on NDI in combination with NNs, MRAC and ESOs is still useful, as it serves as reference for the literature studies performed within this part of the report.

3-3 Review on INDI

INDI, also referred to as simplified or modified NDI, is a variation on NDI for which only the incremental control input with respect to the previous timestep is computed instead of the total control input as is done for NDI. See Chapter 2 for the basic theory and principles of INDI. In general, INDI retains the same advantages and disadvantages as NDI. However, INDI depends less on the model compared to NDI such that the sensitivity to model mismatch and uncertainty is decreased. Therefore, INDI also has an increased tolerance to failures compared to NDI. Instead, INDI uses additional feedback signals, as the feedback of state derivatives is used besides the full-state feedback (Sieberling et al., 2010). Similar to the ESO discussed in Section 3-2 the simplicity and reduced model dependency are beneficial considering the certification of the controller (Heise et al., 2014).

The concept of INDI was first described by Smith and Berry (2000), performing a proof of concept test flight using the VAAC Harrier. However, during the flight test issues related to obtaining accurate measurements of the state derivatives required for feedback, in this case the angular accelerations, were observed. The sensed angular accelerations were of poor quality and filtering and differentiating the angular rates led to oscillatory closed-loop behavior. Note that during the flight test only a pitch rate controller was tested. Bacon, Ostroff, and Joshi (2001) further developed INDI by using washout filters to obtain adequate measurements of the angular acceleration. Bacon et al. (2001) comment that, similar to NDI control, actuator saturation is an issue for an INDI controller. Fortunately, multiple methods are known which can alleviate issues regarding actuator saturation in the proposed research. Bacon et al. (2001) manipulated the INDI control laws to reduce the likelihood of actuator rate or position saturation. Moreover, the PCH technique discussed in Section 3-2 can be used to alleviate actuator saturation issues for an INDI controller (Simplício et al., 2013). Besides actuator saturation, Cox and Cotting (2005) indicate that despite the reduced model dependency the INDI controller developed was not robust to estimates in the control effectiveness matrix.

In recent years the INDI methodology has been studied extensively at Delft University of Technology. Sieberling et al. (2010) mathematically proved the increased robustness against model uncertainties of INDI compared with NDI. Moreover, it was shown that the transfer function from command input to output is independent of any uncertainty besides the sign of the control effectiveness matrix. However, to obtain these mathematical derivations Sieberling et al. (2010) used a set of assumptions which might decrease controller performance in reality compared to a simulated environment. Moreover, Acquatella B. et al. (2012) showed that

INDI outperforms NDI regarding certain external disturbances, time delays and uncertainties. Additionally, INDI was successfully used to control spacecraft and helicopters (Acquatella B. et al., 2012; Simplício et al., 2013). Furthermore, Simplício et al. (2013) showed that the frequency at which the INDI controller operates could affect controller performance.

Lately, Smeur et al. (2016) improved the theory on INDI by properly taking into account time delays due to numerical differentiation and by online estimation of the actuator effectiveness. The latter is used to make INDI adaptive and to further reduce model dependency. Smeur et al. (2016) also successfully flight tested the INDI controller using a multirotor Micro Aerial Vehicle (MAV). These flight test proved that INDI can outperform PID for the MAV platform. Moreover, the flight test confirmed excellent disturbance rejection properties, as found in Acquatella B. et al. (2012). Still, the effect that time delays, (slow) actuator dynamics, sensor dynamics, controller frequency and discrete instead of continuous control, have on the performance of an INDI controlled aircraft have to be investigated. Especially, regarding the application platform of a CS-25 certified fixed-wing aircraft, since aircraft like the PH-LAB Cessna Citation are expected to among others have slower actuators, additional data bus and measurement system delays and lower controller frequency than a multirotor MAV.

Part of these issues were investigated by Vlaar (2014), who worked towards the practical application of INDI in a small fixed-wing unmanned aerial vehicle. Eventually, a flight test with INDI was performed during the thesis project, however these results were never published in peer-reviewed literature. The results of Vlaar (2014) confirm that INDI achieves a reduced sensitivity to model mismatch and measurement errors, also in fixed-wing aircraft. Additionally, the research indicates that unsynchronized time delay between the measured actuator position and the estimated angular acceleration can significantly reduced the controller performance. Within the work a very practical solution for the issue is presented, however no additional theoretical background or explanation is described.

Based on the literature review it can be seen that the issues regarding INDI, i.e. time delays, actuator dynamics, sensor dynamics, controller frequency and discrete control, have to be investigated and potentially mitigated if INDI is to be used in a real-world aircraft. Other research areas might aid in finding a solution to these issues. For example, no comments on the combination of INDI control and discrete control were found in literature. Therefore, theory on discrete control applied to other techniques are of interest. Furthermore, there are multiple control techniques that utilize the principle of incremental control, from which results and solutions can be translated to INDI. For example, Lu and van Kampen (2015) comment that the research considering the effect of actuator dynamics on incremental backstepping, as discussed in Lu, van Kampen, and Chu (2015), can also be used in the analysis of INDI. Similarly, an investigation into the effect of time delay on incremental backstepping might also be valuable for the current research (Koschorke, 2012).

3-4 Conclusions and Recommendations

A few decades ago almost all FCSs were developed based on classical, linear control techniques. However, the methodology is: time consuming, expensive, depends on engineering art, difficult to re-use in other airframes, not flexible regarding design changes within the aircraft design and life cycle, difficult to use for high angle-of-attack flight and not tolerant to system failures.

Most of these issues are inherently connected to the nature of the classical techniques and are thus difficult to mitigate. Consequently, industry and academia have shifted towards using advanced, multivariable control techniques to develop FCSs, of which NDI is most popular.

NDI uses a fundamentally different approach by using a global instead of local linearization and therefore mitigates most of the above mentioned issues. However, among other issues NDI requires an accurate model and accurate full-state feedback to be available. These issues are difficult to alleviate using just NDI and therefore researchers have actively researched variations of NDI control. Flight tests have shown that the use of INDI or NNs, MRAC or ESOs in combination with NDI reduces the effect of model mismatches and measurement errors. The relative simplicity of the INDI and ESOs variations is attractive regarding the clearance of FCSs for certification.

In general, INDI retains the same characteristics as NDI, however INDI is proven to be mathematically less sensitive to model mismatches and uncertainties. This is mainly due to the decreased dependency on the model of the to-be-controlled system. Moreover, on multiple occasions INDI has shown to have better disturbance rejection properties than NDI. A flight test of INDI on a multirotor MAV has successfully validated the above described characteristics. Still, the effect of time delays, (slow) actuator dynamics, sensor dynamics and discrete- instead of continuous-time on INDI are not fully accounted for in literature. Especially, regarding the application platform of a CS-25 certified fixed-wing aircraft, like the PH-LAB Cessna Citation, as it is expected to among others have slower actuators, additional data bus and measurement system delays and a lower controller frequency than a multirotor MAV.

Chapter 4

Assessment Criteria for Controller Performance

The report introduction, see Chapter 1, presented the project objective to further develop the theory on Incremental Nonlinear Dynamic Inversion (INDI), particularly with regard to the implementation of INDI in a CS-25 certified fixed-wing aircraft. Chapter 1 also introduced research sub-question 1 stating: "Which criteria and control modes are relevant for assessing the performance of INDI with each other?".

To answer this question, this chapter contains an in-depth review on assessment criteria used in other research. The use of literature is beneficial as it gives insight into the effectiveness of several criteria. Moreover, the compatibility of the research results and conclusions might be improved by selecting assessment criteria used by various other authors as well. This is considered important as many types of Flight Control Systems (FCSs) have been developed and tested. This makes it increasingly difficult to compare new methodologies, such as INDI, with the current knowledge on FCSs. Quantifiable assessment criteria can be used to more easily compare the results of this project with other results. The chapter focuses on assessment criteria used within Nonlinear Dynamic Inversion (NDI) related literature, due to the nature of the project objective. Moreover, the assessment criteria are chosen such that the criteria could be used during a future flight test. As such, this report can serve as a better reference for all contributors to the future flight test.

First, Section 4-1 discusses the control modes available during test flights with the PH-LAB. In view of potential future flight tests with the PH-LAB, the availability of control modes is important as it might potentially exclude the use of specific assessment criteria. Second, Section 4-2 presents all qualitative assessment criteria found in literature. Third, Section 4-3 describes all quantitative assessment criteria found in literature. Finally, Section 4-4 concludes the chapter by answering the posed research sub-question and providing recommendations.

4-1 Available Assessment Methods

This section discusses the control modes available during test flights with the PH-LAB. In view of potential future flight test, the availability of control modes is important as it might potentially exclude the use of specific assessment criteria. For example, to be able to use qualitative handling qualities criteria, the flight test must be executed with a pilot-in-the-loop control mode. The three control modes considered for this research are: pilot-in-the-loop, passenger-in-the-loop and fully automatic.

The pilot-in-the-loop control mode uses a pilot within the cockpit to give real-time inputs to the control system. To give the control inputs either a sidestick controller or control column might be used. Within the PH-LAB the original control column of the citation is used by the experimental Fly-by-Wire (FBW) system to provide commands to the actuators. Therefore, an additional sidestick controller would be required to execute a pilot-in-the-loop experiment. Unfortunately, it is questionable whether a working sidestick can be installed and certified in the cockpit in the near future. Consequently, the use of the pilot-in-the-loop control mode cannot be used during this project.

The passenger-in-the-loop control mode is a slight variation on the pilot-in-the-loop control mode. Again, a human actively gives real-time inputs to the control system, however this time from the cabin instead of the cockpit. This requires some sort of joystick to be available during the flight test. Fortunately, the opportunity to use a joystick within the cabin is still a possibility for this project. The commands given by the passenger can then be send to the experimental FBW system via the flight test computer on which also the experimental controller will run.

Finally, the fully automatic control mode consist of a set of control inputs developed pre-flight. This control mode does not require any joystick for a human to give real-time inputs to the system. The predefined maneuvers can be performed using the flight control computer running the experimental FCS. This control mode is available during the flight test with the PH-LAB aircraft.

Comparing the various assessment methods two comments are made. First, as mentioned in the section introduction only the pilot-in-the-loop mode can be used if qualitative handling qualities are used as assessment criteria. The passenger-in-the-loop control does provide the option to control the aircraft in real-time. However, the passenger-in-the-loop mode cannot realistically represent a pilot situated in the cockpit. Second, both the passenger-in-the-loop and fully automatic control modes have their advantages. The passenger-in-the-loop mode gives more flexibility during the flight test as input signals can be adjusted real-time. The fully automatic mode reduces the amount of hardware and software required. Moreover, standard flight test maneuvers such as the 3211 and doublet maneuvers can be executed more precisely when designed pre-flight.

4-2 Qualitative Assessment Criteria

This section presents all qualitative assessment criteria found in literature. This consists of two types of criteria: observations of system responses, Subsection 4-2-1, and handling qualities, Subsection 4-2-2.

4-2-1 Observations of System Responses

The most used assessment criterion is the observation of system responses. This assessment criterion is used by almost all researchers for both simulation studies and flight tests. In general, especially the response of the Control Variables (CVs) of the experimental FCS are analyzed. This is quite logical as these variables are directly constrained to be constant or prescribed by the FCS system. Moreover, also the input commands given to the system by the FCS are commonly plotted for analysis. Additionally, plots of external influences, such as the phenomena discussed in Chapter 5, on the system to clarify any unexpected control behavior are also used to support the results. Finally, it is noted that most system responses are presented in the time domain. However, also system responses in the frequency domain are used to present results.

The use of observations is beneficial especially for flight tests due to the reduced repeatability of this type of study. Many controllers are only flight tested once or twice making it difficult to properly use some of the quantitative criteria. Additionally, observations can be used to show outlying behavior due to specific events that occurred. Moreover, the use of observations is useful to provide results on phenomena difficult to capture in quantitative methods, see Section 4-3.

In general, most researchers use observations in combination with one or more quantitative assessment criteria to support the research conclusions. However, interestingly quite some researchers use observations as only assessment criteria to back-up the project conclusions (Smith & Berry, 2000; Johnson & Kannan, 2005; Lombaerts & Looye, 2012; Acquatella B. et al., 2012; Smeur et al., 2016). Although these researchers still properly support their conclusions, the compatibility of their results with other research might be decreased.

Therefore, the current project uses observations of system responses of system input, CVs and/or external influences to support the conclusions of the report. However, it is considered beneficial to select at least one other quantitative assessment criteria to further support the conclusions.

4-2-2 Handling Qualities: Cooper-Harper Rating (CHR)

The second qualitative assessment criterion used within literature is the Cooper-Harper Rating (CHR). The CHR, introduced by Cooper and Harper Jr. (1969), is a scale from 1 to 10, with 1 being best and 10 worst, that pilots can use to evaluate the handling qualities of an aircraft. Note that the handling qualities of an aircraft are defined as: "those qualities or characteristics of an aircraft that govern the ease and precision with which a pilot is able to perform the tasks required in support of an aircraft role" (Cooper & Harper Jr., 1969, p. 2). Despite being a numerical assessment criterion, the criterion is still considered qualitative as it is solely based on pilot opinion. The qualitative evaluation of the handling qualities of an aircraft as its definition directly relates the handling qualities to the pilot. This is also seen in literature, as the use of the CHR scale is popular during flight tests of NDI based controllers (Brinker & Wise, 2001; Walker & Allen, 2002; Bosworth & Williams-Hayes, 2007; Burken, Hanson, Lee, & Kaneshige, 2009; Hanson et al., 2011; Miller, 2011b; Schaefer et al., 2011; Walker, Wurth, & Fuller, 2013).

While using the CHR, it is quite common that different pilots give different ratings to the same aircraft or control law, see e.g. Miller (2011b). This variance in CHR confirms the qualitative characteristic of the rating scale. The variance in rating and the qualitative nature of the CHR also clarifies that it is important that the scale is only used by pilots seated within a proper cockpit. Otherwise, the change in the pilot's environment might cause a change in the pilot's judgment, creating confounds in the research.

Concluding, the use of CHR is not appropriate for the current project. On the other hand, based on decades of experience with flight testing also quantitative measures of handling qualities have been developed. These quantitative measures might be useful for the current project and are discussed in Subsection 4-3-3. Still qualitative handling qualities are considered important for piloted aircraft. Therefore, the use of the CHR is recommended for future research.

4-3 Quantitative Assessment Criteria

This section presents all quantitative assessment criteria found in literature. This consists of six types of criteria: closed-loop eigenvalues, Subsection 4-3-1, gain and phase margin, Subsection 4-3-2, handling qualities, Subsection 4-3-3, performance objectives, Subsection 4-3-4 and Root Mean Square (RMS) tracking error, Subsection 4-3-5. Finally, Subsection 4-3-6 recaps all criteria and selects the quantitative assessment criteria to be used in this project.

4-3-1 Closed-loop Eigenvalues

The concept of closed-loop eigenvalues was developed within linear system theory (Nise, 2011). For linear systems, the behavior of the system is characterized by the eigenvalues of the system matrix commonly denoted by A. The concept of eigenvalues can also be extended to nonlinear control system, such as INDI, by linearizing the closed-loop system locally. Afterwards, the eigenvalues of the system can be determined and analyzed using linear methods. Based on the eigenvalues, the natural frequency and damping ratio of the eigenmotion of the aircraft can be determined. Moreover, the local stability properties of the system can be analyzed using the closed-loop eigenvalues.

The assessment criterion is only used by one other author with regard to an NDI or INDI controlled system (Simplício, 2011). Therefore, the use of this criterion does not directly have any benefits regarding compatibility with other NDI related research. On the other hand, traditional aircraft requirements, which remain in use as guidelines nowadays, define certain ranges of suitable natural frequencies and damping ratios for closed-loop systems (Anon., 1997). Thus, the use of closed-loop eigenvalues does increase compatibility with the knowledge on FCSs in general.

4-3-2 Gain and Phase Margin

The concept of gain and phase margins were also developed within linear system theory (Nise, 2011). Therefore, similar to the closed-loop eigenvalues the system has to be linearized and the linear system response can be validated with the original nonlinear system (Vlaar, 2014).

The use of gain and phase margins provide a sense of robustness of the closed-loop system with respect to instability (Bacon & Ostroff, 2000; Cox & Cotting, 2005). Similarly, the system robustness with respect to model uncertainties can be performed using the concepts of gain and phase margin (Bosworth, 2008). Additionally, the concept can also be used to test the systems robustness with respect to time delays (Bacon & Ostroff, 2000; Miller, 2011b). All analysis can be performed with respect to a combination of one system input and one system output.

The assessment criterion is used by many authors as already seen by the variety of authors cited in the previous paragraph. Moreover, similar to the closed-loop eigenvalues years of linear FCS experience has created a database of reference values for gain and phase margins. Therefore, the use of gain and phase margins would increase compatibility with both the knowledge on FCSs in general and with other research on NDI based controllers.

4-3-3 Handling Qualities

The concept of handling qualities was already introduced in Subsection 4-2-2 from a qualitative point of view. This section discusses quantitative methods developed based on decades of flight test and handling quality experience. The benefit of using quantitative methods is that the pilot-in-the-loop control mode is not specifically required. Therefore, quantitative handling quality criteria can potentially be used in the current project. On the other hand, it has to be noted that by definition handling qualities are subjective and the quantitative criteria can only predict the handling qualities obtained by the system.

Bandwidth The first quantitative handling quality criterion discussed is the bandwidth criterion. This criteria is based on the frequency response of the closed-loop system, similar to the gain and phase margin discussed in Subsection 4-3-2 (Walker & Allen, 2002; Miller, 2011b). Specifically, the bandwidth criterion uses a specific definition of bandwidth combined with the phase delay of the response. A big advantage of this criterion is that a Pilot Induced Oscillation (PIO) prediction can be based on the closed-loop bandwidth (Miller, 2011b). Despite being used by only two researchers, the bandwidth criteria does offer compatibility with general FCS guidelines (Anon., 1997).

Inter-axis coupling The inter-axis coupling criterion is used in a single flight test of NDI based controllers (Schaefer et al., 2011). The criterion is originally derived from helicopter handling quality characteristics, as helicopters naturally suffer from inter-axis coupling more than fixed-wing aircraft. Therefore, Schaefer et al. (2011) already note that the baseline nominal NDI controller used is assumed to have negligible cross coupling. However, as the research investigates simulated failures, which can cause inter-axis couplings, the criterion was still of use. The criterion does lack compatibility with other research and general FCS guidelines.

Lower Order Equivalent System (LOES) Lower Order Equivalent System (LOES) approximates a parametrized model from the flight test data (Miller, 2011b). Parameters might include the Control Anticipation Parameter (CAP), damping ratios, natural frequencies, equivalent time delays and roll mode time constants (Walker & Allen, 2002; Miller, 2011b; Tang, 2014). Note that these parametrized models are generally based on models and transfer functions developed with linear control theory. These traditional parameters, as defined in general FCS guidelines, can be used for handling quality assessments (Anon., 1997). Thus, the criterion is compatible with general FCS guidelines.

Gibson's criteria Gibson's criteria are a set of five criteria used to evaluate the short period mode of the aircraft: the dropback ratio, flight path delay, maximum pitch rate value, time to reach the first peak and time to reach steady state (Steer, 2003; Tang, 2014). The advantage of this set of criteria that all five can be determined directly from the system response. The method has been developed based on a graphical visualization from a pilot's perspective (Gibson, 1999). Moreover, as the criteria are determined from the system response, the method is suitable for nonlinear systems without requiring a linearization. Gibson's criteria have been added to general FCS guidelines with the latest update of these guidelines (Anon., 1997).

Input trace Similar to the inter-axis coupling criterion the input trace criterion is only used by Schaefer et al. (2011). Again, the criterion mainly targets the effect caused by simulated failures during the flight test. The pilot controlling the aircraft adapts to these simulated failures and the input trace of the stick position can be used to analyze the pilot's adaptivity. The criterion does lack compatibility with other research and general FCS guidelines.

Maximum Unnoticeable Added Dynamics (MUAD) Maximum Unnoticeable Added Dynamics (MUAD) are defined by an envelope around the frequency response of the nominal system reference model (Bosworth & Williams-Hayes, 2007; Bosworth, 2008; Miller, 2011b). The MUAD envelope is defined such that the experienced handling quality remain equal as long as the true flight tested system response remains within the envelope. The benefit of using the MUAD criterion is that the nominal system response and MUAD envelope can be computed with a given lower-order system. The metric is also effective when used to test whether simulated failures and adaptive system affect the handling qualities (Bosworth & Williams-Hayes, 2007; Bosworth, 2008). Moreover, the lower-order system required can be used in combination with other metrics described in this section to gain additional insight into the handling quality characteristics of the system.

Neal-Smith criterion The last quantitative handling quality criterion described is the Neal-Smith criterion. This criterion is based on a simple pilot model to estimate the pilot-in-the-loop system response (Miller, 2011b). The observed resonant peak and required pilot lead compensation are then used to determine the handling qualities of the aircraft. The criterion is only used by one author related to NDI based flight tests. Moreover, the criterion is not compatible with the general FCS guidelines.

4-3-4 Performance Objectives

The concept of performance objectives is quite broad and can best be compared with specific requirements put on the FCS by its designer. Performance objectives are found in the form of more traditional parameters such as rise time, overshoot and settling time of the CVs (Wang & Stengel, 2000; Vlaar, 2014). Moreover, performance parameters setting absolute or rate limits on aerospace variables such as pitch angle, airspeed, bank angle, sink rate and vertical velocity are also used (Bauschat et al., 2001; Looye, Joos, & Willemsen, 2001; Schierman et al., 2004). In general, the performance parameters are used to support either Monte-Carlo analysis of the probability of achieving the set performance objectives or to support controller optimization processes (Wang & Stengel, 2000; Looye et al., 2001; Schierman et al., 2004). The concept of performance objectives is used by multiple authors, however almost all authors use their own set of objectives. Therefore, the use of this criteria does not directly benefit the compatibility of the project with previous research. Depending on the objectives selected their might be additional compatibility with general knowledge on FCSs.

4-3-5 Root Mean Square (RMS)

The final assessment criterion discussed is the RMS along the time domain of certain variables such as the input signal or tracking errors. Note that compared to the average, an advantage of the RMS is that the variance of the signal is also taken into account (Sieberling et al., 2010). The RMS offers direct support for the qualitative observations with concrete quantity improving the ease and quality of analysis. The RMS is used on the pilot's input trace as criterion for physical workload (Tang, 2014). Furthermore, the RMS is used on the tracking error of CVs to assess controller accuracy (Burken et al., 2009; Sieberling et al., 2010; Wedershoven, 2010; Hanson et al., 2011; Schaefer et al., 2011; Simplício, 2011; Tang, 2014).

Two variations on the RMS were found in literature. The mean and standard deviation of the RMS can also be used as criteria (Burken et al., 2009). Additionally, the accumulated tracking error within a certain time interval is also used as criteria (Hanson et al., 2011; Schaefer et al., 2011). Finally, similar to the performance objectives of Subsection 4-3-4, the RMS is also used to support batch simulations (Sieberling et al., 2010). The use of this criterion does not increase compatibility with general knowledge on FCSs.

4-3-6 Quantitative Criteria Selection

The previous subsections presented multiple quantitative controller assessment criteria that can be selected to be used in the current project. Although all criteria have some distinctive characteristics, there does not seem to be a best criteria to be selected. However, using all criteria is not feasible due to the time constraints on the project.

The RMS criterion is selected to support the qualitative assessment of the to-be-designed controllers. This criterion can directly give a measure of controller accuracy and performance, while other criteria give an indication on robustness margins and handling qualities. Considering the main goal to implement INDI in an aircraft while preventing performance degradation, the controller accuracy and performance is deemed of primary interest. Moreover, an advantage of the RMS criterion is that it can directly be used by all control systems, without requiring a linearization or parameter estimation.

4-4 Conclusions and Recommendations

There are two control modes available on the PH-LAB are: passenger-in-the-loop and fully automatic. The pilot-in-the-loop mode is not feasible as this would require an additional sidestick controller in the cockpit. The passenger-in-the-loop gives more flexibility during flight testing as it allows for real-time input. On the other hand, the fully automatic control mode reduces the amount of hardware and software required. Additionally, specific flight test maneuvers can be executed more accurately using the fully automatic control mode.

The assessment criteria chosen for this project consist of a mix of qualitative and quantitative criteria. Note that the use of some criteria is not feasible as the pilot-in-the-loop control mode is not available. Although the use of the CHR is not feasible within the current project, the use of the CHR is recommended for future research. This recommendation is based on the notion that qualitative handling qualities for piloted aircraft, like the PH-LAB Cessna Citation, is important.

Observations of system responses of system input, CVs and/or external influences are used to support the conclusions of the report. Additionally, these observations are supported by using the RMS of the variables plotted to provide additional insight into the controller performance and accuracy. The combination of criteria can be used for all types of control systems as only the system inputs and outputs have to be measured.

Chapter 5

Real-World Phenomena to be Investigated

The report introduction, see Chapter 1, presented the project objective to further develop the theory on Incremental Nonlinear Dynamic Inversion (INDI), particularly with regard to the implementation of INDI in a CS-25 fixed-wing aircraft. Chapter 1 also introduced research sub-question 2 stating: "Which phenomena should be included within a simulated environment to emulate reality?". To answer this question, this chapter contains an in-depth review on phenomena causing issues within Flight Control Systems (FCSs), which were observed or mitigated during flight tests documented in literature. Moreover, methods documented in literature to implement these issues within a simulation environment are discussed. The chapter focuses on flight test performed with Nonlinear Dynamic Inversion (NDI) related based controllers, due to the nature of the project objective.

The relevance of this chapter can for example be seen during the initial development of INDI. An INDI controller developed by Smith (1998) showed promising results within a simulated environment, which eventually resulted in a proof of concept flight test with a pitch rate controller based on INDI (Smith & Berry, 2000). However, during the flight test unexpected issues regarding poor quality of sensor measurements and drifting effects were observed. Thus, the simulation environment developed by Smith (1998) did not emulate reality as well as expected. In general, reality may contain phenomena which might go overlooked within a simulated environment. Therefore, identifying the phenomena required to model reality are key for a successful offline analysis. Especially, since availability and costs regarding flight tests, make it difficult to perform multiple iterations within the execution of the flight test.

The literature presented in this section is grouped within various topics. First, Section 5-1 presents literature on bias, i.e. constant disturbances. Second, Section 5-2 discusses literature on discretization, an effect of digital control. Third, Section 5-3 describes literature on model mismatches caused by uncertainties or system changes. Fourth, Section 5-4 shows literature on noise, i.e. random disturbances. Fifth, Section 5-5 reviews literature on time delays within FCSs. Finally, Section 5-6 presents a brief discussion leading up to the conclusions answering the posed research question.

5-1 Bias

This section discusses the topic of bias, which is defined to include all constant disturbances that can affect the FCS. Three studies discuss the topic of bias with regard to flight test results. First, Schierman et al. (2004) comments on atmospheric disturbances and wind to affect controller performance for a controller with a dynamic inversion inner loop. Despite thorough offline analysis with regard to these issues, the controller still was not able to cope with severe wind conditions. Second, Johnson and Turbe (2006) comment that the exclusion of atmospheric disturbances, including bias, within simulation resulted in a reduced performance during a flight test of a controller combining Neural Networks (NNs) with NDI. Third, Lombaerts and Looye (2012) show that the inclusion of wind as a constant disturbance to airspeed in simulation was used to develop an NDI controller which successfully attenuated bias during the flight test. Note that Lombaerts and Looye (2012) use the German Aerospace Center (DLR)'s ATTAS aircraft as flight test vehicle, which is also an adapted fixed-wing aircraft like the PH-LAB Cessna Citation.

The studies mentioned above take into account constant disturbances that serve as input to the airframe. Note that Smeur et al. (2016) also planned to test this phenomenon on an INDI controller by generating artificial indoor aerodynamic disturbances. These disturbances would be realistic, however due to repeatability issues this test was not performed. Instead, additional weight was added to the airframe during flight to simulate the effect of bias as input to the airframe. This weight addition can also be considered a model mismatch, discussed in Section 5-3.

In general, literature adds bias as input to the airframe, however bias can also be added to the measured feedback signals. For example, Johnson and Turbe (2006) indicate that a bias on the measurement signals due to erroneous GPS measurements caused a performance reduction during flight testing. Moreover, two recent studies on INDI control in a simulated environment take bias on measured feedback signals into account (Falkena, Borst, Chu, & Mulder, 2011; Acquatella B. et al., 2012).

For the current research project, both bias as input to the airframe and bias as addition to the measured feedback signals are considered important to be included in the simulated environment. This importance is mainly based on the negative effect of both types of bias observed in multiple flight tests of NDI based controllers. Therefore, potential problems regarding bias during the flight test can be mitigated by examining these problems in simulation. Fortunately, by definition bias can simply be added as a constant value to one or more variables within the simulation. The effect can be analyzed for each signal separately to increase the accuracy of the analysis.

Both types of bias can also be encountered during a flight test with the PH-LAB Cessna Citation. Still, it would depend on some uncontrollable factors whether effects due to bias actually are observed. For example, the occurrence of bias due to a steady wind depends on the weather during testing, which cannot actively be controlled. Furthermore, the occurrence of bias in measurement signals depends on the sensors used and the calibration of these sensors. The uncertainty regarding the occurrence of both types of bias stresses the importance of including the bias phenomenon in the simulation environment.

5-2 Discretization

This section presents the topic of discretization, which is the result of the use of digital (flight) control systems. In general, most researchers perform their studies in the continuous time domain and do not specifically consider the effects of the discrete time domain on controller performance. Unfortunately, all control system have to be discretized in order to be implemented in a Fly-by-Wire (FBW) system. Nise (2011) already indicates that the discretization of a control system can influence its performance and even its stability properties.

The negative effect of discretization is also confirmed by two different research projects. Bauschat et al. (2001) indicate that errors due to quantization on measurements observed during flight tests resulted in a setback within the research program, as this issue was not included within the simulation model. Note that the research program tested an autopilot with NDI inner loop. Similarly, Johnson and Turbe (2006) observed that quantization errors on measurements, not included within the simulation model, resulted in degraded performance during flight testing. Lombaerts and Looye (2012) also include these quantization effects on some feedback signals within the simulation model, however no comments on the effect of the quantization of measurements on the results were made. The two flight test programs testing INDI controllers do not comment on the quantization effects of measurements.

Besides the quantization of measurements, also controller frequency is mentioned in literature as potential phenomenon affecting INDI control performance due to discretization (Simplício et al., 2013). Simplício et al. (2013) first notice issues with controller performance due to frequency when the frequency dropped to 60 Hz. Contrary, in the work of Smeur et al. (2016) no issues related to controller performance were found during a flight test with a controller running at a frequency of 512 Hz.

For the current research project, only the controller frequency phenomenon seems to be of interest. Carefully revising literature on quantization errors shows that these issues were mentioned by a study performed in 2001 (Bauschat et al., 2001), 15 years ago, and a study using a Micro Aerial Vehicle (MAV) (Johnson & Turbe, 2006). Therefore, both studies were relatively limited in computational resources compared to today's standard in aircraft, which can be the main cause of the quantization errors. This is also confirmed as a study in 2012 on a platform similar to the PH-LAB Cessna Citation does not mention any issues related to quantization of measurements (Lombaerts & Looye, 2012). Therefore, the inclusion of quantization errors does not seem important for the proposed research.

Due to the nature of INDI control as incremental control technique, controller frequency has shown to have a significant effect on controller performance. The effect of controller frequency is also confirmed within the theoretical derivation of INDI control, as instantaneous control inputs and actuator deflections are assumed (Sieberling et al., 2010). Obviously, lower frequencies are less instantaneous than higher frequencies, thus invalidating the assumptions made. Therefore, it is concluded that the research can benefit from investigating this effect in simulation. Especially, since INDI is integrated into the PH-LAB Cessna Citation as a digital FCS running at a certain frequency. This means that the simulation should be ran with a specified fixed step size for both the airframe model as well as the controller model, instead of a variable step size. Note that continuous time can be emulated for the airframe model by selecting a small variable step size with high order nonlinear solver.

5-3 Model Mismatches

This section presents the topic of model mismatches, which result from uncertainties within the model or system changes. The effect of uncertainty within the aircraft model used was demonstrated during a flight test of a baseline NDI controller (Miller, 2011a). A small deviation between the modeled and true pitch surface effectiveness, i.e. a uncertainty, caused a noticeable effect on the pitch handling qualities. Similarly, Bosworth and Williams-Hayes (2007) show that the response of an NDI controller deviates from the desired response and even produces Pilot Induced Oscillation (PIO) tendencies due to a simulated failure. On the other hand, a flight test with NDI controller artificially changing the system by destabilizing the plant also showed a reduced controller performance (Bosworth, 2008).

The effect of model uncertainties in pitch control effectiveness was also investigated in the first flight test of INDI (Smith & Berry, 2000). During the flight test both an increase and decrease in modeled control effectiveness caused the aircraft behavior to change significantly. As already mentioned in Section 5-1, Smeur et al. (2016) tested a change in model mass and model mass distribution. These test concluded the successful rejection of these deviations within the controlled system.

For the current research project, model mismatches are not considered to be of primary interest. Although this section does discuss multiple flight tests reporting issues regarding model mismatches, all issues besides Miller (2011a) were due to simulated uncertainties or simulated failures. Therefore, it is considered more important to focus on the non-artificial phenomena that can affect controller performance. On the other hand, INDI was developed to improve the robustness of NDI based controller, thus testing model mismatches on an aircraft can still be of added value.

Model uncertainties can be incorporated by changing properties of the to-be-controlled system. For example, the inertia matrix or the overall mass distribution of the system can be changed (Acquatella B. et al., 2012; Smeur et al., 2016). Moreover, the high fidelity model can be analyzed and simplified to a lower fidelity model to emulate a limited amount of knowledge. During the planned flight test, simple tricks like changing the weight distribution of the aircraft, see Smeur et al. (2016), can be used to create model mismatches.

Failures can be simulated during a flight test by for example locking a control surfaces or by limiting the power of an engine (Schaefer et al., 2011; Heise et al., 2014). Note that simulated failures have not been discussed in flight tests performed with INDI controllers. However, research regarding failures is limited as pilots of the PH-LAB Cessna Citation can only control the engines, speedbrakes, gears, and flaps, while the FBW system is used to test an experimental controller. On the other hand, there is of course always a possibility that systems fail during the flight test unexpectedly.

5-4 Noise

This section discusses the topic of noise, which is defined to include all random disturbances that affect the FCS. Analogous to bias discussed in Section 5-1, which included all constant disturbances, atmospheric disturbances also cause random external disturbances that serve as input to the airframe. The same researchers that commented on the phenomenon of bias also comment on the issue of noise. Schierman et al. (2004) again despite a thorough offline analysis notes that the controller was not able to cope with severe turbulent conditions. Johnson and Turbe (2006) comments that the exclusion of atmospheric disturbances, including noise, within simulation resulted in a reduced performance during flight tests. Finally, also Bauschat et al. (2001) comment that issues related to high levels of turbulence negatively affected the controller performance during their flight test.

Additionally, two flight test programs confirm that noise can also act upon measured feedback signals. First, Lombaerts and Looye (2012) states that the first flight performed failed due to noise in the lateral accelerometer. Flight test could only continue after partial redesign of the NDI controller. Second, as mentioned in the introduction Smith and Berry (2000) already showed that INDI can be sensitive to sensor noise when implemented in reality. This was later also confirmed in a simulation environment (Falkena et al., 2011). An example of noise magnitudes for various feedback signals that can be used for platforms like the PH-LAB are presented by Wedershoven (2010), who performed simulation studies on both NDI and INDI.

For the current research, both noise as input to the airframe and noise as addition to the measured feedback signals is considered important. Adding a randomly generated signal to either the airframe input or measured feedback signals is beneficial as it facilitates the analysis of the effects of noise before the controller is flight tested. Fortunately, by definition noise can simply be added as a random number with specified mean and variance to one or more variables in the simulation. Similar to bias, the noise can be applied to various feedback signals separately as well. Again, this increases the accuracy with which the performance of the controller can be analyzed, such that more valid conclusions can be drawn.

The occurrence of noise during the flight test with the PH-LAB Cessna Citation is still uncertain. Similar to bias, this depends on the weather conditions and the sensors used by the aircraft. This uncertainty regarding the occurrence of both types of noise again stresses the importance of including the phenomenon of noise in the simulation environment. Moreover, sensor noise is a common phenomena and additionally the rate gyro signals have to be differentiated to obtain rotational acceleration, see Chapter 6. The differentiation will further amplify the noise underlining the importance of including noise in the simulated environment (Smeur et al., 2016).

5-5 Time Delay

This section presents the topic of time delay, which can have a significant negative influence on the performance of FCSs. For example, during the development of an NDI controller for the X-35, the predecessor of the F-35, pilot induced oscillations occurred due to large time delays within the system (Walker & Allen, 2002). This is also confirmed by the research of Burken et al. (2009), which concludes that delays as small as 0.05 seconds can cause constant errors within the closed-loop system. Moreover, time delay can also be the result of the designed control due to the use of numerical filters (Smeur et al., 2016). However, time delay is still left out of simulation environments within many researches, despite the significant effect that others observe.

The importance of including time delays within the simulated environment is also confirmed by previous research on INDI control (Sieberling et al., 2010; Smeur et al., 2016). The difference in time delay between the feedback of the state derivative and actuator position can have a detrimental effect on controller performance. Additionally, other incremental control methods display the high sensitivity to a mismatch in time delay (Koschorke, 2012).

Time delay is considered the most important phenomenon to include within the simulation environment for this project. Contrary to bias, discretization and noise, which in general only caused a decrease in controller performance, time delays can create PIOs. Moreover, seemingly small delays of 0.05 seconds can already cause persistent errors. Simulating time delay is fairly straightforward as signals can simply be delayed a few time steps. As discussed by Falkena (2012) these time delays can be introduced within sensors, actuators and the digital control system itself. Within the PH-LAB Cessna Citation, time delays will occur naturally, due to either signal filtering, similar to Smeur et al. (2016), or pure time delays within the FBW system and data buses.

5-6 Conclusions and Recommendations

This section discusses the conclusions that can be drawn regarding the research question: Which phenomena should be included within a simulation environment to emulate reality? First of all, note that the PH-LAB Cessna Citation is a certified flight testing aircraft for testing experimental controllers. Therefore, the inclusion of phenomena in the simulation environment is purely focused on obtaining the best results instead of ensuring safety. Obviously, the inclusion of all phenomena discussed within this paper would never harm the outcome of the research. However, including all phenomena has its disadvantages as it would result in a tedious.

Therefore, it is concluded that the following phenomena are included within the simulation environment emulating reality:

- Bias, i.e. a constant disturbance, should be included as input to the simulated airframe as well as within each measured feedback signal separately;
- Discretization effects should be included by analyzing the controller frequency of the simulated controller, while quantization effects on each measured feedback signal can be disregarded;
- Model mismatch in the form of uncertainties and system changes can be disregarded;
- Noise, i.e. a random disturbance, should be included as input to the simulated airframe as well as within each measured feedback signal separately;
- Time delay should be included within the actuator dynamics as well as within each measurement signal separately.

Note that time delay is considered the most important phenomenon as literature has shown stronger effects regarding controller performance due the time delay than due to bias, discretization or noise. Furthermore, it is recommended that the fault tolerant properties of INDI be flight tested within an aircraft in future research.

Chapter 6

INDI FCS Design

This chapter contains the detailed theory required to eventually design a Flight Control System (FCS) for an aircraft using Incremental Nonlinear Dynamic Inversion (INDI). The content of this chapter can be used in the remainder of the thesis to answer the sub-question 4: "Which measures are required to prevent any observed performance degradation?". As such, this chapter presents measures suggested in literature to prevent any performance degradation observed in other research on INDI. The content of this chapter builds upon the basic Nonlinear Dynamic Inversion (NDI) and INDI theory and principles as discussed in Chapter 2. Additionally, the issues and phenomena discussed in Chapters 3 and 5 are used starting point for the literature study.

The outline of this section is as follows. First, Section 6-1 discusses both the bias and model mismatch phenomena. Second, Section 6-2 discusses all theory related to sensor noise. Third, Section 6-3 describes the theory related to actuators and also the control saturation that is associated with actuators. Fourth, the issues related to time delay are presented in Section 6-4. Finally, Section 6-5 discusses the conclusions and recommendations of this chapter.

6-1 Bias & Model Mismatches

This section discusses both the bias and model mismatch phenomena. INDI was developed with the purposed to increase the robustness to model mismatches with respect to NDI. The mathematical derivation supporting this claim can be found in Section 2-5 and in literature, see Section 3-3. In practice the claim does not always hold, as for example Smeur et al. (2016) uses an adaptive control effectiveness matrix. Still, it is assumed that the inherent properties of INDI prevent performance degradation.

Part of the bias phenomena as discussed in Section 5-1 is inherently rejected by the INDI controller. As such, it is assumed that most types of bias do not cause performance degradation due to inherent properties of INDI. Acquatella B. et al. (2012) concludes that a basic INDI controller, contrary to NDI, fully rejects the constant external disturbances. Moreover, it has been mathematically proven that disturbances in the state derivatives are rejected provided that the actuator dynamics are stable (Smeur et al., 2016). This effect is only noticeable over time, such that only the constant long term disturbances, i.e. bias, are rejected. On the other hand, the short term disturbances, i.e. noise, were not proven to be rejected. Besides bias in state derivatives, Section 5-1 also considered bias in sensor measurements. Fortunately, bias on the Control Variables (CVs) of the inner loop are compensated for by the outer loop (Simplício, 2011).

6-2 Sensor Noise

This section discusses all theory related to sensor noise. The theory of Section 2-2 already introduced the notion that INDI requires the derivative of the CVs to be measured. For continuous-time INDI controller these CVs derivatives can be obtained using various methods (van 't Veld, 2016). However, as discussed in Part I and Chapter 7 this report uses a discrete-time INDI controller, which inherently uses a first-order difference approximation.

The use of signal differentiation is important to consider regarding the noise phenomenon, as the differentiation of a noisy signal amplifies this noise (Smeur et al., 2016). Fortunately, the actuator dynamics already act as low-pass filters within the INDI setup, alleviating noise issues (Falkena et al., 2011). Still, additional signal filtering is probably required to completely mitigate noise issues. However, signal filtering does add artificial delays to the system, this is further discussed in Section 6-4. An overview of filter methods used in literature in combination with a first-order difference scheme are as follows:

- No filter (Bacon, Ostroff, & Joshi, 2000; Vlaar, 2014)
- First-order low-pass filter (Wedershoven, 2010; Simplício, 2011; Acquatella B. et al., 2012)
- Second-order low-pass filter (Wedershoven, 2010; Vlaar, 2014; Smeur et al., 2016)
- Two low-pass filters, before and after differentiation (Smith & Berry, 2000)

Two methods from the list above have been flight tested together with INDI, all approximating the angular accelerations. Smith and Berry (2000) has flight tested the use of two low-pass filters, before and after differentiation. Smeur et al. (2016) flight tested INDI using a second-order low-pass filter. Note that both methods were flight tested successfully. A choice between these options based on literature is difficult due to the similarity between the options. Therefore, this choice is not made based on literature study, but on the performance of the filters within the simulated environment.

6-3 Actuator Dynamics & Control Saturation

The state-of-the-art review on INDI, see Section 3-3, concluded that the effect of (slow) actuator dynamics is not fully accounted for in literature. This issue is caused by the assumption of instantaneous control surface deflections of the to-be-controlled system (Sieberling et al., 2010). Additionally, the absolute and rate limits on a system's control surfaces cause control saturation. When subjected to control saturation, the controls do not comply with the assumption of instantaneous deflections. Note that the issue of control saturation also causes performance degradation for NDI control.

Unfortunately, literature on control saturation and NDI has not yet found a solution completely eliminating the issues. The most intuitive solution to avoid control saturation is to scale down the commands given to the controller to a level achievable by the controller. However, adapting the commands also negatively affects the controller performance. Moreover, it might be difficult to determine the exact input still achievable by the controller. For example, Ostroff and Bacon (2002) adaptively penalizes the control allocation methodology used to avoid control saturation for an INDI controller. However, the methodology used cannot prevent that saturation limits are violated. Moreover, adaptive features have an additional downside related to certification clearance, see Chapter 1. Alternatively, Lu et al. (2015) presents the use of actuator compensation for another incremental control method, incremental backstepping, to avoid the assumption of instantaneous actuator dynamics. As the method is also based on incremental inputs the compensator might be feasible in combination with INDI, however this has not been proven in literature.

At this moment Pseudo Control Hedging (PCH) seems to be the most promising method to alleviate the issues related to control saturation in NDI and INDI controllers. The PCH method was originally developed to support Neural Network (NN) controller and aims at compensating for actuator dynamics and control saturation by modifying a reference model signal. (Johnson & Calise, 2000). The signal modification is performed by computing the difference between the desired virtual input and actual virtual input achieved by the system. The combination of PCH and INDI has been implemented within a simulation environment successfully (Simplício et al., 2013). Moreover, PCH has also performed a successful test flight together with NDI (Lombaerts & Looye, 2012).

PCH is effective in reducing the level and duration of control saturation, however it cannot eliminate it (Lam, Hindman, Shell, & Ridgely, 2005). An additional advantage is that the PCH methodology can be combined with the time-scale separation principle. Furthermore, when control saturation occurs in one of the CVs, PCH can prevent performance degradation of the non-saturated CVs. Without the use of PCH, the performance regarding all CVs will degrade as INDI is a multivariable method computing control inputs for all CVs simultaneously. Additionally, PCH could potentially be a useful addition to the inner-loop acting as an anti-windup technique for the PI-controller used to compute the virtual control input (Lombaerts & Looye, 2012).

6-4 Time Delay

The state-of-the-art review on INDI of Section 3-3 concluded that another issue not yet fully accounted for in literature is the issue of time delay. Moreover, the significant effect of time delay within an INDI based control system is described in Section 5-5. Especially within a relatively large platform as the PH-LAB aircraft, the total accumulated time delay can become significant. Furthermore, Section 6-2 already concluded that some sort of filter will be used within the INDI controller adding additional artificial delay. As discussed in Section 3-3 the most important issue regarding delay is the difference in delay between the estimated angular acceleration and measured actuator deflections. Throughout the remainder of the report this specific delay is referred to as unsynchronized delay.

The first solution posed in literature for these issue is the use of the predictive filter, see also Section 6-2. However, disadvantages of the predictive filter are that it has to be trained and that it is not robust regarding noise. Therefore, the use of a simpler first- or second-order filter is preferred, but this choice will add artificial delays to the system. Fortunately, Smeur et al. (2016) has flight tested and as such proven that the additional artificial delays can correctly be taken into account by filtering both the gyro and actuator measurement with a filter with similar dynamics. As such, the artificial delay added to both signals is equal avoiding the unsynchronized time delay issues.

Unfortunately, using similar filters only solves the issues regarding the artificial delay added to the system, hence the natural delays within the system remains. For these delays the work of Vlaar (2014) provides a very practical trial-and-error solution by estimating the difference in natural delay between the estimated angular accelerations and measured actuator deflections. The estimation is performed with a hardware in the loop test and assumes that the delay is constant. The estimated difference in unsynchronized time delay is then artificially added to one of the signal channels.

6-5 Conclusions and Recommendations

This section presents the conclusions and recommendations regarding the detailed theory on INDI required to design a FCS. The chapter concluded that for model mismatches and some types of bias performance degradation is inherently prevented. The types of bias include the external disturbances to the airframe as well as measurement bias on the inner loop CVs signals. Thus, no solutions are required to mitigate the effect of these phenomena. Still, bias on other feedback signals used may cause performance degradation.

Moreover, to compensate for sensor noise, mostly due to the numerical differentiation of the CVs required, three filters were proposed. These three methods are: a first-order low-pass filter, a second-order low-pass filter and two low-pass filters. A choice between these options could not be made based on literature and should be based on simulation results.

Furthermore, to compensate for control saturation PCH is selected. Although PCH cannot completely eliminate the issues related to saturation, PCH is effective in reducing the level and duration of control saturation. Furthermore, when control saturation occurs in one of the CVs, PCH can prevent performance degradation of the non-saturated CVs. Additionally, PCH could potentially be a useful addition to the inner-loop acting as an anti-windup technique for the PI-controller used to compute the virtual control input.

Regarding time delay, especially the unsynchronized time delay between the measured control surface deflections and estimated angular accelerations are of interest. This unsynchronized delay can be compensated for by filtering both signals with the same filter dynamics. Moreover, natural time delay between both signals has to be estimated and artificially added to the appropriate channel. No method was found in literature to automatically estimate the natural time delay in real-time.

Part III

Additional Derivations & Results

Chapter 7

Incremental Nonlinear Dynamic Inversion (INDI) Derivations

This chapter presents the detailed derivation of Discrete Incremental Nonlinear Dynamic Inversion (DINDI), in support of Section II of the research paper in Part I, via two methods. Section 7-2 presents the derivation of DINDI by first discretization then linearization. Section 7-3 presents the derivation of DINDI by first linearization then discretization. To support the derivation of DINDI, Section 7-1 recaps the derivation and notation of Continuous Incremental Nonlinear Dynamic Inversion (CINDI).

7-1 Continuous INDI (CINDI)

The CINDI derivation starts from a general nonlinear system, see Eq. (7-1). (Sieberling et al., 2010; Simplício et al., 2013)

$$\underline{\dot{x}} = \underline{f}(\underline{x}, \underline{u}) \tag{7-1}$$

The system of Eq. (7-1) can be linearized about the current point in time indicated by the subscript '0', see Eq. (7-2). As such the variables $\underline{x}_0$ and $\underline{u}_0$ are given by the latest available measurements. Note that the linearization is based on the assumptions of a small sampling time and instantaneous control effectors. The notation of Eq. (7-2) can be simplified by defining $\left.\frac{\partial \underline{f}(\underline{x},\underline{u})}{\partial \underline{x}}\right|_{\underline{x}=\underline{x}_0, \underline{u}=\underline{u}_0} = F(\underline{x}_0, \underline{u}_0)$ and $\left.\frac{\partial \underline{f}(\underline{x},\underline{u})}{\partial \underline{u}}\right|_{\underline{x}=\underline{x}_0, \underline{u}=\underline{u}_0} = G(\underline{x}_0, \underline{u}_0)$.

$$\begin{aligned} \underline{\dot{x}} &\approx \underline{f}(\underline{x}_0, \underline{u}_0) + \left.\frac{\partial \underline{f}(\underline{x},\underline{u})}{\partial \underline{x}}\right|_{\underline{x}=\underline{x}_0, \underline{u}=\underline{u}_0} (\underline{x} - \underline{x}_0) + \left.\frac{\partial \underline{f}(\underline{x},\underline{u})}{\partial \underline{u}}\right|_{\underline{x}=\underline{x}_0, \underline{u}=\underline{u}_0} (\underline{u} - \underline{u}_0) \\ \underline{\dot{x}} &= \underline{\dot{x}}_0 + F(\underline{x}_0, \underline{u}_0)(\underline{x} - \underline{x}_0) + G(\underline{x}_0, \underline{u}_0)(\underline{u} - \underline{u}_0) \end{aligned} \tag{7-2}$$

The time-scale separation principle as defined in Eq. (7-3) is assumed to hold, again based on small sampling time. Therefore, Eq. (7-2) can be simplified to Eq. (7-4), which can be used to develop a control law by defining the virtual control input as $\underline{\nu} = \dot{\underline{x}}$.

$$F(\underline{x}_0, \underline{u}_0)(\underline{x} - \underline{x}_0) << G(\underline{x}_0, \underline{u}_0)(\underline{u} - \underline{u}_0) \tag{7-3}$$

$$\dot{\underline{x}} = \dot{\underline{x}}_0 + G(\underline{x}_0, \underline{u}_0)(\underline{u} - \underline{u}_0) \tag{7-4}$$

$$\underline{u} = \underline{u}_0 + G^{-1}(\underline{x}_0, \underline{u}_0)(\underline{\nu} - \dot{\underline{x}}_0) \tag{7-5}$$

Concluding, the physical control input u can be computed using Eq. (7-5), the latest available measurements ($\dot{\underline{x}}_0$,$\underline{x}_0$,$\underline{u}_0$) and the virtual control input $\underline{\nu}$. This virtual control input is to be designed, e.g. using a linear PID-controller.

7-2 Discrete INDI (DINDI) Discretization-Linearization

DINDI can be derived from the system of Eq. (7-1) by first performing a discretization then a linearization. The discrete-time system equivalent to Eq. (7-1) is given in Eq. (7-6).

$$\underline{x}_{k+1} = \underline{x}_k + \int_{t_k}^{t_{k+1}} f(\underline{x}, \underline{u})dt \tag{7-6}$$

For small sampling times $\dot{\underline{x}}$ can be assumed constant between two consecutive samples. Consequently, Eq. (7-6) simplifies to Eqs. (7-7) to (7-9) with $\Delta t = t_{k+1} - t_k$.

$$\underline{x}_{k+1} \approx \underline{x}_k + \Delta t \underline{f}(\underline{x}_k, \underline{u}_k) \tag{7-7}$$

$$\frac{\underline{x}_{k+1} - \underline{x}_k}{\Delta t} = \underline{f}(\underline{x}_k, \underline{u}_k) \tag{7-8}$$

$$\frac{\underline{x}_k - \underline{x}_{k-1}}{\Delta t} = \underline{f}(\underline{x}_{k-1}, \underline{u}_{k-1}) \tag{7-9}$$

Similar to CINDI, the right-hand side of Eq. (7-8) can be linearized about the current point in time indicated by the subscript 'k-1', see Eq. (7-10). As such the variables $\underline{x}_{k-1}$ and $\underline{u}_{k-1}$ are given by the latest available measurements. Moreover, the linearization again implies small sampling time and instantaneous control effectors. Again the notations $\frac{\partial \underline{f}(\underline{x},\underline{u})}{\partial \underline{x}}\Big|_{\underline{x}=\underline{x}_{k-1},\underline{u}=\underline{u}_{k-1}} = F(\underline{x}_{k-1}, \underline{u}_{k-1})$ and $\frac{\partial \underline{f}(\underline{x},\underline{u})}{\partial \underline{u}}\Big|_{\underline{x}=\underline{x}_{k-1},\underline{u}=\underline{u}_{k-1}} = G(\underline{x}_{k-1}, \underline{u}_{k-1})$ are introduced together with a substitution based on Eq. (7-9), see Eq. (7-11).

$$\begin{aligned}\frac{\underline{x}_{k+1} - \underline{x}_k}{\Delta t} \approx \underline{f}(\underline{x}_{k-1}, \underline{u}_{k-1}) + \frac{\partial \underline{f}(\underline{x}, \underline{u})}{\partial \underline{x}}\Big|_{\underline{x}=\underline{x}_{k-1},\underline{u}=\underline{u}_{k-1}} (\underline{x}_k - \underline{x}_{k-1}) + \cdots \\ \cdots + \frac{\partial \underline{f}(\underline{x}, \underline{u})}{\partial \underline{u}}\Big|_{\underline{x}=\underline{x}_{k-1},\underline{u}=\underline{u}_{k-1}} (\underline{u}_k - \underline{u}_{k-1})\end{aligned} \tag{7-10}$$

$$\frac{\underline{x}_{k+1} - \underline{x}_k}{\Delta t} = \frac{\underline{x}_k - \underline{x}_{k-1}}{\Delta t} + F(\underline{x}_{k-1}, \underline{u}_{k-1})(\underline{x}_k - \underline{x}_{k-1}) + G(\underline{x}_{k-1}, \underline{u}_{k-1})(\underline{u}_k - \underline{u}_{k-1}) \tag{7-11}$$

Based on the given definitions of $F(\underline{x}_{k-1}, \underline{u}_{k-1})$ and $G(\underline{x}_{k-1}, \underline{u}_{k-1})$ the time-scale separation principle given by Eq. (7-3) also holds for Eq. (7-11) and the equation reduces to Eq. (7-12).

This equation can be inverted to obtain the DINDI control law, Eq. (7-13), by defining the virtual control input as Eq. (7-14).

$$\frac{\underline{x}_{k+1} - \underline{x}_k}{\Delta t} \approx \frac{\underline{x}_k - \underline{x}_{k-1}}{\Delta t} + G(\underline{x}_{k-1}, \underline{u}_{k-1})(\underline{u}_k - \underline{u}_{k-1}) \tag{7-12}$$

$$\underline{u}_k = \underline{u}_{k-1} + G^{-1}(\underline{x}_{k-1}, \underline{u}_{k-1})(\underline{\nu}_k - \frac{\underline{x}_k - \underline{x}_{k-1}}{\Delta t}) \tag{7-13}$$

$$\underline{\nu}_k = \frac{\underline{x}_{k+1} - \underline{x}_k}{\Delta t} \tag{7-14}$$

However, the control law of Eq. (7-13) requires the future state $\underline{x}_k$ to be known, since the $\underline{x}_{k-1}$ state was defined to be given by the latest available measurements. To obtain a usable control law, the term $\frac{\underline{x}_k - \underline{x}_{k-1}}{\Delta t}$ is considered to represent the forward difference approximation of $\dot{\underline{x}}_{k-1}$ and can be replaced by the backward difference approximation $\frac{\underline{x}_{k-1} - \underline{x}_{k-2}}{\Delta t}$.

Concluding the physical control input u_k can be computed using Eq. (7-15), the latest available measurements ($\underline{x}_{k-1}$,$\underline{u}_{k-1}$), the previous measurements, $\underline{x}_{k-2}$, and the virtual control input, $\underline{\nu}_k$. Again the virtual control input is to be designed.

$$\underline{u}_k = \underline{u}_{k-1} + G^{-1}(\underline{x}_{k-1}, \underline{u}_{k-1})(\underline{\nu}_k - \frac{\underline{x}_{k-1} - \underline{x}_{k-2}}{\Delta t}) \tag{7-15}$$

7-3 DINDI Linearization-Discretization

DINDI can also be derived from the system of Eq. (7-1) by first performing a linearization then a discretization. Therefore, the initial derivation of DINDI via this road is equal to the CINDI derivation including all assumptions of Section 7-1 up to Eq. (7-4).

$$\dot{\underline{x}} = \dot{\underline{x}}_0 + G(\underline{x}_0, \underline{u}_0)(\underline{u} - \underline{u}_0) \tag{7-4}$$

Eq. (7-4) can be seen as the combination of two linear state-space systems, Eqs. (7-16) and (7-17), both with $F(\underline{x}_0, \underline{u}_0) = 0$.

$$\dot{\underline{x}} = F(\underline{x}_0, \underline{u}_0)\underline{x} + G(\underline{x}_0, \underline{u}_0)\underline{u} \tag{7-16}$$

$$\dot{\underline{x}}_0 = F(\underline{x}_0, \underline{u}_0)\underline{x}_0 + G(\underline{x}_0, \underline{u}_0)\underline{u}_0 \tag{7-17}$$

The discrete counterpart of such a linear state-space systems is known, see Eq. (7-18) (Mulder, van der Vaart, & Mulder, 2007). Considering $F(\underline{x}_0, \underline{u}_0) = 0$, the discretized system simplifies to Eqs. (7-19) and (7-20).

$$\begin{aligned} \underline{x}_{k+1} &= \Phi(\underline{x}_0, \underline{u}_0)\underline{x}_k + \Gamma(\underline{x}_0, \underline{u}_0)\underline{u}_k \\ \Phi &= I + \Delta t F + \frac{\Delta t^2}{2!}F^2 + \frac{\Delta t^3}{3!}F^3 + \cdots \\ \Gamma &= \Delta t G + \frac{\Delta t^2}{2!}FG + \frac{\Delta t^3}{3!}F^2 G + \cdots \end{aligned} \tag{7-18}$$

$$\underline{x}_{k+1} = \underline{x}_k + \Delta t G(\underline{x}_0, \underline{u}_0)\underline{u}_k \tag{7-19}$$

$$\frac{\underline{x}_{k+1} - \underline{x}_k}{\Delta t} = G(\underline{x}_0, \underline{u}_0)\underline{u}_k \tag{7-20}$$

Using Eq. (7-20) to discretize both Eqs. (7-16) and (7-17) and combining these as in Eq. (7-4) results in Eq. (7-21). Additionally, Sections 7-1 and 7-2 presented the latest available measurements to be indicated by the '0' and 'k-1' subscripts respectively. Therefore, Eq. (7-21) can be rewritten using $\underline{x}_{0_k} = \underline{x}_{k-1}$ and $\underline{u}_{0_k} = \underline{u}_{k-1}$ to obtain Eq. (7-22).

$$\frac{\underline{x}_{k+1} - \underline{x}_k}{\Delta t} = \frac{\underline{x}_{0_{k+1}} - \underline{x}_{0_k}}{\Delta t} + G(\underline{x}_{0_k}, \underline{u}_{0_k})(\underline{u}_k - \underline{u}_{0_k}) \tag{7-21}$$

$$\frac{\underline{x}_{k+1} - \underline{x}_k}{\Delta t} = \frac{\underline{x}_k - \underline{x}_{k-1}}{\Delta t} + G(\underline{x}_{k-1}, \underline{u}_{k-1})(\underline{u}_k - \underline{u}_{k-1}) \tag{7-22}$$

Eq. (7-22) is equal to Eq. (7-13), which shows that the order of linearization and discretization in the derivation of the DINDI control law does affect the result. Consequently, Eq. (7-22) can be used to obtain the DINDI control law of Eq. (7-15) based on the procedure described in Section 7-2.

$$\underline{u}_k = \underline{u}_{k-1} + G^{-1}(\underline{x}_{k-1}, \underline{u}_{k-1})(\underline{\nu}_k - \frac{\underline{x}_{k-1} - \underline{x}_{k-2}}{\Delta t}) \tag{7-15}$$

Chapter 8

Analytical Stability

This chapter presents the detailed analytical stability analysis method of a sampled-data control system based on Discrete Incremental Nonlinear Dynamic Inversion (DINDI). The crux of sampled-data control systems is the combination of a discrete controller controlling a continuous system. First, Section 8-1 presents the stability conditions of a fully continuous closed-loop system based on Continuous Incremental Nonlinear Dynamic Inversion (CINDI). Second, Section 8-2 presents the detailed analysis method for the sampled-data system based on DINDI. All in support of Section III of the research paper in Part I.

8-1 Continuous-Time System

To support the results of the sampled-data system based on DINDI, first a continuous system based on CINDI is analyzed. The system considered is given by Eq. (8-1) and is controlled by the CINDI law of Eq. (8-2). The continuous-time system and control law can be combined into a state-space system, see Eq. (8-3).

$$\begin{aligned}\dot{x} &= Fx + Gu \\ \dot{u} &= K_u(u_c - u_0) = K_u \Delta u\end{aligned} \tag{8-1}$$

$$\Delta u = (G + \Delta G)^{-1}(K_x(x_d - x_0) - \dot{x}_0) \tag{8-2}$$

$$\begin{bmatrix}\dot{x} \\ \dot{u}\end{bmatrix} = \begin{bmatrix} F & G \\ -K_u \frac{K_x + F}{G + \Delta G} & -K_u \frac{G}{G + \Delta G}\end{bmatrix}\begin{bmatrix} x \\ u \end{bmatrix} + \begin{bmatrix} 0 \\ K_u \frac{K_x}{G + \Delta G}\end{bmatrix} \tag{8-3}$$

The characteristic polynomial of this state-space system is given by Eq. (8-4), using the definition of the control effectiveness uncertainty ratio, γ, in Eq. (8-5). Based on this characteristic polynomial the stability conditions of the closed-loop system are given by Eq. (8-6). These stability conditions can be clearly found in the results of DINDI stability as described in Section III of the paper.

$$\lambda^2 + (K_u\gamma - F)\lambda - K_u\gamma F + K_u\gamma(K_x + F) \tag{8-4}$$

$$\gamma = \frac{G}{G + \Delta G} \tag{8-5}$$

$$\begin{aligned} K_u\gamma - F &> 0 \\ K_u K_x \gamma &> 0 \end{aligned} \tag{8-6}$$

8-2 Sampled-Data Analysis Method

This section presents the method used to analyze a sampled-data system consisting of both discrete and continuous components, based on Nise (2011). Figure 8-1 presents a DINDI controller in combination with a generic system, $\dot{x} = Fx + Gu$, with actuator dynamics. The closed-loop system also includes samplers, converting continuous signals to discrete signals, as well as a zero-order hold converting a discrete signal to a continuous signal, $\frac{1-e^{-Ts}}{s}$. The discrete-time part of the system has sampling time, T.

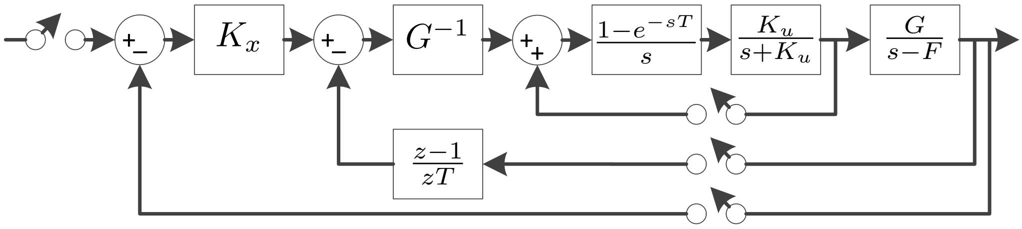

Figure 8-1: Sampled-data system including the DINDI controller in combination with generic system with actuator dynamics

The goal of the method is to reduce the block diagram of Figure 8-1 into its discrete equivalent. To retain clear block diagrams the following transfer functions are introduced: $K(z) = K_x$, $I(z) = G^{-1}$, $H(s) = \frac{1-e^{-Ts}}{s}$, $A(s) = \frac{K_u}{s+K_u}$, $S(s) = \frac{G}{s-F}$ and $D(z) = \frac{z-1}{zT}$. Moreover phantom samplers are added at the output of any block that has sampled input, provided that it does not change the nature of the signal sent to another block, see Figure 8-2.

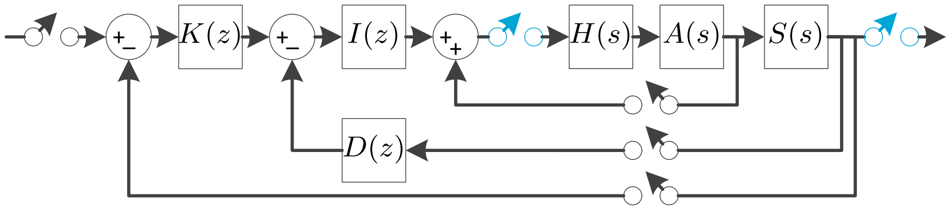

Figure 8-2: Sampled-data system with phantom samplers (blue) added

For this process it is important to realize that the z-transform has the following property: $\mathcal{Z}\{H_1(s)H_2(s)\} = \mathcal{Z}\{H_1H_2(s)\} = H_1H_2(z) \neq H_1(z)H_2(z)$. Moreover, a continuous (series of) transfer function(s) can only be converted to a discrete transfer function in combination with a sampler in front and behind the (series of) transfer function(s). Therefore, the phantom sampler, $H(s)$ and $A(s)$ blocks are pushed to the right of the pickoff point, see Figure 8-3.

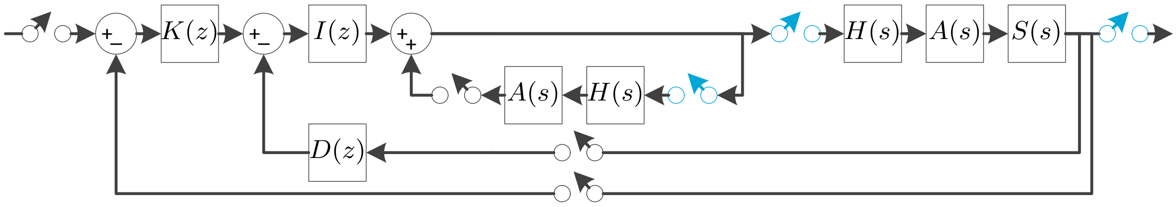

Figure 8-3: Sampled-data system with the phantom sampler, $H(s)$ and $A(s)$ pushed to the right of the pickoff point

Finally, the discrete equivalent of the sampled-data system is obtained by converting the two series of continuous transfer functions combined with the samplers to discrete transfer functions, see Figure 8-4. This discrete system can then be converted to the transfer function of Eq. (8-7).

$$\frac{K(z)I(z)HAS(z)}{1 - HA(z) + [D(z) + K(z)]I(z)HAS(z)} \tag{8-7}$$

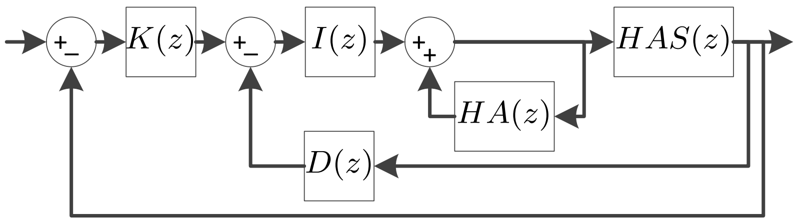

Figure 8-4: Discrete equivalent of the sampled-data system

To be able to use the transfer function of Eq. (8-7) for analysis the $HA(z)$ and $HAS(z)$ transfer functions have to be obtained. Typically, these transfer functions are obtained via tables combining z- and s-transforms (Nise, 2011). To be able to use these standard tables the original continuous transfer functions is expanded using partial fraction expansion. Using this method, the discrete transfer functions of $HA(z)$ and $HAS(z)$ are obtained in Eqs. (8-8) to (8-11).

$$\mathcal{Z}\{HA(s)\} = \mathcal{Z}\left\{(1 - e^{-sT})\frac{K_u}{s(s+K_u)}\right\} = (1 - z^{-1})\mathcal{Z}\left\{\frac{1}{s} - \frac{1}{s+K_u}\right\} \tag{8-8}$$

$$HA(z) = \frac{z-1}{z}\left\{\frac{z}{z-1} - \frac{z}{z - e^{-K_u T}}\right\} = \frac{1 - e^{-K_u T}}{z - e^{-K_u T}} \tag{8-9}$$

$$\begin{aligned} \mathcal{Z}\{HAS(s)\} &= \mathcal{Z}\left\{(1 - e^{-sT})\frac{K_u}{s(s+K_u)}\frac{G}{s-F}\right\} \\ &= (1 - z^{-1})\mathcal{Z}\left\{\frac{K_u G}{F(F+K_u)}\frac{1}{s-F} + \frac{G}{F+K_u}\frac{1}{s+K_u} - \frac{G}{F}\frac{1}{s}\right\} \end{aligned} \tag{8-10}$$

$$\begin{aligned} HAS(z) &= \frac{z-1}{z}\left\{\frac{K_uG}{F(F+K_u)}\frac{z}{z-e^{FT}}+\frac{G}{F+K_u}\frac{z}{z-e^{-K_uT}}-\frac{G}{F}\frac{z-1}{z}\right\} \\ &= \frac{K_uG}{F(F+K_u)}\frac{z-1}{z-e^{FT}}+\frac{G}{F+K_u}\frac{z-1}{z-e^{-K_uT}}-\frac{G}{F} \end{aligned} \tag{8-11}$$

To analyze the stability of the sampled-data system, the characteristic polynomial of Eq. (8-7) has to be obtained. Fortunately, the characteristic polynomial only depends on the denominator, $1-HA(z)+[D(z)+K(z)]I(z)HAS(z)$, see Eq. (8-12). From this denominator the characteristic polynomial can be derived via mathematical manipulation, see Eqs. (8-13) and (8-14).

$$1-\frac{1-e^{-K_uT}}{z-e^{-K_uT}}+\left[\frac{z-1}{zT}+K_x\right]\frac{1}{G}\left(\frac{K_uG}{F(F+K_u)}\frac{z-1}{z-e^{FT}}+\frac{G}{F+K_u}\frac{z-1}{z-e^{-K_uT}}-\frac{G}{F}\right) \tag{8-12}$$

$$\begin{aligned} &Tz^3+\left(-T-Te^{FT}+(K_xT+1)(Ae^{FT}+Be^{-K_uT}-C)\right)z^2+... \\ &\left(Te^{FT}+(K_xT+1)(Ae^{-K_uT}+Be^{FT}-Ce^{(F-K_u)T})-Ae^{FT}-Be^{-K_uT}+C\right)z+... \\ &(-Ae^{-K_uT}-Be^{FT}+Ce^{(F-K_u)T}) \end{aligned} \tag{8-13}$$

$$A=\frac{K_u}{F(F+K_u)};B=\frac{1}{F+K_u};C=\frac{1}{F} \tag{8-14}$$

The closed-loop system is asymptotically stable if and only if all roots of the characteristic polynomial have a magnitude smaller than one. To avoid having to solve all the roots of the characteristic polynomial, Jury's stability criterion is used to check the system's stability based on a tabular method (Jury, 1965). As such, Jury's criterion is the discrete-time counterpart of the continuous-time Routh-Hurwitz criterion.

Considering the general characteristic polynomial, Eq. (8-15), Jury's stability criterion is generated by using Eqs. (8-16) and (8-17). The closed-loop system is stable if and only if the table consists of n+1 rows and all entries in the left most column have the same sign. A numerical approach was used to evaluate these stability conditions and obtain the results as presented in Section III of the paper in Part I.

$$F(z)=a_0+a_1z+a_2z^2+...a_nz^n \quad a_n\neq 0 \tag{8-15}$$

$$\begin{array}{cccccc} a_n & a_{n-1} & \cdots & a_2 & a_1 & a_0 \\ b_{n-1} & b_{n-2} & \cdots & b_1 & b_0 & \\ c_{n-2} & c_{n-3} & \cdots & c_0 & & \\ \vdots & \vdots & & & & \end{array} \tag{8-16}$$

$$\begin{aligned} b_i &= a_{i+1}-a_{n-1-i}\frac{a_0}{a_n}, \quad i=0,1,\cdots,n-1 \\ c_i &= b_{i+1}-b_{n-2-i}\frac{b_0}{b_{n-1}}, \quad i=0,1,\cdots,n-2 \\ d_i &= c_{i+1}-c_{n-3-i}\frac{c_0}{c_{n-2}}, \quad i=0,1,\cdots,n-3 \end{aligned} \tag{8-17}$$

Chapter 9

Additional Simulation Results

This chapter presents additional simulation results in support of Sections V and VI of the research paper in Part I. As the paper has to be consice not all results can be displayed, these remaining results are presented in this chapter. First, Figures 9-1 and 9-2 present the roll and sideslip angle command and responses for the controller based on Incremental Nonlinear Dynamic Inversion (INDI) and INDI+, i.e. INDI with solutions, for all phenomena causing performance degradation. The results of Figures 9-1 and 9-2 show that the results presented in Section V of the paper based on the pitch response also hold for the roll and sideslip responses.

Second, the results of Section VI of the paper are supported with additional plots. Figure 9-3 shows the principle of latency in closer detail. Figure 9-3a shows the original control commands and the control deflection measurements. Additionally, the figure shows the measurements shifted by the identified latency of 110 ms to obtain a measurement signal that is overlaying the control command. Note that the simulated actuator measurement delay is 39.7 ms. Similarly, Figure 9-3b shows that the angular rate latency of 210 ms matches both command and measurement signals, while the simulated delay is 128 ms. The difference between actual delay and latency is caused by system dynamics, which naturally adds latency to the system. Fortunately, the difference in latency, in this case 100 ms, is still a good indication on the difference in delay, in this case 90 ms (rounded).

Third, the evolution of identified delay mismatch can be seen in Figure 9-4. The algorithm logically has to run for a couple of seconds to obtain an appropriate estimate. Afterwards, the algorithm steadily converges to a steady-state answer. This identified delay does differ from the actual delay by 20 ms, however as shown in Part I this still results in adequate controller performance without oscillations.

Finally, Figure 9-5 shows the delay identification error for the INDI controller with PCH, but not affected by real-world phenomena. Clearly, the overall average error depicted in Figure 9-5 is smaller than the overall average error shown in Part I for the system affected by real-world phenomena. This supports the claim made in the paper that the real-world phenomena degrade algorithm performance. Fortunately, as shown in the paper the degradation is within the bounds of adequate controller performance.

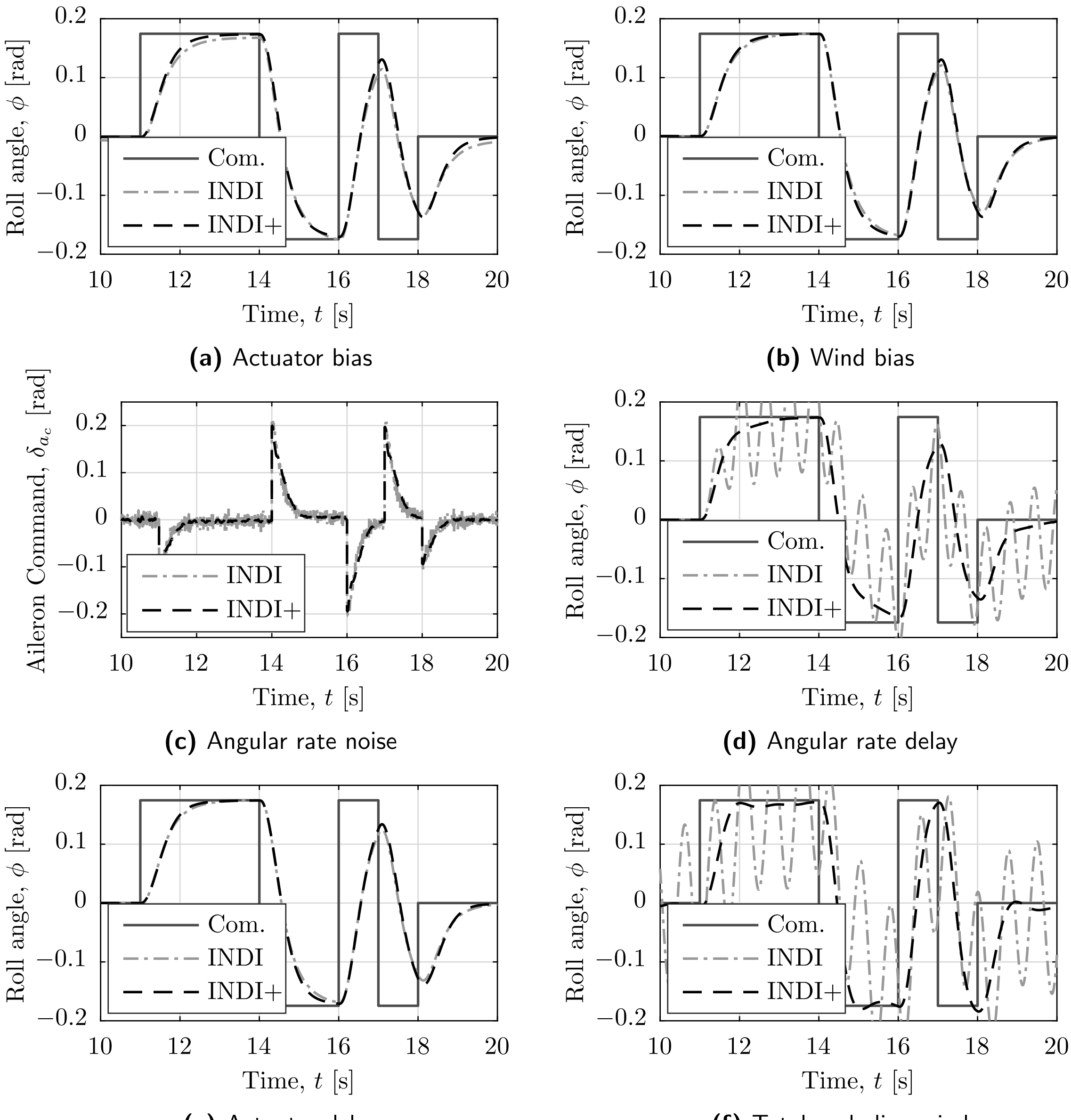

(a) Actuator bias

(b) Wind bias

(c) Angular rate noise

(d) Angular rate delay

(e) Actuator delay

(f) Total excluding wind

Figure 9-1: Roll response subjected to selected phenomena for INDI with and without solutions

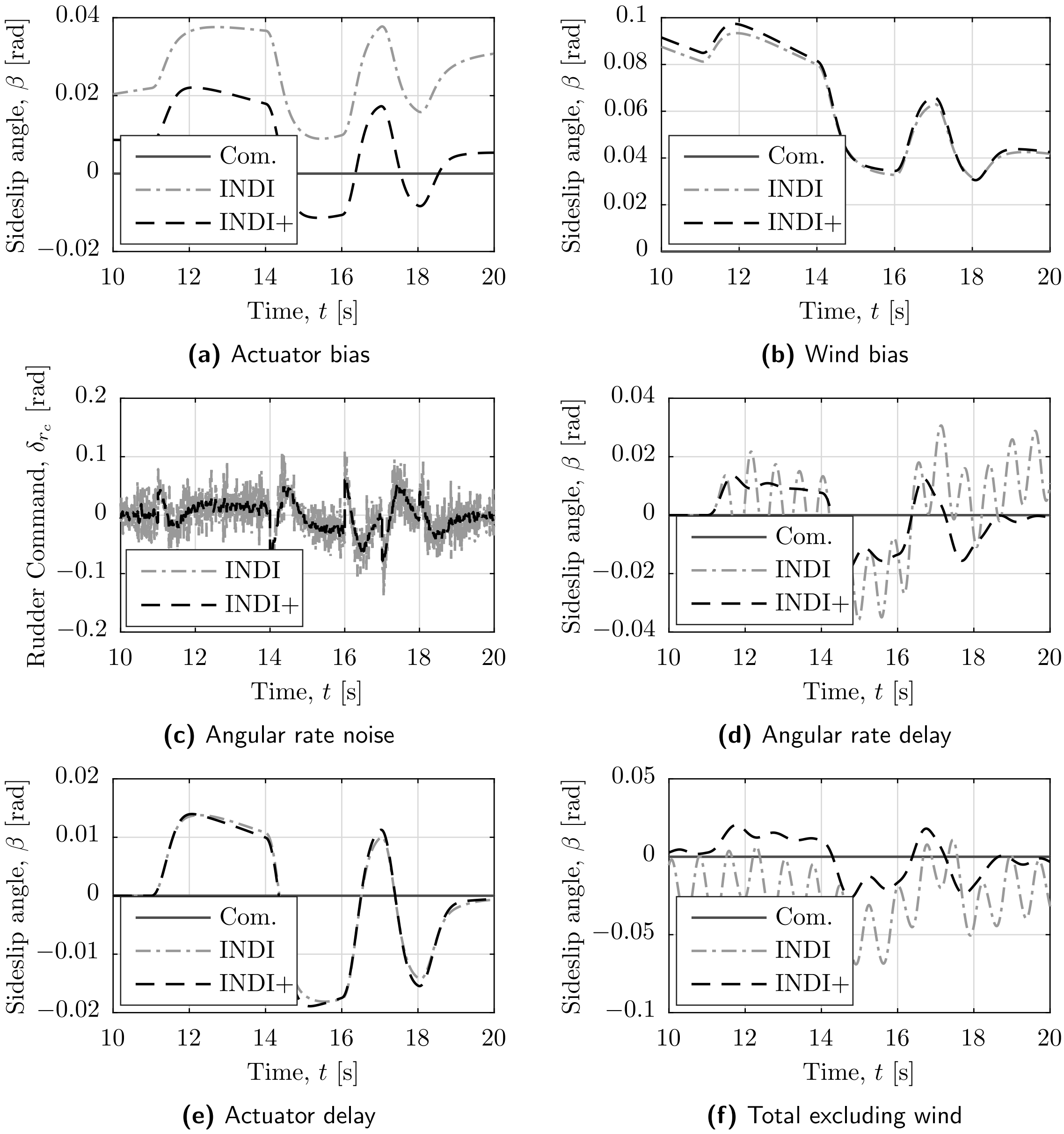

Figure 9-2: Sideslip response subjected to selected phenomena for INDI with and without solutions

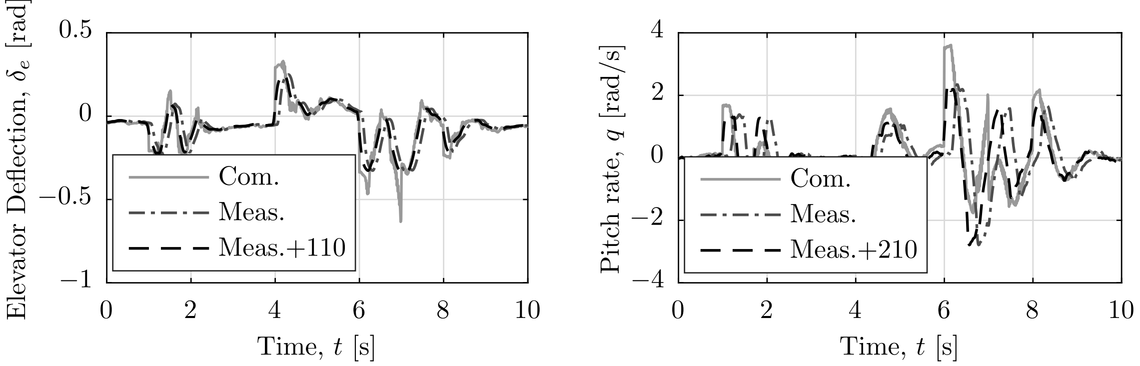

(a) Actuator delay 39.7 ms, latency 110ms **(b)** Angular rate delay 128 ms, latency 210 ms

Figure 9-3: Latency identification with disturbances and PCH

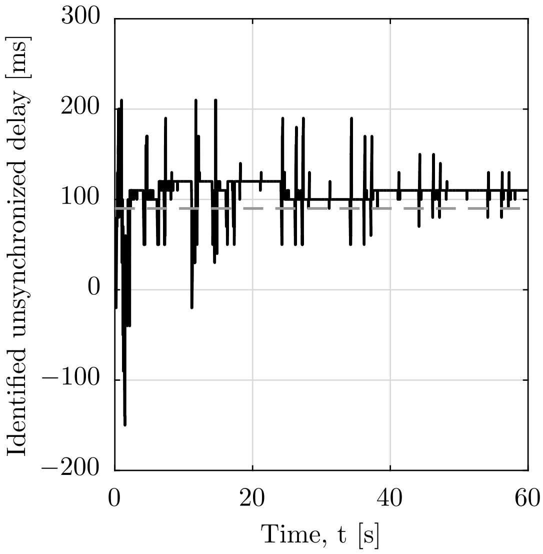

Figure 9-4: Evolution of identified unsynchronized delay for system with 90 ms actual unsynchronized delay

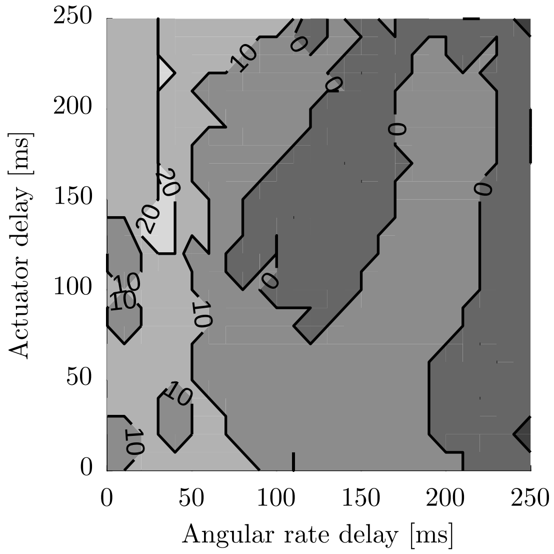

Figure 9-5: Delay identification error after 40 seconds without real-world phenomena and with PCH

Chapter 10

PH-LAB Cessna Citation Characteristics

Throughout this project the PH-LAB aircraft is used as example aircraft, as discussed in Chapter 1. Therefore, this chapter uses previous flight test data from the PH-LAB, obtained on September 16th 2015, to generate aircraft characteristics used to run all simulations. As such, this chapter supports Section V of the research paper in Part I. The measurement bias, noise, delay and sampling time characteristics are found in Section 10-1. The numerical values of the control effectiveness matrix are presented in Section 10-2.

10-1 Real-World Phenomena Characteristics

This section presents the bias, noise, delay and sampling time characteristics of the PH-LAB Cessna Citation. All numerical values were found based on two periods, 4 and 5 minutes long, of relative straight flight.

The control surface deflections, (δ_a, δ_e, δ_r), are measured using a single synchro per type of control surface and are sent to the Flight Test and Instrumentation System (FTIS) as a group. The angular rates, (p, q, r), the attitude angles, (ϕ, θ), and the lateral acceleration, n_y, are all measured using the Attitude and Heading Reference System (AHRS). The PH-LAB has two independent AHRSs and the data is sent to the FTIS via an ARINC data bus. Finally, the true airspeed, V_{TAS}, is measured by two independent Digital Air Data Computers (DADCs) and its data is also sent to the FTIS via an ARINC data bus.

To obtain measurement bias estimates of the angular rates, attitude angles and lateral acceleration, the difference between the mean of both AHRSs is used. Similarly, the bias of the airspeed is determined using the difference between the mean of both DADCs. Unfortunately, there were not two independent synchro systems available during the flight test. Therefore, the bias of the control surface deflections is determined based on the mean between the two periods of straight flight. However, as the flight conditions between both periods of straight flight differ, thus requiring a different elevator setting, only the results of the aileron and rudder are used. The resulting bias characteristics are presented in Tables 10-1 and 10-2.

Table 10-1: PH-LAB flight test data bias characteristics (AHRS & DADC)

	100 - 400 sec			3660 - 3900 sec		
Mean	AHRS1	AHRS2	Bias	AHRS1	AHRS2	Bias
ϕ [rad]	$-2.60 \cdot 10^{-4}$	$1.26 \cdot 10^{-3}$	$1.52 \cdot 10^{-3}$	$1.02 \cdot 10^{-2}$	$1.17 \cdot 10^{-2}$	$1.51 \cdot 10^{-3}$
θ [rad]	$5.98 \cdot 10^{-2}$	$5.70 \cdot 10^{-2}$	$2.86 \cdot 10^{-3}$	$2.68 \cdot 10^{-2}$	$2.30 \cdot 10^{-2}$	$3.81 \cdot 10^{-3}$
p [rad/s]	$-1.67 \cdot 10^{-5}$	$-4.06 \cdot 10^{-5}$	$2.39 \cdot 10^{-5}$	$5.28 \cdot 10^{-6}$	$1.05 \cdot 10^{-6}$	$4.22 \cdot 10^{-6}$
q [rad/s]	$5.53 \cdot 10^{-5}$	$3.40 \cdot 10^{-5}$	$2.13 \cdot 10^{-5}$	$-3.89 \cdot 10^{-5}$	$-6.94 \cdot 10^{-5}$	$3.06 \cdot 10^{-5}$
r [rad/s]	$-6.35 \cdot 10^{-5}$	$-5.96 \cdot 10^{-5}$	$3.88 \cdot 10^{-6}$	$7.26 \cdot 10^{-5}$	$6.51 \cdot 10^{-5}$	$7.46 \cdot 10^{-6}$
n_y [g]	$6.37 \cdot 10^{-4}$	$-1.85 \cdot 1-^{-3}$	$2.49 \cdot 10^{-3}$	$-9.11 \cdot 10^{-3}$	$-1.12 \cdot 10^{-2}$	$2.07 \cdot 10^{-3}$
	DADC1	DADC2	Bias	DADC1	DADC2	Bias
V_{TAS} [m/s]	101.9	100.1	1.74	134.2	131.5	2.68

Table 10-2: PH-LAB flight test data bias charachteristics (Synchro)

Mean	100-400s	3660-3900s	Bias
δ_a [rad]	$-1.21 \cdot 10^{-2}$	$-7.63 \cdot 10^{-3}$	$4.42 \cdot 10^{-3}$
δ_e [rad]	$1.07 \cdot 10^{-2}$	$3.58 \cdot 10^{-2}$	n.a.
δ_r [rad]	$-3.64 \cdot 10^{-2}$	$-3.44 \cdot 10^{-2}$	$2.02 \cdot 10^{-3}$

As seen in Tables 10-1 and 10-2, all sets of variables, that is the angular rates, attitude angles, etc. all have quite similar and consistent bias values. Therefore, the largest bias value within each group is selected from the results and used within simulation, see Table 10-6. Note that the steady rudder deflection, almost 2 degrees, is due to the pilots trimming the rudder pre-flight against asymmetries. Therefore, this steady deflection should not be seen as a measurement bias.

To obtain measurement noise estimates, all measurement signals were filtered using Eq. (10-1) and subtracted from the original measurements. The variance of the remainders was taken as estimate of the noise variance. Additionally, the estimate of both the AHRSs and DADCs were averaged to obtain a final noise estimate, see Table 10-3. For the synchro measurements the estimates from the two periods were averaged to obtain a final estimate, see Table 10-4. Similar to the bias estimates, the noise estimates are quite similar and consistent within each set of variables. Therefore, the largest noise value within each group is selected from the results and used within simulation, see Table 10-6. Note that these values are larger than noise values of the PH-LAB used in literature (Wedershoven, 2010).

$$x_{filt}[k] = \frac{1}{16}x[k-3] + \frac{2}{16}x[k-2] + \frac{3}{16}x[k-1] + \frac{4}{16}x[k] + \frac{3}{16}x[k+1] + \frac{2}{16}x[k+2] + \frac{1}{16}x[k+3] \tag{10-1}$$

Besides measurement bias and noise, also bias and noise disturbances as input to the system are taken into account, see Chapter 5. Based on flight test data, a constant wind is implemented as bias with a total velocity of 25 m/s split across all three axes. Additionally,

Table 10-3: PH-LAB flight test data noise characteristics (AHRS & DADC)

	100 - 400 sec			3660 - 3900 sec		
Variance	AHRS1	AHRS2	Noise	AHRS1	AHRS2	Noise
ϕ [rad^2]	$1.22 \cdot 10^{-9}$	$1.23 \cdot 10^{-9}$	$1.22 \cdot 10^{-9}$	$7.74 \cdot 10^{-10}$	$7.65 \cdot 10^{-10}$	$7.69 \cdot 10^{-10}$
θ [rad^2]	$4.02 \cdot 10^{-10}$	$4.07 \cdot 10^{-10}$	$4.05 \cdot 10^{-10}$	$2.93 \cdot 10^{-10}$	$3.28 \cdot 10^{-10}$	$3.10 \cdot 10^{-10}$
p [rad^2/s^2]	$3.94 \cdot 10^{-7}$	$3.84 \cdot 10^{-7}$	$3.89 \cdot 10^{-7}$	$2.91 \cdot 10^{-7}$	$3.00 \cdot 10^{-7}$	$2.96 \cdot 10^{-7}$
q [rad^2/s^2]	$3.05 \cdot 10^{-8}$	$7.15 \cdot 10^{-8}$	$5.10 \cdot 10^{-8}$	$3.42 \cdot 10^{-8}$	$9.10 \cdot 10^{-8}$	$6.26 \cdot 10^{-8}$
r [rad^2/s^2]	$3.92 \cdot 10^{-8}$	$4.03 \cdot 10^{-8}$	$3.97 \cdot 10^{-8}$	$3.68 \cdot 10^{-8}$	$3.66 \cdot 10^{-8}$	$3.67 \cdot 10^{-8}$
n_y [g]	$1.75 \cdot 10^{-5}$	$1.07 \cdot 10^{-5}$	$1.41 \cdot 10^{-5}$	$1.74 \cdot 10^{-5}$	$1.03 \cdot 10^{-5}$	$1.39 \cdot 10^{-5}$
	DADC1	DADC2	Noise	DADC1	DADC2	Noise
V [m^2/s^2]	$4.79 \cdot 10^{-4}$	$1.19 \cdot 10^{-3}$	$8.37 \cdot 10^{-4}$	$1.48 \cdot 10^{-4}$	$4.09 \cdot 10^{-4}$	$2.78 \cdot 10^{-4}$

Table 10-4: PH-LAB flight test data noise charachteristics (Synchro)

Mean	100-400s	3660-3900s	Bias
δ_a [rad^2]	$4.67 \cdot 10^{-7}$	$6.39 \cdot 10^{-7}$	$5.53 \cdot 10^{-7}$
δ_e [rad^2]	$1.51 \cdot 10^{-7}$	$1.65 \cdot 10^{-7}$	$1.58 \cdot 10^{-7}$
δ_r [rad^2]	$7.70 \cdot 10^{-9}$	$7.99 \cdot 10^{-9}$	$7.84 \cdot 10^{-9}$

atmospheric turbulence is implemented as noise using the Dryden model with $\sigma = 1\text{m}^2/\text{s}^2$ and $L_g = 150\text{m}$ (Mulder et al., 2007).

The time delay characteristics of the signals cannot be obtained using the two periods of straight flight. Contrary, the time delay characteristics are obtained using parts of the flight in which 3211 and doublet maneuvers were performed in pitch and roll. The commands for these maneuvers were given directly to the actuators in an open-loop fashion without interference of a control system. In total 26 samples were obtained throughout these maneuvers at which the time delay characteristics were observed. The time delay itself was determined by obtaining the difference between the timing of the command signal and the observed response of the control surface deflections and the angular accelerations. The delay of the control surfaces serves as an indication of the delay for the synchro measurements. The delay of the angular accelerations serve as an indication of the delay for the AHRS measurements.

Table 10-5: PH-LAB statistics on time delay for synchro and AHRS measurements

Description	Samples	Mean [ms]	σ [ms]	Mean [ms]	σ [ms]
Pitch: δ_e & $\dot{q}$	16	37.1	8.16	125	6.36
Roll: δ_a & $\dot{p}$	10	44.0	4.85	134	8.78
Total	26	39.7	7.77	128	8.59

Collecting all results presented in this section results in the combination of phenomena characteristics as seen in Table 10-6. This table also includes the sampling time for all sets of variables, which is constant throughout the entire flight test for all variables. Additionally, no delay for the DADC measurement of the airspeed was obtained, therefore a value of 0.1s is used. This delay is not as vital as other delays, since the airspeed does not vary quickly.

Table 10-6: PH-LAB real-world phenomena characteristics

	Bias	Noise	Delay [s]	Sampling Time [s]
p, q, r [rad/s]	$3 \cdot 10^{-5}$	$4 \cdot 10^{-7}$	0.128	0.0192
V_{TAS} [m/s]	2.5	$8.5 \cdot 10^{-4}$	0.1	0.0625
δ_a, δ_e, δ_r [rad]	$4.5 \cdot 10^{-3}$	$5.5 \cdot 10^{-7}$	0.0397	0.01
ϕ, θ [rad]	$4 \cdot 10^{-3}$	$1 \cdot 10^{-9}$	0.128	0.0192
n_y [g]	$2.5 \cdot 10^{-3}$	$1.5 \cdot 10^{-5}$	0.128	0.0192

10-2 Control Effectiveness Matrix Estimation

This section presents an estimation of the control effectiveness matrix of the PH-LAB to be used in simulation. The control effectiveness matrix consists of five control derivatives, which are all implemented within the high fidelity simulation model of the Citation. The estimation of the control derivatives is based on a 2 minute simulation with the PH-LAB model. The average value of the control derivatives is taken to be used within the Incremental Nonlinear Dynamic Inversion (INDI) controller, see Table 10-7.

Table 10-7: PH-LAB control effectiveness matrix over 2 minute simulation run

Symbol	Initial [-]	Mean [-]	Std. [-]	Min./Max. [-]	Dependence
$C_{l_{\delta_a}}$	-0.185	-0.185	0	[-0.185,-0.185]	-
$C_{l_{\delta_r}}$	0.0316	0.0332	0.00477	[0.0203,0.0438]	α, M
$C_{m_{\delta_e}}$	-1.32	-1.26	0.100	[-1.40,-1.14]	α, δ_{flap}, V_{EAS}
$C_{n_{\delta_a}}$	-0.00623	-0.00826	0.00624	[-0.0201,0.00831]	α, δ_{flap}, M
$C_{n_{\delta_r}}$	-0.101	-0.101	0	[-0.101,-0.101]	-

Chapter 11

PH-LAB Cessna Citation Specific Issues

This section discusses PH-LAB Cessna Citation specific issues related to flight testing an Incremental Nonlinear Dynamic Inversion (INDI) controller. Originally, a flight test with the PH-LAB was included in the project plan, as discussed in Chapter 1. To prevent any confounds during such a flight test it is important to understand whether some PH-LAB specific issues and characteristics can lead to performance degradation of an INDI controller. Therefore, this chapter answers research sub-question 5: "Which measures are required to implement an INDI controller together with the Fly-by-Wire (FBW) system of the PH-LAB Cessna Citation?"

Section 11-1 describes a potential issue related to the maximum servo power available and the elevator trim. Section 11-2 discusses issues related to the control surface deflection measurements. Additionally, the topic of maneuver design is presented in Section 11-3. Although the flight test was not executed during this project, the conclusions and recommendations of this chapter as presented in Section 11-4 are still considered useful for any future contributors to the flight test.

11-1 Maximum Servo Power and Elevator Trim

Flight testing an experimental controller on the PH-LAB would require the controller to be connected to the FBW system of the aircraft. Consequently, the limitations of this FBW will also limit the experimental controller. An example of such a limitation is the maximum servo power available for automatic control system. The limitation has been put into place as human pilots should at all times be able to overpower the automatic control system for certification and safety purposes. This servo power is limited in the PH-LAB by clipping the current sent to the servo within the original autopilot computer made by Cessna.

Additionally, a second current limit exists within the autopilot computer. Once this higher current limit is reached the complete autopilot is switched off. When either current limit is reached the experimental controller running is powerless as the feedback loop is effectively ruined by the clipping. See Figure 11-1, in which the control surface seems to remain in the same position multiple times after t=2700 s. Note that the results in the figure present the flight test data of October 9th, 2015 between t=2480 to 2820s.

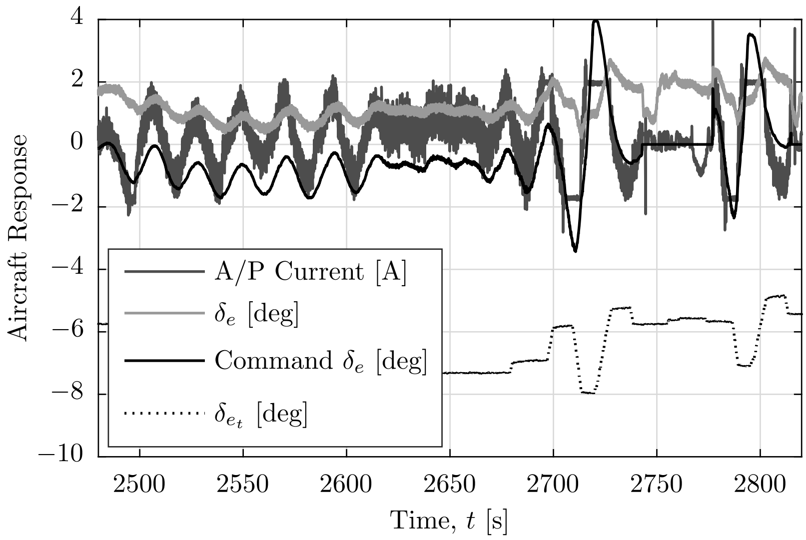

Figure 11-1: Output response of A/P current, commanded elevator deflection, true elevator deflection and elevator trim tab deflection

To prevent current clipping, the elevator trim tab is used to reduce the amount of power to be delivered by servo motor. Within the original Cessna autopilot the trim tab is deflected when the load exerted by the servo exceeds a certain voltage for a 3 second period. Thus, the autotrim is hardwired into the analog autopilot, as a measure to reduce the power required to deflect the elevator during the maneuvers. As such the autotrim feature is very beneficial for the autopilot. On the other hand, it is clear from Figure 11-1 that the elevator trim tab cannot follow fast oscillations in the system response due to the 3 second delay, thus causing the maximum current to be reached.

Still, the limitation is not necessarily an issue. During the flight test presented in Figure 11-1 flew at a high velocity, about 330 knots. High velocities also create high aerodynamic forces and as such the maximum servo power is reached quickly. Therefore, it is recommended that the flight test be executed at lower velocities to reduce the chance of hitting the maximum servo power.

11-2 Control Surface Deflection Measurements

The research paper of Part I extensively discussed the effect of actuator measurements on the controller performance. Additionally, the PH-LAB aircraft might have additional issues related to nonlinear actuator measurements. First, the actuators are deflected asymmetrically with only one of the surfaces being measured by the synchro. As such, the measured deflection

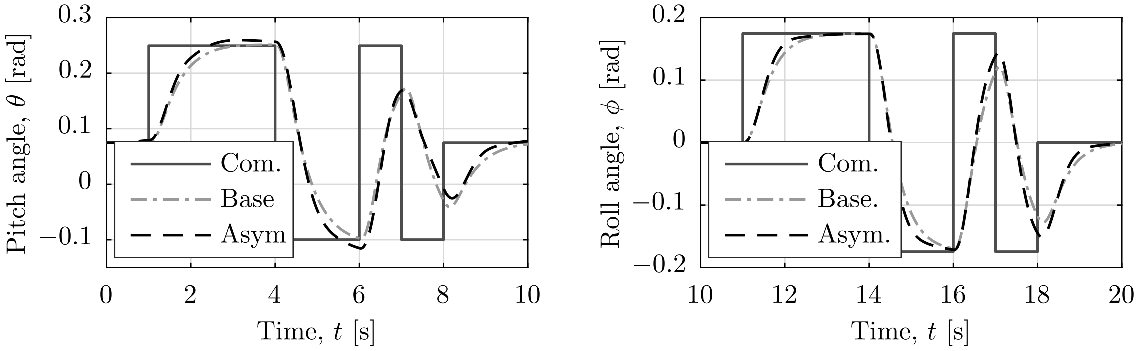

(a) Pitch response

(b) Roll response

Figure 11-2: Aircraft response for INDI with solutions, baseline and subjected to asymmetric actuator measurements

is not equal to the effective combined deflection. Second, the synchros are connected to the actual control surfaces using mechanical links with unequal lengths. As such, an nonlinear trigonometric relation is added to the measurement system.

The effect of nonlinear actuator measurements on the aircraft pitch and roll response is presented in Figure 11-2. Clearly, the phenomenon adds unwanted additional overshoot and steady-state error in the pitch response. The roll response is affected through an unwanted change in the transient response, but without steady-state error. The difference between both responses is caused by the fact that ailerons are not deflected in a steady-state, while the elevator is. Fortunately, it is possible to perform a ground test calibrating all control surface synchros, such that the relation between synchro measurement and control surface deflection are properly known. This ground test is recommended to be executed before the flight test to investigate the performance degradation due to this phenomenon.

11-3 Maneuver Design

Regarding maneuver design for the flight test it is recommended to check the vertical speeds and normal loads beforehand in simulation. The normal loads are recommended to be kept between 0.6 and 1.4g and it should be noted that especially low g-values can be uncomfortable during the flight test. Additionally, it is recommended that maneuvers are designed well below the aircraft maximum speed to avoid manual pilot interference to be required. Pilots will not let the aircraft exceed a specified maximum speed as this requires an extensive ground check before the aircraft is deemed airworthy again.

11-4 Conclusions and Recommendations

This section presents the conclusions and recommendations regarding PH-LAB Cessna Citation specific issues. The issues are to be solved before the flight test to prevent confounds within the research. First, previous flight test have shown that the maximum servo power is limited. The limitation has been put into place as human pilots should at all times be able to overpower the automatic control system for certification and safety purposes. Therefore, it is recommended that the flight test be executed at lower velocities to reduce the chance of hitting the maximum servo power.

Second, a lower velocity is also recommended as it avoids a potential manual interference by the pilot when the aircraft is about to hit the maximum speed. Moreover, checks on the normal loads and vertical speeds are also recommended such that the loads on the aircraft are kept small and serious passenger discomfort is avoided.

Third, it is recommended that a ground test be executed before the flight test calibrating all control surface synchros. As such, the relation between synchro measurement and control surface deflection are properly known. This should avoid performance degradation due to nonlinear actuator measurement effects.

Chapter 12

Conclusions and Recommendations

This chapter presents the conclusions and recommendations of this report. The research objective used for this report is to further develop the theory on Incremental Nonlinear Dynamic Inversion (INDI), particularly with regard to the implementation of INDI in a CS-25 certified commercial fixed-wing aircraft. INDI is a promising control technique that could contribute to safer, cheaper Flight Control Systems (FCSs) with shorter development periods, straightforward certification and increased performance. This report has shown that performance degradation due to typical aircraft characteristics can be prevented to retain the advantages of INDI as proven on other application platforms.

The controller performance was assessed based on a mix of qualitative and quantitative criteria. As qualitative criterion, observations of system responses of system input were used, while the Root Mean Square (RMS) was used as quantitative criteria. The developed controller consists of an inner loop with the angular rates as Control Variables (CVs) and attitude angles together with the sideslip angle as outer loop CVs. Additionally, a Proportional-Integral-Derivative (PID) controller was developed, such that the performance of INDI could be put into perspective.

An analytical stability analysis showed that implementing discrete-time INDI with a smaller sampling time results in larger stability margins regarding system characteristics and controller gains. More specifically, the analysis concluded that sampling times smaller than 0.02s result in large stability margins. Moreover, the artificial unit delay of the actuator measurements implemented by some other authors was found to degrade system stability.

The effect of the real-world phenomena, bias, discretization, noise and time delay on an INDI controlled aircraft were investigated. Four phenomena showed significant performance degradation requiring controller adaptation: actuator measurement bias, angular rate measurement noise, angular rate measurement delay and actuator measurement delay.

Fortunately, the performance degradation can be prevented using a combination of three solutions without introducing additional model dependencies into the controller. First, using PI-control to design the virtual control input of the inner loop prevents a steady-state error due to actuator measurement bias. Second, a second-order low-pass filter can be used to reduce noise in the control input signal due to angular rate measurement noise. Third, the measurement delay of the angular rate and actuator measurements have to be synchronized to prevent oscillatory behavior, although a small mismatch between the delay in both signals is acceptable.

The importance of synchronizing the measurements was confirmed by both the analytical stability analysis and simulations with an INDI controlled aircraft. Moreover, both methods also showed that INDI is inherently more sensitive to a surplus of angular rate delay compared with a surplus of actuator delay. Part of this effect can be counteracted using Pseudo Control Hedging (PCH), which favorably shifts the region of adequate performance towards a surplus of angular rate delay.

To synchronize the measurements a real-time time delay identification algorithm based on the concept of latency was proposed. The latency of both actuator and angular rate measurements with respect to the values commanded by the controller are identified using the Average Square Difference Function (ASDF). The difference in latency between the actuator and angular rate measurements is a measure of the unsynchronized delay between these signals. The unsynchronized delay is successfully identified by the algorithm with only a small error range. As such, the controller can fly with each combination of actuator and angular rate delay for values well above typical delays for aircraft. An additional benefit of the algorithm is that it does not introduce additional model dependencies into the controller as only already available signals are used.

Besides the conclusions of this report that can be applied to aircraft in general, also some conclusions and recommendations can be made with regard to the PH-LAB Cessna Citation aircraft. There are two control modes available on the PH-LAB: passenger-in-the-loop and fully automatic. It is recommended that the flight test be executed on at least two points of the flight envelope by performing typical flight test maneuvers such as 3211 maneuvers, doublets or angle captures. Moreover, it is recommended that the Cooper-Harper Rating (CHR) be used as assessment criteria for future flight tests, based on the notion that qualitative handling qualities for piloted aircraft are important. However, for this to be possible a pilot-in-the-loop control mode has to be available.

Finally, to avoid any confounds in future research all PH-LAB specific issues have to be solved. It is recommended that the flight test be executed at lower velocities to reduce the chance of hitting the maximum servo power as well as avoiding manual interference by the pilot. Moreover, checks on the normal loads and vertical speeds are also recommended such that the loads on the aircraft are kept small and serious passenger discomfort be avoided. Third, it is recommended that a ground test be executed before the flight test calibrating all control surface synchros. This should avoid performance degradation due to nonlinear actuator measurement effects.

Bibliography

Acquatella B., P., Falkena, W., van Kampen, E.-J., & Chu, Q. P. (2012). Robust Nonlinear Spacecraft Attitude Control using Incremental Nonlinear Dynamic Inversion. In *AIAA Guidance, Navigation, and Control Conference*. Minneapolis, MN, USA: AIAA. doi:10.2514/6.2012-4623

Adams, R. J. & Banda, S. S. (1993). Robust Flight Control Design using Dynamic Inversion and Structured Singular Value Synthesis. *IEEE Transactions on Control Systems Technology*, *1*(2), 80–92. doi:10.1109/87.238401

Anon. (1997). *Flying Qualities of Piloted Aircraft.* Departmant of Defense, MIL-HDBK-1797. Washington, D.C., USA.

Anon. (2008). *Civil Aviation Safety Data: 1993-2007.* Civil Aviation Authority of the Netherlands (CAANL). The Hague, the Netherlands.

Anon. (2013). *State of Global Aviation Safety.* International Civil Aviation Organization (ICAO). Montreal, Canada.

Bacon, B. J. & Ostroff, A. J. (2000). Reconfigurable Flight Control using Nonlinear Dynamic Inversion with a Special Accelerometer Implementation. In *AIAA Guidance, Navigation, and Control Conference and Exhibit.* Denver, CO, USA: AIAA. doi:10.2514/6.2000-4565

Bacon, B. J., Ostroff, A. J., & Joshi, S. M. (2000). Nonlinear Dynamic Inversion Reconfigurable Controller Utilizing a Fault Tolerant Accelerometer Approach. In *Proceedings of the 19th Digital Avionics Systems Conference* (6F5/1–6F5/8). Philadelphia, PA, USA: IEEE. doi:10.1109/DASC.2000.884920

Bacon, B. J., Ostroff, A. J., & Joshi, S. M. (2001). Reconfigurable NDI Controller using Inertial Sensor Failure Detection & Isolation. *IEEE Transactions on Aerospace and Electronic Systems*, *37*(4), 1373–1383. doi:10.1109/7.976972

Baer, S. (2014). F-35A High Angle-of-Attack Testing. In *AIAA Atmospheric Flight Mechanics Conference*. Atlanta, GA, USA: AIAA. doi:10.2514/6.2014-2057

Balas, G. J. (2003). Flight Control Law Design: An Industry Perspective. *European Journal of Control*, *9*(2-3), 207–226. doi:10.3166/ejc.9.207-226

Balas, G. J. & Hodgkinson, J. (2009). Control Design Methods for Good Flying Qualities. In *AIAA Atmospheric Flight Mechanics Conference*. Chicago, IL, USA: AIAA. doi:10.2514/6.2009-6319

Bauschat, J.-M., Mönnich, W., Willemsen, D., & Looye, G. (2001). Flight Testing Robust Autoland Control Laws. In *AIAA Guidance, Navigation, and Control Conference and Exhibit*. Montreal, Canada: AIAA. doi:10.2514/6.2001-4208

Bosworth, J. T. (2008). Flight Results of the NF-15B Intelligent Flight Control System (IFCS) Aircraft with Adaptation to a Longitudinally Destabilized Plant. In *AIAA Guidance, Navigation, and Control Conference and Exhibit*. Honolulu, HI, USA: AIAA. doi:10.2514/6.2008-6985

Bosworth, J. T. & Williams-Hayes, P. S. (2007). Flight Test Results from the NF-15B Intelligent Flight Control System (IFCS) Project with Adaptation to a Simulated Stabilator Failure. In *AIAA Infotech@Aerospace 2007 Conference and Exhibit*. Rohnert Park, CA, USA: AIAA. doi:10.2514/6.2007-2818

Brinker, J. S. & Wise, K. A. (2001). Flight Testing of Reconfigurable Control Law on the X-36 Tailless Aircraft. *Journal of Guidance, Control, and Dynamics*, *24*(5), 903–909. doi:10.2514/2.4826

Burken, J. J., Hanson, C. E., Lee, J. A., & Kaneshige, J. T. (2009). Flight Test Comparison of Different Adaptive Augmentations of Fault Tolerant Control Laws for a Modified F-15 Aircraft. In *AIAA Infotech@Aerospace Conference*. Seattle, WA, USA: AIAA. doi:10.2514/6.2009-2056

Cooper, G. E. & Harper Jr., R. P. (1969). *The Use of Pilot Rating in the Evaluation of Aircraft Handling Qualities*. National Aeronautics and Spac Administration, NASA TN D-5153. Washington, D.C., USA.

Cox, T. H. & Cotting, M. C. (2005). A Generic Inner-Loop Control Law Structure for Six-Degree-of-Freedom Conceptual Aircraft Design. In *43rd AIAA Aerospace Sciences Meeting and Exhibit*. Reno, NV, USA: AIAA. doi:10.2514/6.2005-31

Enns, D., Bugajski, D., Hendrick, R., & Stein, G. (1994). Dynamic Inversion: An Evolving Methodology for Flight Control Design. *International Journal of Control*, *59*(1), 71–91. doi:10.1080/00207179408923070

Falkena, W. (2012). *Investigation of Practical Flight Control Systems for Small Aircraft* (PhD Thesis, Delft University of Technology, Delft, the Netherlands).

Falkena, W., Borst, C., Chu, Q. P., & Mulder, J. A. (2011). Investigation of Practical Flight Envelope Protection Systems for Small Aircraft. *Journal of Guidance, Control, and Dynamics*, *34*(4), 976–988. doi:10.2514/1.53000

Fielding, C., Varga, A., Bennani, S., & Selier, M. (Eds.). (2002). *Advanced Techniques for Clearance of Flight Control Laws*. Heidelberg, Germany: Springer-Verlag. doi:10.1007/3-540-45864-6

Gibson, J. C. (1999). *Development of a Design Methodology for Handling Qualities Excellence in Fly by Wire Aircraft* (PhD Thesis, Delft University Press, Delft, the Netherlands).

Hanson, C., Schaefer, J., Burken, J. J., Johnson, M., & Nguyen, N. (2011). Handling Qualities Evaluations of Low Complexity Model Reference Adaptive Controllers for Reduced Pitch and Roll Damping Scenarios. In *AIAA Guidance, Navigation, and Control Conference*. Portland, OR, USA: AIAA. doi:10.2514/6.2011-6607

Heise, C. D., Falconí, G. P., & Holzapfel, F. (2014). Hexacopter Outdoor Flight Test Results of an Extended State Observer based Controller. In *2014 IEEE International Conference on Aerospace Electronics and Remote Sensing Technology* (pp. 26–33). Yogyakarta, Indonesia: IEEE. doi:10.1109/ICARES.2014.7024373

Honeywell & Lockheed Martin. (1996). *Application of Multivariable Control Theory to Aircraft Control Laws. Final Report: Multivariable Control Design Guideline*. Wright Laboratory, Air Force Materiel Command, WL-TR-96-3099. Wright Patterson AFB, OH, USA.

Jacklin, S. A. (2008). Closing the Certification Gaps in Adaptive Flight Control Software. In *AIAA Guidance, Navigation and Control Conference and Exhibit*. Honolulu, HI, USA: AIAA. doi:10.2514/6.2008-6988

Johnson, E. N. & Calise, A. J. (2000). Pseudo-Control Hedging: A New Method for Adaptive Control. In *Advances in Navigation Guidance and Control Technology Workshop*. Redstone Arsenal, AL, USA.

Johnson, E. N. & Kannan, S. K. (2005). Adaptive Trajectory Control for Autonomous Helicopters. *Journal of Guidance, Control, and Dynamics*, *28*(3), 524–538. doi:10.2514/1.6271

Johnson, E. N. & Turbe, M. A. (2006). Modeling, Control, and Flight Testing of a Small Ducted-Fan Aircraft. *Journal of Guidance, Control, and Dynamics*, *29*(4), 769–779. doi:10.2514/1.16380

Jury, E. I. (1965). A Modified Stability Table for Linear Discrete Systems. *Proceedings of the IEEE*, *53*(2), 184–185. doi:10.1109/PROC.1965.3612

Koschorke, J. (2012). *Advanced Flight Control Design and Evaluation: An Application of Time Delayed Incremental Backstepping* (Master's Thesis, Delft University of Technology, Delft, the Netherlands).

Lam, Q. M., Hindman, R., Shell, W. M., & Ridgely, D. B. (2005). Investigation and Preliminary Development of a Modified Pseudo Control Hedging for Missile Performance Enhancement. In *AIAA Guidance, Navigation, and Control Conference and Exhibit*. San Francisco, CA, USA: AIAA. doi:10.2514/6.2005-6458

Lombaerts, T. J. J., Huisman, H. O., Chu, Q. P., Mulder, J. A., & Joosten, D. A. (2009). Nonlinear Reconfiguring Flight Control based on Online Physical Model Identification. *Journal of Guidance, Control, and Dynamics*, *32*(3), 727–748. doi:10.2514/1.40788

Lombaerts, T. J. J. & Looye, G. H. N. (2012). Design and Flight Testing of Nonlinear Autoflight Control Laws. In *AIAA Guidance, Navigation, and Control Conference*. Minneapolis, MN, USA: AIAA. doi:10.2514/6.2012-4982

Looye, G., Joos, H.-D., & Willemsen, D. (2001). Application of an Optimisation-based Design Process for Robust Autoland Control Laws. In *AIAA Guidance, Navigation, and Control Conference and Exhibit*. Montreal, Canada: AIAA. doi:10.2514/6.2001-4206

Lu, P., van Kampen, E., & Chu, Q. P. (2015). Robustness and Tuning of Incremental Backstepping. In *AIAA Guidance, Navigation, and Control Conference*. Kissimmee, FL, USA: AIAA. doi:10.2514/6.2015-1762

Lu, P. & van Kampen, E.-J. (2015). Active Fault-Tolerant Control for Quadrotors Subjected to a Complete Rotor Failure. In *2015 IEEE/RSJ International Conference on Intelligent Robots and Systems* (pp. 4698–4703). Hamburg, Germany: IEEE/RSJ. doi:10.1109/IROS.2015.7354046

Marino, R. (1986). On the Largest Feedback Linearizable Subsystem. *Systems & Control Letters*, *6*(5), 345–351. doi:10.1016/0167-6911(86)90130-1

Miller, C. J. (2011a). Nonlinear Dynamic Inversion Baseline Control Law: Architecture and Performance Predictions. In *AIAA Guidance, Navigation, and Control Conference*. Portland, OR, USA: AIAA. doi:10.2514/6.2011-6467

Miller, C. J. (2011b). Nonlinear Dynamic Inversion Baseline Control Law: Flight-Test Results for the Full-scale Advanced Systems Testbed F/A-18 Airplane. In *AIAA Guidance, Navigation, and Control Conference*. Portland, OR, USA: AIAA. doi:10.2514/6.2011-6468

Mulder, J. A., van der Vaart, J. C., & Mulder, M. (2007). *AE4304: Atmospheric Flight Dynamics*. Delft, the Netherlands: Faculty of Aerospace Engineering, Delft University of Technology.

Mulder, J. A., van Staveren, W. H. J. J., van der Vaart, J. C., de Weerdt, E., de Visser, C. C., in 't Veld, A. C., & Mooij, E. (2013). AE3202: Flight Dynamics. Delft: Faculty of Aerospace Engineering, Delft University of Technology.

Naidu, D. S. & Calise, A. J. (2001). Singular Perturbations and Time Scales in Guidance and Control of Aerospace Systems: A Survey. *Journal of Guidance, Control, and Dynamics*, *24*(6), 1057–1078. doi:10.2514/2.4830

Nise, N. S. (2011). *Control Systems Engineering* (6th ed.). Asia: John Wiley & Sons, Inc.

Ostroff, A. J. & Bacon, B. J. (2002). Enhanced NDI Strategies for Reconfigurable Flight Control. In *Proceedings of the 2002 American Control Conference* (pp. 3631–3636). Anchorage, AK, USA: IEEE. doi:10.1109/ACC.2002.1024492

Rajput, J. & Weiguo, Z. (2014). Fundamental Methodologies for Control of Nonlinear Nonminimum-Phase Systems: An Overview. *Journal of Systems and Control Engineering*, *228*(8), 553–564. doi:10.1177/0959651814535573

Schaefer, J., Hanson, C., Johnson, M. A., & Nguyen, N. (2011). Handling Qualities of Model Reference Adaptive Controllers with Varying Complexity for Pitch-Roll Coupled Failures. In *AIAA Guidance, Navigation, and Control Conference*. Portland, OR, USA: AIAA. doi:10.2514/6.2011-6453

Schierman, J. D., Ward, D. G., Hull, J. R., Gandhi, N., Oppenheimer, M. W., & Doman, D. B. (2004). Integrated Adaptive Guidance and Control for Re-Entry Vehicles with Flight-Test Results. *Journal of Guidance, Control, and Dynamics*, *27*(6), 975–988. doi:10.2514/1.10344

Schumacher, C. & Khargonekar, P. P. (1998). Stability Analysis of a Missile Control System with a Dynamic Inversion Controller. *Journal of Guidance, Control, and Dynamics*, *21*(3), 508–515. doi:10.2514/2.4266

Sieberling, S., Chu, Q. P., & Mulder, J. A. (2010). Robust Flight Control using Incremental Nonlinear Dynamic Inversion and Angular Acceleration Prediction. *Journal of Guidance, Control, and Dynamics*, *33*(6), 1732–1742. doi:10.2514/1.49978

Simplício, P. V. M. (2011). *Helicopter Nonlinear Flight Control: An Acceleration Measurements-based Approach using Nonlinear Dynamic Inversion* (Master's Thesis, Delft University of Technology, Delft, the Netherlands).

Simplício, P., Pavel, M. D., van Kampen, E., & Chu, Q. P. (2013). An Acceleration Measurements-based Approach for Helicopter Nonlinear Flight Control using Incremental Nonlinear Dynamic Inversion. *Control Engineering Practice*, *21*(8), 1065–1077. doi:10.1016/j.conengprac.2013.03.009

Slotine, J.-J. E. & Li, W. (1991). *Applied Nonlinear Control* (3rd ed.). Upper Saddle River, NJ, USA: Prentice-Hall.

Smeur, E. J. J., Chu, Q. P., & de Croon, G. C. H. E. (2016). Adaptive Incremental Nonlinear Dynamic Inversion for Attitude Control of Micro Air Vehicles. *Journal of Guidance, Control, and Dynamics*, *39*(3), 450–461. doi:10.2514/1.G001490

Smith, P. R. (1998). A Simplified Approach to Nonlinear Dynamic Inversion Based Flight Control. In *23rd Atmospheric Flight Mechanics Conference* (pp. 762–770). Boston, MA, USA: AIAA. doi:10.2514/6.1998-4461

Smith, P. & Berry, A. (2000). Flight Test Experience of a Non-Linear Dynamic Inversion Control Law on the VAAC Harrier. In *Atmospheric Flight Mechanics Conference* (pp. 132–142). Denver, CO, USA: AIAA. doi:10.2514/6.2000-3914

Steer, A. J. (2003). Handling Quality Design Criteria for Advanced Supersonic Aircraft Flight Control. In *AIAA Atmospheric Flight Mechanics Conference and Exhibit*. Austin, TX, USA: AIAA. doi:10.2514/6.2003-5308

Tang, S. H. (2014). *Fault-Tolerant Flight Control with Sensor-based Nonlinear Dynamic Inversion: Application and Evaluation in the SIMONA Research Simulator* (Master's Thesis, Delft University of Technology, Delft, the Netherlands).

van 't Veld, R. C. (2016). *Incremental Nonlinear Dynamic Inversion Flight Control: Practical Implementation on a Commercial Fixed-Wing Aircraft* (Preliminary Master's Thesis, Delft University of Technology, Delft, the Netherlands).

Vlaar, C. M. (2014). *Incremental Nonlinear Dynamic Inversion Flight Control: Implementation and Flight Test on a Fixed Wing UAV* (Master's Thesis, Delft University of Technology, Delft, the Netherlands).

Wacker, R., Munday, S., & Merkle, S. (2001). X-38 Application of Dynamic Inversion Flight Control. In *24th Annual AAS Guidance and Control Conference*. Breckenridge, CO, USA: AAS.

Walker, G. P. & Allen, D. A. (2002). X-35B STOVL Flight Control Law Design and Flying Qualities. In *2002 Biennial International Powered Lift Conference and Exhibit*. Williamsburg, VA, USA: AIAA. doi:10.2514/6.2002-6018

Walker, G., Wurth, S., & Fuller, J. (2013). F-35B Integrated Flight-Propulsion Control Development. In *2013 International Powered Lift Conference*. Los Angeles, CA, USA: AIAA. doi:10.2514/6.2013-4243

Wang, Q. & Stengel, R. F. (2000). Robust Nonlinear Control of a Hypersonic Aircraft. *Journal of Guidance, Control, and Dynamics*, *23*(4), 577–585. doi:10.2514/2.4580

Wedershoven, J. A. M. M. (2010). *Analysis of Nonlinear Dynamic Inversion based Control Law Designs: Application to an F-16 Model* (Master's Thesis, Delft University of Technology, Delft, the Netherlands).